DYNAMIC MODELING AND CONTROL OF SEMI-ACTIVE SUSPENSION SYSTEM FOR ROAD VEHICLE

A THESIS SUBMITTED IN PARTIAL FULFILLMENT OF THE REQUIREMENT FOR THE AWARD OF THE DEGREE OF

MASTER OF TECHNOLOGY
(COMPUTATIONAL DESIGN)
TO

DELHI TECHNOLOGICAL UNIVERSITY

SUBMITTED BY

NILANJAN BHARADWAJ
ROLL NO.- 2K14/CDN/10

UNDER THE GUIDANCE OF

DR. VIKAS RASTOGI
PROFESSOR

DELHI TECHNOLOGICAL UNIVERSITY

DEPARTMENT OF MECHANICAL, PRODUCTION & INDUSTRIAL AND AUTOMOBILE ENGINEERING
DELHI TECHNOLOGICAL UNIVERSITY
BAWANA ROAD, DELHI-110042
JUNE 2016

DELHI TECHNOLOGICAL UNIVERSITY

(Formerly Delhi College of Engineering)

Shahbad Daulatpur, Bawana Road,

Delhi-110042

STUDENT'S DECLARATION

I, **Nilanjan Bharadwaj,** hereby certify that the work which is being presented in this thesis entitled **"Dynamic Modeling and Control of Semi-Active Suspension System for Road Vehicle"** is submitted in the partial fulfillment of the requirement for degree of **Master of Technology (Computational Design)** in Department of Mechanical Engineering at **Delhi Technological University** is an authentic record of my own work carried out under the supervision of **Prof. Vikas Rastogi.** The matter presented in this thesis has not been submitted in any other University/Institute for the award of Master of Technology Degree. Also, it has not been directly copied from any source without giving its proper reference.

Signature of Student

This is to certify that the above statement made by the candidate is correct to the best of my knowledge.

Signature of Supervisor

The Master of Technology Viva-Voce examination of Mr. Nilanjan Bharadwaj has been held on ……. and accepted.

Signature of Supervisor **Signature of HOD**

Signature of External Examiner

DELHI TECHNOLOGICAL UNIVERSITY

(Formerly Delhi College of Engineering)

Shahbad Daulatpur, Bawana Road,

Delhi-110042

CERTIFICATE

This is to certify that this thesis report entitled, **"Dynamic Modeling and Control of Semi-Active Suspension System for Road Vehicles"** being submitted by **Nilanjan Bharadwaj (Roll No. 2K14/CDN/10)** at Delhi Technological University, Delhi for the award of the Degree of Master of Technology as per academic curriculum. It is a record of bonafide research work carried out by the student under my supervision and guidance, towards partial fulfillment of the requirement for the award of Master of Technology degree in Computational Design. The work is original as it has not been submitted earlier in part or full for any purpose before.

Dr. Vikas Rastogi

Professor

Mechanical Engineering Department

Delhi Technological University

Delhi-110042

ACKNOWLEDGEMENT

First and foremost, praises and thanks to the God, the Almighty, for His showers of blessings throughout my research work to complete the research successfully.

I would like to extend my gratitude to **Prof. R. S. Mishra, Head,** Department of Mechanical Engineering, Delhi Technological University, for providing this opportunity to carry out the present thesis work.

The constant guidance and encouragement received from **Dr. A. K. Agrawal, M.Tech. Coordinator and Associate Professor,** Department of Mechanical Engineering, Delhi Technological University, has been of great help in carrying out the present work and is acknowledged with reverential thanks.

I would like to express my deep and sincere gratitude to my research supervisor, **Prof. Vikas Rastogi,** Department of Mechanical Engineering, Delhi Technological University, for giving me the opportunity to do research and providing invaluable guidance throughout this research. His dynamism, vision, sincerity and motivation have deeply inspired me. He has taught me the methodology to carry out the research and to present the research works as clearly as possible. It was a great privilege and honor to work and study under his guidance. I am extremely grateful for what he has offered me. I would also like to thank him for his friendship, empathy, and great sense of humor. Without the wise advice and able guidance, it would have been impossible to complete the thesis in this manner.

I would like to extend my thanks to **Mr. Ashish Gupta**, PhD Scholar, Delhi Technological University, without the help of whom the project would not have been completed. I am also grateful to all the faculty members of the Mechanical Engineering Department for molding me at correct time so that I can have a touch at final destination and to all my friends, especially Shreyansh Upadhyaya for the help, moral support and encouragement; they had given to me during completion of dissertation work.

I am extremely grateful to my parents and family for their love, prayers, caring and sacrifices for educating and preparing me for my future.

NILANJAN BHARADWAJ
M.Tech. (COMPUTATIONAL DESIGN)
2K14/CDN/10

ABSTRACT

The vehicle suspension system is generally considered as the linkage between the vehicle body and wheels. The main task of the suspension system is to provide a comfortable and safe ride. The good ride quality requires high damping setting at low frequencies to suppress pitch, and lower damping setting at higher frequencies to prevent harshness. However, to improve handling performance, springs and dampers must be made stiffer at all frequencies to reduce body attitude. The design of a better-quality suspension system remains an important development objective for the automotive industry. An ideal vehicle suspension should have the capability to reduce the displacement and acceleration of the vehicle body, and thus; maximizing the ride comfort.

Present work analyzes the dynamic behavior of a road vehicle through bond graph and MATLAB/Simulink®, where vertical and longitudinal dynamics have been evaluated. A two degrees of freedom quarter car model and a four degrees of freedom half car model have been considered for the performance assessment. Simulations have been carried out on SYMBOLS Sonata® and MATLAB® software environments. The results obtained are used to evaluate the performance of the system.

The work also includes different types of suspension systems such as passive and semi-active suspension system, where physical and mathematical models of quarter car and half car have been evaluated. Different semi-active suspension control algorithms have been incorporated to the system models to optimize the efficiency of the vehicle for bump type and random road inputs.

Key Words: Bond graph modeling, Vehicle dynamics, Car model, Semi-active suspension, Passive suspension, Skyhook control, Groundhook control, Balance logic, Hybrid control logic.

TABLE OF CONTENTS

LIST OF FIGURES

LIST OF TABLES

APPENDIX

Bond Graph Modeling

The bond graph modeling is the representation (by a bond) of power as the product of an effort and a flow, with elements acting between these variables and junction structures to put the process plant together. The power exchanged between two process plants A and B is indicated by a bond and is the product of two variables – a potential variable (i.e., pressure, electric potential, temperature, chemical potential, force, etc.) called effort (e) and a current variable (i.e., volume flow, current, entropy flow, velocity, molar flow, etc.) referred to as flow (f). The determination of causes and effects in the process plant is directly deduced from the graphical representation. In the bond graph, it is denoted by the cross-stroke indicating how 'e' and 'f' simultaneously are determined causally on a bond. The direction of action is indicated by an arrow on each connection. Independently of the causality, the direction of the positive power is indicated by a half-arrow on the bond.

Since power interactions are always present when two multiport are connected, the various power variables are classified in a universal scheme and to describe all types of multiport in a common language. Table 1 gives power variables called effort and flow for some of physical domains. This type of bond graph is then called true bond graph. The power P_u corresponds to the product of the power variables effort and flow.

$$P_u = e(t) \cdot f(t)$$

Table 1: Power variables in a true bond graph

Domain	Effort $e(t)$	Flow $f(t)$
Electric	Voltage *u* (V)	Current *i* (A)
Mechanics rotation	Torque Γ (Nm)	Angular velocity ω (rad/s)
Mechanics translation	Force *F* (N)	Velocity *v* (m/s)
Hydraulics	Pressure (Pa)	Volume flow rate $\dot{V}$ (m^3/s)
Thermodynamics	Temperature (K)	Entropy flow (J/Ks)
Chemistry		
Transformation phenomenon	Chemical potential μ (J/mol)	Molar flow rate $\dot{n}$ (mol/s)
Kinetic phenomenon	Chemical affinity *A*	Speed of reaction $\dot{\xi}$

Energy variables

Two additional physical quantities are used in bond graph modeling. They are called energy variables and are important for dynamic system representation and are associated with state variables. Two kinds of energy variables are used: generalized momentum $p(t)$ (charge, volume, entropy, etc.) and generalized displacement $q(t)$ (angular momentum, pressure momentum, etc.). They are obtained by integration of power variables (effort or flow) with respect to time:

$$q(t) = \int_0^t f(\tau)d\tau$$

$$p(t) = \int_0^t e(\tau)d\tau$$

The state vector in a bond graph model is composed by the energy variables p and q. Those variables appear in their derivative form in C ($\dot{q} = f$) and I ($\dot{p} = e$) elements. The dimension of the state vector is equal to the number of C and I elements in integral causality. Finally, the bond graph symbol gives four information's: (1) the physical link between two systems with the bond, (2) the type of power (electric, mechanical, etc.) with the power variables, (3) the power direction with the half arrow, and (4) the causality with the stroke.

Bond graph elements

There are nine basic energetic multiport elements and two information's elements, grouped into four categories according to their energy characteristics. These elements and definitions (constitutive equations) are summarized in Table 2. In bond graph language, two active elements (called sources) (Se and Sf), three generalized passive elements (I, C and R), two junctions (0 and 1) and two transducers (TF and GY) are used to model any energetic process. When the exchanged power is negligible, it is represented by an information bond, which corresponds to block diagrams arrows. It is shown in as full arrow on the bond and can represent the signal transmitted by sensors, integrators, etc.

Table 2: Elements of bond graph

	Symbol	Constitutive equation	Name
Sources	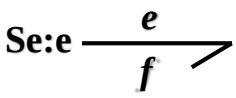	$\begin{cases} e(t)\ given\ by\ the\ source \\ f(t)\ arbitrary \end{cases}$	Source of effort
	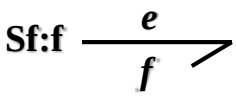	$\begin{cases} f(t)\ given\ by\ the\ source \\ e(t)\ arbitrary \end{cases}$	Source of flow
Passive elements Dissipater	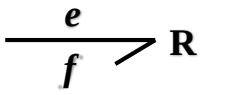	$\Phi_R(e,f) = 0$	Resistance
Energy stores	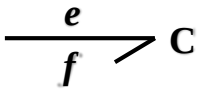	$\Phi_C(e,f) = 0$	Capacitance
	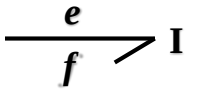	$\Phi_I(e,f) = 0$	Inertance
Junctions Transducers	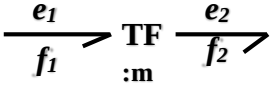	$\begin{cases} e_1 = me_2 \\ f_2 = mf_1 \end{cases}$	Transformer
	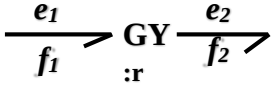	$\begin{cases} e_1 = rf_2 \\ e_2 = rf_1 \end{cases}$	Gyrator
Junctions	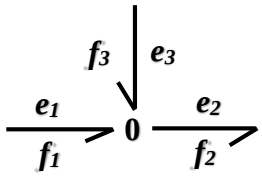	$\begin{cases} e_1 = e_2 = e_3 \\ f_1 - f_2 + f_3 = 0 \end{cases}$	Zero junction: common effort junction
	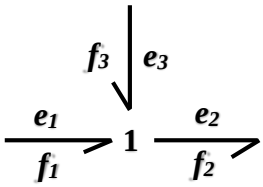	$\begin{cases} f_1 = f_2 = f_3 \\ e_1 - e_2 + e_3 = 0 \end{cases}$	One junction: common flow junction
Sensors	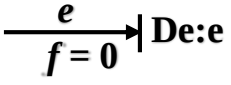	$\begin{cases} e = e(t) \\ f = 0 \end{cases}$	Sensors (Detectors)
	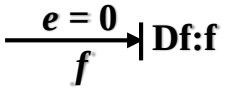	$\begin{cases} f = f(t) \\ e = 0 \end{cases}$	

CHAPTER 1

INTRODUCTION

1.1 Background

India has road networks of 3.314 million kilometres, which is one of the largest road networks in the world, consisting of National Highways, Expressways, State Highways etc. About 65% of freight and 86.7% passenger traffic is carried by roads. In 2012, the loss to the Indian economy due to Road Traffic Accidents was estimated as 3% of GDP. According to the Road Accident Report (2014) published by the Ministry of Road Transport and Highways, while 4,726 people lost their lives in accidents due to humps, 6,672 were killed in crashes caused due to potholes and speed breakers [1, 2]. Road roughness is a main source of vibration in vehicles and a well-known cause of wear and damage to sensitive payloads, to the vehicle itself, as well as to bridges and pavements. Vehicle vibration in turn, also brings whole-body vibration (WBV) exposure to drivers and passengers. WBV is a root cause of work related accidents and work related diseases like spinal compression stress, heart disease and musculoskeletal problems (ROADEX-III report, under National Periphery Program, European Union) [3].

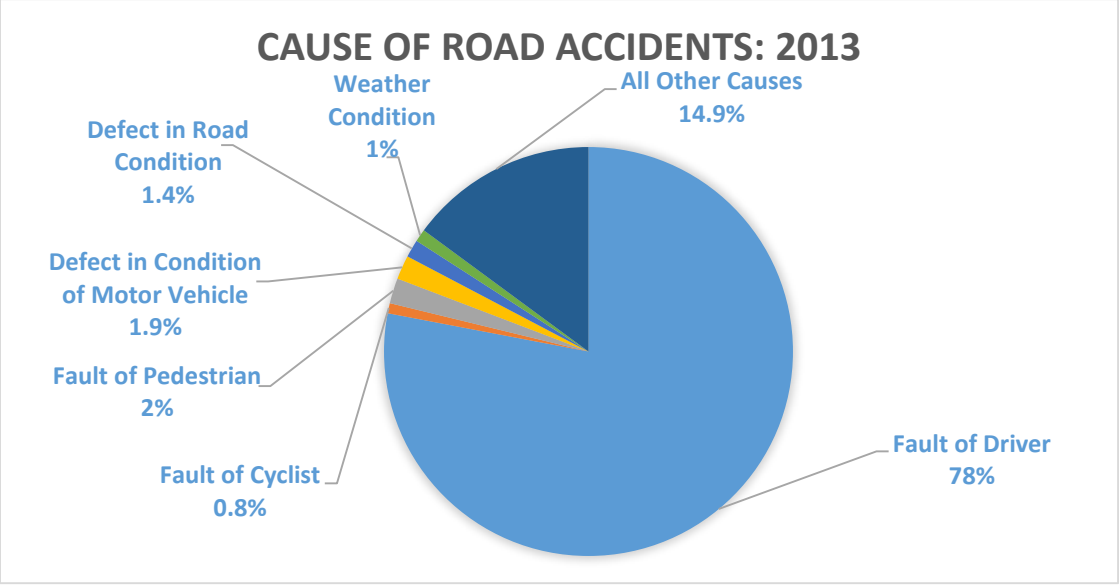

Fig. 1.1: Causes of Road Accidents (Government of India, Ministry of Road Transport and Highways, Transport Research Wing, New Delhi) [4].

As shown in Fig. 1.1, fault of driver accounted to 78% of the road accidents in India in the year 2013. The nature of surface of roads (Pot Holes) accounted for 9,699 road accidents and 2,607 road accident fatalities in 2013. As a share, the total road accidents and fatalities, due to pot holes constituted 2.0 per cent and 1.9 per cent, respectively [4]. Ride comfort of the driver is therefore of utmost importance as WBV caused by the unevenness of the road may lead to fatigue of the driver in turn degrading driver's performance and concentration.

1.2 Motivation

Vehicle design is an expensive and time consuming process that is initiated with an extensive analysis of the vehicle system and observing any faults related with the design in order to determine the desired characteristics and efficiency of the vehicle. This is followed by detail design of numerous sub-systems and components to envision the real model of the vehicle.

The motivation of this study came from the recent trends in the increase of road accidents due to bad road conditions leading to fatigue of the operator. Vibration isolation as well as ride comfort is of utmost importance to check the accidents due to bad road conditions. Road holding is one of the major factors to study the performance of a vehicle. A vehicle tire must always be in contact with the road for better handling of the vehicle. But, due to harsh road conditions, the contact between the tire and the road may be compromised leading to accidents. Suspension system plays a vital role in diminishing the vibration caused by the road roughness and prevent it from transmitting to the driver and the passengers. Moreover, a suspension system should be able to provide good road holding force for better vehicle handling in rough road conditions.

1.3 Types of Suspension Systems

Vehicle suspension performs a vital role in vehicle dynamics, contributing to enhance the ride comfort and the vehicle stability. The vehicle suspension system design is an active research area, where one of the goals is to alleviate the passenger's comfort through the vibration reduction of the internal engine as well as external road disturbances. Suspension systems can be classified into three basic classes, passive suspensions, semi-active suspensions and active suspensions.

1.3.1 Passive suspension

A passive suspension system is one in which the spring stiffness and the damping coefficient are fixed. These characteristics are decided by the designer of the suspension, according to the design objectives and the intended application. Passive suspension can provide a compromise between vehicle handling and ride comfort as shown in Fig. 1.2.

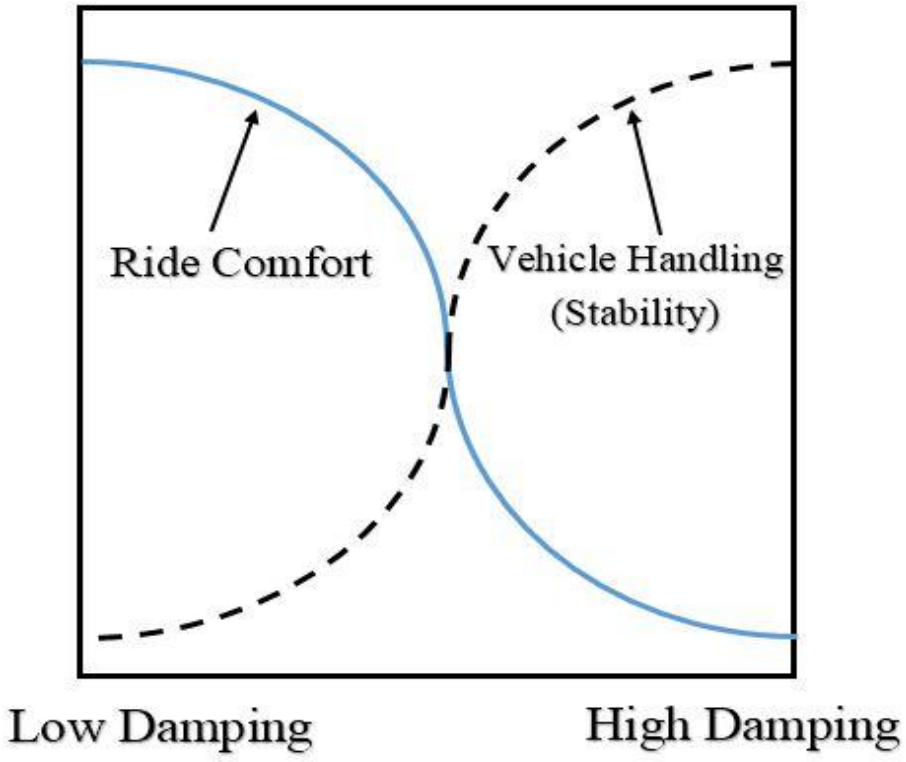

Fig. 1.2: Damping compromise for passive damper

A heavily damped suspension will provide good vehicle handling, but it will transmit much of the road input to the vehicle body. When the vehicle is traversing a rough road at low speed or a straight line at high speed, this will be regarded as a harsh ride. The driver and passengers may find the harsh ride unacceptable, or it may damage freight. A lightly damped system will give a more comfortable ride, but can significantly lessen the vehicle stability in turns or lane change manoeuvres. Good design of a passive suspension can optimize ride comfort and stability to some extent, but the compromise cannot be completely eliminated.

1.3.2 Active suspension

In an active suspension, force actuator is used instead of passive damper or both damper and spring as shown in Fig. 1.3. The force actuator is capable of adding and dissipating energy from the system, whereas a passive damper can only dissipate energy. The force applied by the force actuator does not dependent on the relative velocity or displacement across the suspension. Implementing an appropriate control strategy, a better compromise between ride comfort and vehicle stability can be achieved as shown in Fig. 1.4.

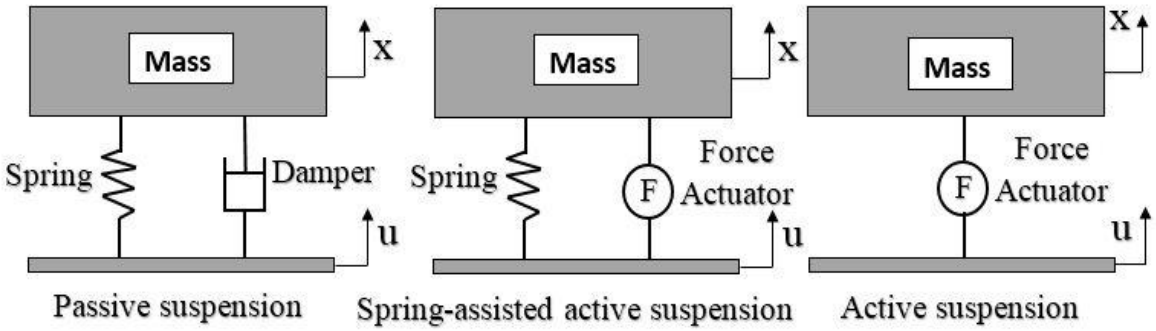

Fig. 1.3: Passive and active suspensions

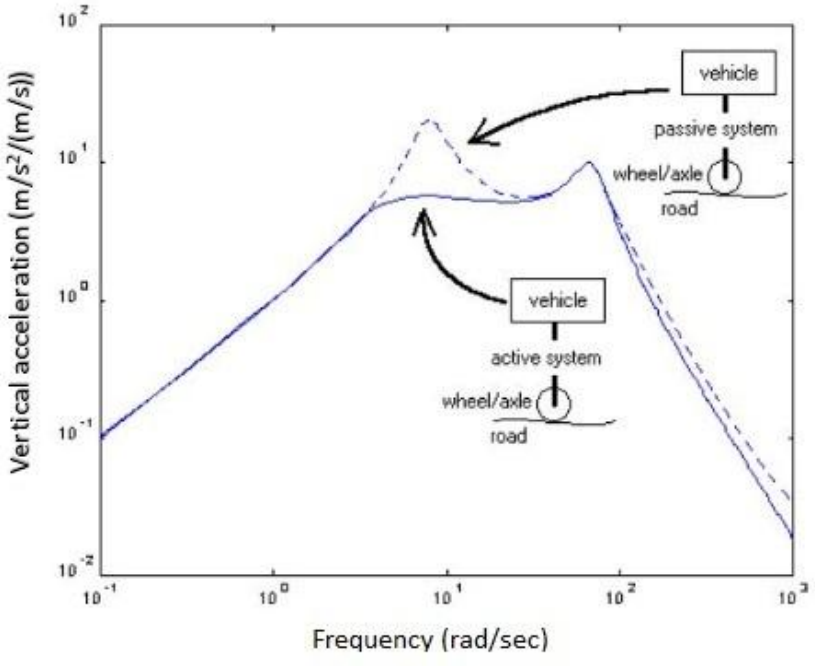

Fig. 1.4: Comparison of passive and active suspensions

Active suspension systems have the added benefit of controlling the attitude of a vehicle. They can reduce the consequences of braking, which makes a vehicle to nose-dive, or acceleration, which compels a vehicle to squat. They also decrease the vehicle roll, when the vehicle is traversing cornering manoeuvres.

Though active suspension systems are capable of improving ride comfort as well as stability, they have some added disadvantages. The force actuators required for an active suspension system generally have large power requirements (typically 4-5 hp). The power requirements reduce the overall efficiency of the vehicle, and are hence usually unacceptable. Moreover, if the actuator fails, the vehicle would be left undamped, and probably unsprung. This is a potentially hazardous situation for both the vehicle and driver.

1.3.3 Semi-active suspension

Semi-active suspensions came into picture in early 1970's. In semi-active suspension system, the conventional spring element is kept, but the damper is substituted with a controllable damper as shown in Fig. 1.5.

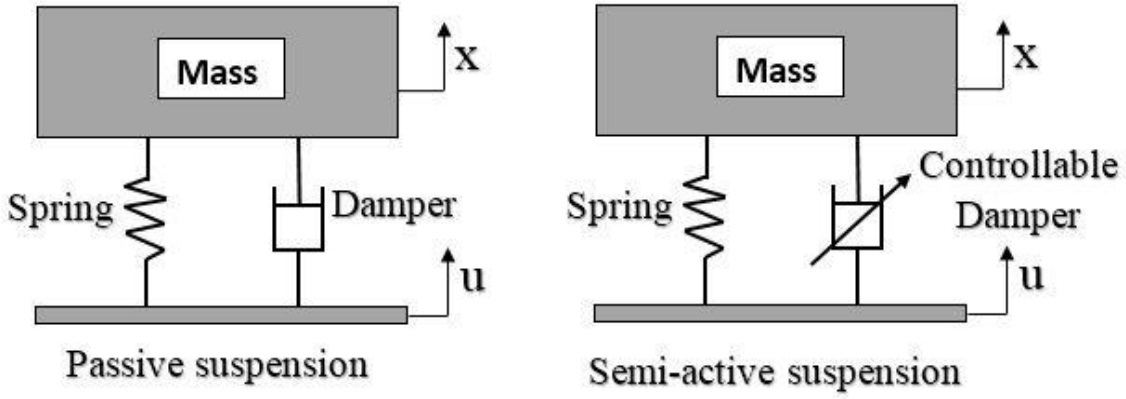

Fig. 1.5: Passive and Semi-active suspensions

A semi-active system uses external power only to regulate the damping levels, and operate an embedded controller and a group of sensors. The controller decides the damping level on the basis of a control strategy, and accordingly adjusts the damper to attain that damping. If the controllable damper required in a semi-active suspension fails, it will simply

turn back to a conventional damper. Semi-active systems not only have a less critical failure mode, but are also less complex, less likely to fail mechanically, and have much lower power requirements as compared to active systems.

1.4 Importance of Suspension System

The ride comfort level and vehicle stability are two of the factors that are of paramount importance in a vehicle's performance evaluation. There are many aspects of a vehicle that regulate these two properties, especially the suspension components, which isolate the vehicle frame from the axle and wheel assemblies. Ideally the suspension should seclude the body from road disturbances and inertial disturbances associated with cornering and braking or acceleration. The suspension must also be able to diminish the vertical force transferred to the passengers for their comfort. In the design of a traditional suspension system there is a compromise between the two factors; ride comfort and vehicle stability. If the design of the suspension is such that it optimizes stability and handling, the driver may find the ride to be a rough and uncomfortable one. On the contrary, if the suspension is designed by keeping passenger comfort in mind, the vehicle may not be very stable during maneuvers.

There are two basic elements in a conventional suspension system - spring and damper. The function of a spring in a vehicle suspension system is to support the static weight of the vehicle. The function of a damper is to dissipate energy and control the road input that is transmitted to the vehicle.

1.5 Literature Review

A review of literature is reported keeping in view the scope and objectives of the project. Therefore, numbers of studies regarding vehicle modeling, semi-active suspension control and hybrid control are presented here.

1.5.1 Vehicle modeling

The dynamic analysis of vehicle requires a mathematical model of the car (quarter/half/full model), suspension and the road excitation. There are various researchers who have studied about quarter/half/full car model.

Optimum design of road-friendly vehicle suspension systems subjected to rough pavement surfaces has been proposed by Lu Sun [5]. Further this work presented an optimum concept to design road-friendly vehicles with the recognition of pavement loads as a primary objective function of vehicle suspension design. Chikhale et al. [6] presented comparative analysis of vehicle suspension system in MATLAB-SIMULINK and MSc- ADAMS with the help of a quarter car model. Vibration analysis was done by giving step input. Xueying et al. [7] presented the study on accurate modeling of suspension based on ADAMS. The torque vibration derived from in-wheel-motor transmits to body frame through suspension system without the absorption of mechanical transmission parts, which influenced the quality of the vehicle and also aimed to build an accurate suspension system model to analyze the vibration transmission property.

Pathare et al. [8] presented design and development of quarter car suspension test rig model and its simulation. He developed a simplified and cost effective setup for testing suspension system. A quarter car setup was made, which was reduced from a full car model, to reduce the complications and cost of development in its design and manufacturing process. Hadi Adibi-asl et al. [9] presented bond graph modeling and simulation of a full car model with active suspension. This paper shows the advantages of the bond graph modeling method to simulate the capability of an active suspension system to enhance ride and handling. The control matrix elements were assigned to scale down the sprung mass acceleration (bounce, roll and pitch) and thus enhance ride comfort as well as road holding. Simulations were carried out using commercial software that permits hybrid bond graph and block diagram models. The construction of model, simulation, design of control strategy and evaluation of performance can be efficiently done in one software environment. The model presented in this paper had specific state equations because the mass velocities and spring deflections are independent. The results demonstrated a significant decline in bounce and pitch acceleration and, also some betterment in roll acceleration of the body for different road profiles. It is found that the bounce acceleration decreases considerably as compared passive suspension, especially at resonance frequency of 2 Hz. Pitch accelerations have also been reduced for lower frequencies whereas, roll accelerations only showed a little improvement.

Silva et al. [10] had discussed bond graph based fault diagnosis of 4w-vehicles suspension systems. He discussed the model-based ARR technique, implemented on diagnostic bond graph, to the problem of detecting and isolating faults in vehicle suspensions. The main contribution was the proposition of simplified diagnostic bond graph that, allow solving a FDI problem on a reduced subsystem decoupled from the wheel dynamics. The simulation results presented illustrate the method ability of monitoring and isolating all the possible suspension faults considered.

1.5.2 Semi-active suspension control

Many researchers have addressed the advantages of semi-active systems over conventional passive systems in many studies. Karnopp et al. [11] investigated the performance of a skyhook controlled semi-active system and compared it with that of a traditional passive system [11,12]. Semi-active systems can provide the versatility, flexibility and higher performance of fully active systems with a miniscule amount of energy while maintaining the reliability of passive systems. Alanoly and Sankar [13,14] studied the balance logic for vibration and shock isolation. Liu et al. [15] studied the "on-off" and "continuous" forms of both skyhook and balance logic and compared it to adaptive passive damping control system. Shamsi and Choupani [16] presented the on-off and continuous skyhook control for half car roll plane model and compared the frequency and transient responses with that of a passive system.

Strecker et al. [17] presented the comparison between three semi-active control algorithms viz. groundhook, skyhook and modified groundhook and passive system. Simulation were conducted for three different response time of magnetorheological (MR) damper; 1.5, 8 and 20ms. The effect of the MR damper response time on the efficiency of semi-active suspension system has been studied. The algorithms are presented below:

Groundhook:

$$F_{gh} = \begin{cases} c_{max}(\dot{x}_1 - \dot{x}_2), & (\dot{x}_2 - \dot{x}_{in})(\dot{x}_1 - \dot{x}_2) < 0 \\ c_{min}(\dot{x}_1 - \dot{x}_2), & (\dot{x}_2 - \dot{x}_{in})(\dot{x}_1 - \dot{x}_2) \geq 0 \end{cases} \tag{1.1}$$

Skyhook:

$$F_{sa} = \begin{cases} c_{max}(\dot{x}_1 - \dot{x}_2), & \dot{x}_1(\dot{x}_1 - \dot{x}_2) \geq 0 \\ c_{min}(\dot{x}_1 - \dot{x}_2), & \dot{x}_1(\dot{x}_1 - \dot{x}_2) < 0 \end{cases} \tag{1.2}$$

Modified Groundhook:

$$F_{ghmod} = \begin{cases} c_{max}(\dot{x}_1 - \dot{x}_2), & \ddot{x}_2(\dot{x}_1 - \dot{x}_2) \geq 0 \\ c_{min}(\dot{x}_1 - \dot{x}_2), & \ddot{x}_2(\dot{x}_1 - \dot{x}_2) < 0 \end{cases} \quad (1.3)$$

Results show that the MR damper with modified groundhook shows better grip for shorter response time of 1.5 ms. If the response time is long (20ms), the comfort level achieved is slightly better than that of a passive system. On the contrary, the influence of response time on the suspension quality is less for the skyhook control strategy. Here, better comfort can be achieved even with longer response time of 20ms. Overall, better performance is shown by the damper with less response time.

Bakar et al. [18] compared skyhook and modified skyhook control algorithms for a validated full car model. The modified skyhook control strategy is adopted to reduce the water hammer effect of the original skyhook control. It includes the effect of both the passive and skyhook dampers. The skyhook logic employed is as given below

$$\begin{aligned} &If\ v_1 v_{12} \geq 0\ then\ F_d = c_{sky} v_1 \\ &If\ v_1 v_{12} < 0\ then\ F_d = 0 \end{aligned} \quad (1.4)$$

where, v_1 is the absolute velocity of the sprung mass, v_{12} is the relative velocity of the sprung mass as compared to the unsprung mass, F_d is the damping force and c_{sky} is the skyhook damping constant. The modified skyhook logic used includes both the passive damper and the skyhook damper. The logic is given by

$$F_d = c_{ms}\left[\alpha\left(\dot{Z}_u - \dot{Z}_s\right) + (1-\alpha)\dot{Z}_s\right] \quad (1.5)$$

where, c_{ms} is the modified skyhook damping, α is the passive to skyhook ratio, $\dot{Z}_u$ and $\dot{Z}_s$ are the unsprung body velocity and the sprung body velocity respectively. In general, the semi-active system performance is better than that of a conventional system. However, the semi-active system performance is dependent on the control algorithm used. The results have shown that for random road input, the overall performance of the skyhook logic is better than that of modified skyhook by 3.2%. The modified skyhook performs better in case of vertical and roll motion though.

Zhang et al. [19] examined the skyhook based semi-active control of full vehicle suspension system incorporated with MR damper. A 7-DOF full vehicle dynamic model is set up by using the modified Bouc-wen hysteretic model of MR damper and a modified skyhook

control is proposed to individually control the four MR quarter vehicle sub-systems of the full vehicle. The modified skyhook control proposed is as given below:

$$i_{di} = \begin{cases} k_d|\dot{x}_{si}|^m, & \dot{x}_{si}(\dot{x}_{si} - \dot{x}_{ui}) > 0, \\ 0, & \dot{x}_{si}(\dot{x}_{si} - \dot{x}_{ui}) \leq 0, \end{cases} \quad i = 1, 2, 3, 4, \tag{1.6}$$

where i_{di} are controlled driver currents for four MR dampers, k_d is the controller gain, $m(m \geq 0)$ represents the controller order. $\dot{x}_{si}$ and $\dot{x}_{ui}$ are velocities of sprung and unsprung masses of the four quarter car sub-suspensions. Controller parameters are taken as $m = 2$ and $k_d = 3$. The vertical motion characteristics have been inspected using harmonic excitations with delay time. The results show that the peak value of the vehicle body acceleration decreases by 30% for the suspension incorporated with MR damper in comparison with passive system. However, the unsprung mass acceleration shows abrupt responses. The pitch angular acceleration and the roll angular acceleration are found to be less in the semi-active MR suspension system. The vehicle dynamic model was also subjected to rounded pulse excitations to assess the vibration diminishment performance of the suspension system. Results exhibit that the performance of the MR suspension is better than that of a passive system in terms of shock diminishment whereas, road handling and ride comfort have been slightly compromised. In case of random road inputs, the semi-active MR suspension has potential of resonance attenuation for low frequency range (0.5-2.0Hz).

Ikhwan et al. [20] studied the skyhook logic for a 7-DOF ride model of an armored vehicle. The skyhook controller proposed by them consists of an outer loop and an inner loop. The purpose of the outer loop is to control the body acceleration, pitch acceleration and roll accelerations due to road excitations whereas, the inner loop controls the damping characteristics. The outer loop utilizes PID control while the inner loop uses skyhook logic to control the damping force. The semi-active damping force is given by

$$F_{sa} = -c_{sa}(\dot{x}_2 - \dot{x}_1) = -c_{sky}\dot{x}_1 \tag{1.7}$$

where, F_{sa} is the damping force, c_{sa} is the semi-active damping coefficient, c_{sky} is the skyhook damping coefficient, $\dot{x}_1$ is the velocity of the sprung mass and $\dot{x}_2$ is the velocity of the unsprung mass. High mobility multipurpose wheeled vehicle (HMMWV) is considered as the paper focuses on armored vehicles. The simulation results show that the body acceleration, pitch acceleration and roll acceleration have been significantly reduced by the proposed skyhook

control as compared to PID control of semi-active system or passive suspension. This will in turn improve the comfort level and the ride performance of the armored vehicle.

Anand Raj et al. [21] adopted a fuzzy logic controller based on skyhook logic to control a semi-active suspension system. The fuzzy logic, which is a multi-valued logic was introduced in 1965 by Lotfi Zadeh. The fuzzy controller based on skyhook logic is supposed to operate between a high damping state and a low damping state. There are two inputs to the system, viz. velocity of sprung mass and relative velocity. The output is the damping coefficient of the semi-active damper. The linguistic variables for input are Negative Big (NB), Negative Small (NS), Zero (Z), Positive Small (PS) and Positive Big (PB). The outputs are LV (Large Value), L_{AVG} (Large Average), L (Large), M (Medium), S (Small), S_{AVG} (Small Average) and SS (Small Small). The rules are defined by the Rule Matrix as shown in Table 1.1.

A PID controller was also embedded with the fuzzy logic, which will give better ride comfort by smoothing the velocity and the displacement. A sinusoidal road input was provided into the system to evaluate the performance. The results show considerable improvement in case of semi-active suspension using continuous skyhook, fuzzy logic based on skyhook control and fuzzy PID as compared to on-off skyhook or passive system. The fuzzy controller embedded with continuous skyhook logic shows better performance in terms of displacement of sprung mass and sprung mass acceleration than simple on-off skyhook or continuous skyhook. However, inclusion of PID with fuzzy gives better ride comfort by smoothing the velocity.

Table 1.1: Rule Matrix

	Velocity					
Relative Velocity		NB	NS	Z	PS	PB
	NB	LV	L_{AVG}	M	S_{AVG}	SS
	NS	L_{AVG}	L	M	S	S_{AVG}
	Z	M	M	S	M	M
	PS	S_{AVG}	S	M	L	L_{AVG}
	PB	SS	S_{AVG}	M	L_{AVG}	LV

1.5.3 Hybrid control strategies

Strydom et al. [22] investigated the applicability of hybrid control to a small off-road vehicle. The suspension system consists of controllable dampers and passive spring-damper units. Skyhook and groundhook control is used to control the nonlinear, three-dimensional, 12-DOF dynamic model. The skyhook control provides reduced vehicle body motion, thus improving ride comfort at the expense of unsprung mass motion. On the contrary, groundhook control results in decreased unsprung mass motion, thus better road handling at the expense of ride comfort. A hybrid control has been adapted by Strydom, et al. to incorporate the relative velocity over the damper, which is given by

$$\begin{aligned} \dot{Z}_s\dot{x}_{cl} > 0: &\quad \sigma_{sky} = \dot{Z}_s \\ \dot{Z}_s\dot{x}_{cl} \leq 0: &\quad \sigma_{sky} = 0 \\ \dot{Z}_u\dot{x}_{cl} < 0: &\quad \sigma_{gnd} = -\dot{Z}_u \\ \dot{Z}_u\dot{x}_{cl} \geq 0: &\quad \sigma_{gnd} = 0 \end{aligned} \tag{1.8}$$

where, $\dot{Z}_s$ is the sprung mass velocity, $\dot{Z}_u$ is the unsprung mass velocity, $\dot{x}_{cl}$ is the relative velocity across the damper, σ_{sky} and σ_{gnd} are the skyhook and groundhook control inputs to the semi-active force, $F_{SA,z}$, which is given by

$$F_{SA,z} = G\left[a\sigma_{sky} + (1-a)\sigma_{gnd}\right] \tag{1.9}$$

where, G is the controller gain and a is the skyhook to groundhook ratio. The ride comfort evaluation shows that improvement can be achieved by implementation of skyhook logic with a control gain of 1200Ns/m. The groundhook logic is capable of diminishing the vertical acceleration of the wheels. In case of road holding, an uncontrolled system with low damping gives the best results. The skyhook control system incorporated with passive suspension lessens the roll motion and improves road-tire contact. However, for a vehicle system with more degrees of freedom, the groundhook logic was found to be less effective despite the fact that its primary objective is to reduce wheel hop and increase road holding.

Kashem et al. [23] introduced a modified continuous skyhook strategy along with adaptive gain that directs the semi-active vehicle suspension. They have scrutinized 11 sets of suspension parameters and considered a set of parameters that demonstrated better performance in terms of peak amplitude and settling time. The proposed system first

apprehends the road input and determines the best value of skyhook gain (SG). In the meantime, the system is controlled by the new skyhook algorithm as given below,

$$f_d = \begin{cases} C_{max}(\dot{z}_2 - \dot{z}_1), & if\ \dfrac{\dot{z}_2}{(\dot{z}_2 - \dot{z}_1)} \geq \dfrac{C_{sky}}{C_{max}} \\ C_{sky}\dot{z}_2, & if\ \dfrac{C_{sky}}{C_{max}} > \dfrac{\dot{z}_2}{(\dot{z}_2 - \dot{z}_1)} > \dfrac{C_{sky}}{C_{min}} \\ C_{min}(\dot{z}_2 - \dot{z}_1), & otherwise \end{cases} \quad (1.10)$$

where, C_{max} and C_{min} are the maximum and the minimum damping coefficients of the semi-active damper. C_{sky} is the skyhook damping constant and varied corresponding to the road input. $\dot{z}_2$ and $\dot{z}_1$ are the velocities of the sprung and the unsprung masses. A comparison of the above control strategy is made with three skyhook control strategies proposed by Karnopp et al. [11]; Bessinger et al. [24]; and Nguyen et al. [25] respectively. Ride comfort has been found to be enhanced by 38.4% for the modified skyhook logic by Kashem et al. as compared to a passive system, whereas improvements of 27.3% for optimal skyhook control by Nguyen, et al.; 2.8% for modified skyhook control by Bessinger et al. and 5.9% for continuous skyhook control by Karnopp et al. have been observed. Moreover, the proposed modified skyhook control system provides superior ride comfort as compared to passive or any of the skyhook control considered.

Espinoza et al. [26] has studied three hybrid control strategies for semi-active suspension system viz., hybrid Sky Hook-Ground Hook, hybrid Mix-1-Sensor and Frequency Estimation-Based controller. A commercial magneto-rheological damper was designed by using an artificial neural network (ANN) approach. The automotive semi-active suspension was appointed in a commercial controller area network (CAN) system; and the control logics were enforced in a micro-controller system with the goals to optimize comfort and road holding. Results show the usefulness of this approach in commercial utilization. All control algorithms have better results than the default solutions. Using the pseudo-Bode diagrams hybrid solutions exhibit good results in both frequencies range of interest (comfort and road holding); these results were also validated with the RMS index.

1.6 Research Gap Identification

After going through the literature review, it can be summarized that lots of the work has been done on suspension systems. Several researchers have worked on semi-active suspension

system and passive suspension system. Different semi-active control strategies have been studied through different practical method and software like MATLAB/Simulink® etc. Comparison of different semi-active control policies with passive suspension has also been done. It has been observed that very limited studies are developed computational model of suspension controller through Bond graph modeling. Although different studies have been done on bond graph modeling of vehicle systems, incorporation of semi-active control strategies in bond graph modeling is a research area still to be explored. Moreover, hybrid combination of skyhook and groundhook control logics have been studied by many researchers. But combination of other control logics for the formulation of different hybrid control logics have not gained popularity.

1.7 Objectives of the Research

The research objectives are as follows:

- To create computational model of a quarter car and a half car model of vehicle through bond graph as well MATLAB/Simulink®.
- To incorporate different semi-active control strategies and hybrid control logics for control of the vehicle suspension model.
- Simulation of the bond graph and Simulink models for variable parameters to obtain performance of vehicle for different semi-active control strategies.
- Comparison of performance of the different control strategies for semi-active suspension for quarter car and half car as well as comparison with a passive suspension system.
- Validation of results and performance evaluation of different semi-active control algorithms.

1.8 Organization of Thesis

The chapters of the thesis are arranged in the following manner. *Chapter one* presents the background of this project along with a summary of the literature review. The primary aim of this chapter is to provide the reader with a basic idea of the work presented in the thesis. *Chapter two* demonstrates the mathematical modeling of the various vehicle models (quarter/half). *Chapter three* describes the computational modeling of the vehicle models in bond graph and Simulink software environment. *Chapter four* depicts different control

strategies for the control of semi-active suspension system of a vehicle. *Chapter five* presents the simulation study where the numerical parameters and road profile inputs are illustrated. *Chapter six* provides the results obtained by the simulation study and discusses the performance of different semi-active vehicle models. Finally, *Chapter seven* concludes the thesis and provides suggestions for future work.

CHAPTER 2

MODEL FORMULATION: MATHEMATICAL MODEL

2.1 Introduction

The road vehicle models considered in this work are a 2-DOF quarter car model and a 4-DOF half car model. The chapter presents the mathematical modelling of the quarter car model and the half car model. Vertical translation and rotation (in case of a half car model) about transverse axis have been included for vehicle body.

2.2 Mathematical Model of 2-DOF Quarter Car with Passive Suspension

The model in Fig. 2.1 consists of two masses. The top mass M_s represents the vehicle body whereas the bottom mass M_u represents the wheel. The parallel spring and damper combinations placed in between the vehicle body and the tire represent the stiffness (k_s) and damping (c_d) of the suspension system. The tire stiffness is shown by the spring k_t. x_1, x_2 and x_{in} are the vehicle displacement, wheel displacement and the road input to the quarter car model.

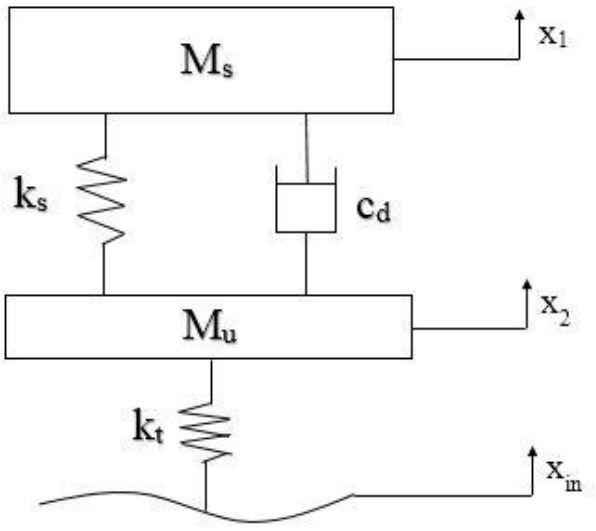

Fig. 2.1: 2-DOF quarter car model with passive suspension

According to Newton's law, the governing equation of the system can be represented as

$$M_s\ddot{x}_1 + k_s(x_1 - x_2) + c_d(\dot{x}_1 - \dot{x}_2) = 0 \quad (2.1)$$

$$M_u\ddot{x}_2 - k_s(x_1 - x_2) - c_d(\dot{x}_1 - \dot{x}_2) + k_t(x_2 - x_{in}) = 0 \quad (2.2)$$

The same can be represented in the matrix form as:

$$\begin{bmatrix} M_s & 0 \\ 0 & M_u \end{bmatrix}\begin{Bmatrix} \ddot{x}_1 \\ \ddot{x}_2 \end{Bmatrix} + \begin{bmatrix} c_d & -c_d \\ -c_d & c_d \end{bmatrix}\begin{Bmatrix} \dot{x}_1 \\ \dot{x}_2 \end{Bmatrix} + \begin{bmatrix} k_s & -k_s & 0 \\ -k_s & k_s + k_t & -k_t \end{bmatrix}\begin{Bmatrix} x_1 \\ x_2 \\ x_{in} \end{Bmatrix} = 0 \quad (2.3)$$

2.3 Mathematical Model of 2-DOF Quarter Car with Semi-Active Suspension

The model for 2-DOF quarter vehicle with semi-active suspension is as shown in Fig. 2.2. The mass M_s represents the vehicle body; the mass M_u represents the wheel. The parallel spring and damper combinations placed in between the vehicle body and the wheel (k_s and c_d) represent the stiffness and damping of the suspension system. The damper used in this case is a controllable damper which is necessary for a semi-active suspension. A controller is incorporated which regulates an actuator which in turn, controls the damping level of the controllable damper. The tire stiffness is shown by the spring k_t. x_1, x_2 and x_{in} are the vehicle displacement, wheel displacement and the road input to the quarter car model.

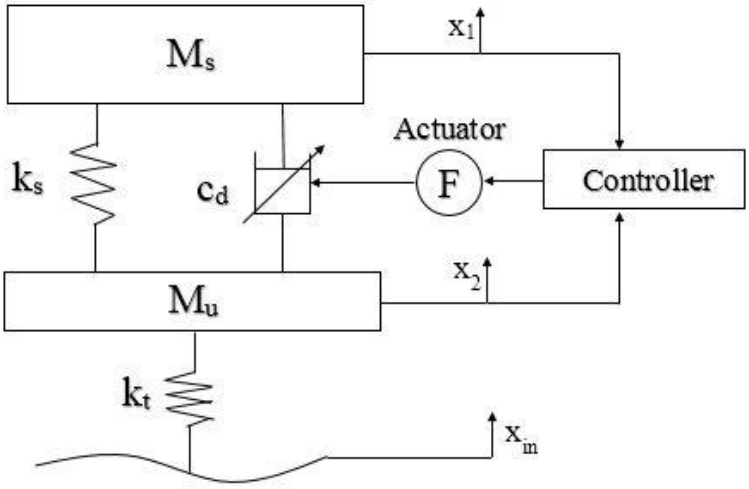

Fig. 2.2: 2-DOF quarter car model with controllable damper

Now, for the semi-active suspension system, the governing equations can be represented as,

$$M_s\ddot{x}_1 + k_s(x_1 - x_2) + F_d = 0 \tag{2.4}$$

$$M_u\ddot{x}_2 - k_s(x_1 - x_2) - F_d + k_t(x_2 - x_{in}) = 0 \tag{2.5}$$

where, F_d represents the damping force of the controllable damper which can be regulated by controlling the value of the damping coefficient, and given as;

$$F_d = c_d(\dot{x}_1 - \dot{x}_2) \tag{2.6}$$

The state-space representation for the same can be given by the following equations,

$$\begin{bmatrix} M_s & 0 \\ 0 & M_u \end{bmatrix}\begin{Bmatrix} \ddot{x}_1 \\ \ddot{x}_2 \end{Bmatrix} + \begin{bmatrix} 1 \\ -1 \end{bmatrix}\{F_d\}\begin{bmatrix} k_s & -k_s & 0 \\ -k_s & k_s + k_t & -k_t \end{bmatrix}\begin{Bmatrix} x_1 \\ x_2 \\ x_{in} \end{Bmatrix} = 0 \tag{2.7}$$

2.4 Mathematical Model of 4-DOF Half Car with Passive Suspension

Similarly, a 4-DOF half vehicle model is also considered to evaluate the vehicle performance, which is shown in Fig. 2.2. Here M_s is the vehicle body mass $M_{u,f}$ is the unsprung mass or wheel mass of front suspension and $M_{u,r}$ is the same for rear suspension. $k_{s,f}$ and $k_{s,r}$ are the stiffnesses of the front and rear suspensions; $c_{d,f}$ and $c_{d,r}$ are the damping coefficients of the front and rear suspensions and $k_{t,l}$ and $k_{t,r}$ are the stiffnesses of the front and the rear tires respectively. x_1 and θ_1 represent the heave and pitch motions of vehicle body; $x_{2,f}$ and $x_{2,r}$ represent the heave motions of the front and the rear wheels; $x_{in,l}$ and $x_{in,r}$ represent the road inputs to the front and the rear tires of the system.

The dynamics of the model in Fig. 2.3 are described by:

$$\begin{aligned} M_s\ddot{x}_1 + c_{d,f}\left(\dot{x}_1 - \dot{x}_{2,f} - d_a\dot{\theta}_1\right) + c_{d,r}\left(\dot{x}_1 - \dot{x}_{2,r} + d_b\dot{\theta}_1\right) \\ + k_{s,f}\left(x_1 - x_{2,f} - d_a\theta_1\right) + k_{s,r}\left(x_1 - x_{2,r} + d_b\theta_1\right) = 0 \end{aligned} \tag{2.8}$$

$$\begin{aligned} I_{yy}\ddot{\theta}_1 - d_a c_{d,f}\left(\dot{x}_1 - \dot{x}_{2,f} - d_a\dot{\theta}_1\right) + d_b c_{d,r}\left(\dot{x}_1 - \dot{x}_{2,r} + d_b\dot{\theta}_1\right) \\ - d_a k_{s,f}\left(x_1 - x_{2,f} - d_a\theta_1\right) + d_b k_{s,r}\left(x_1 - x_{2,r} + d_b\theta_1\right) = 0 \end{aligned} \tag{2.9}$$

$$\begin{aligned} M_{u,f}\ddot{x}_{2,f} - c_{d,f}\left(\dot{x}_1 - \dot{x}_{2,f} - d_a\dot{\theta}_1\right) - k_{s,f}\left(x_1 - x_{2,f} - d_a\theta_1\right) \\ + k_{t,f}\left(x_{2,f} - x_{in,f}\right) = 0 \end{aligned} \tag{2.10}$$

$$\begin{aligned} M_{u,f}\ddot{x}_{2,f} - c_{d,f}\left(\dot{x}_1 - \dot{x}_{2,f} - d_a\dot{\theta}_1\right) - k_{s,f}\left(x_1 - x_{2,f} - d_a\theta_1\right) \\ + k_{t,f}\left(x_{2,f} - x_{in,f}\right) = 0 \end{aligned} \tag{2.11}$$

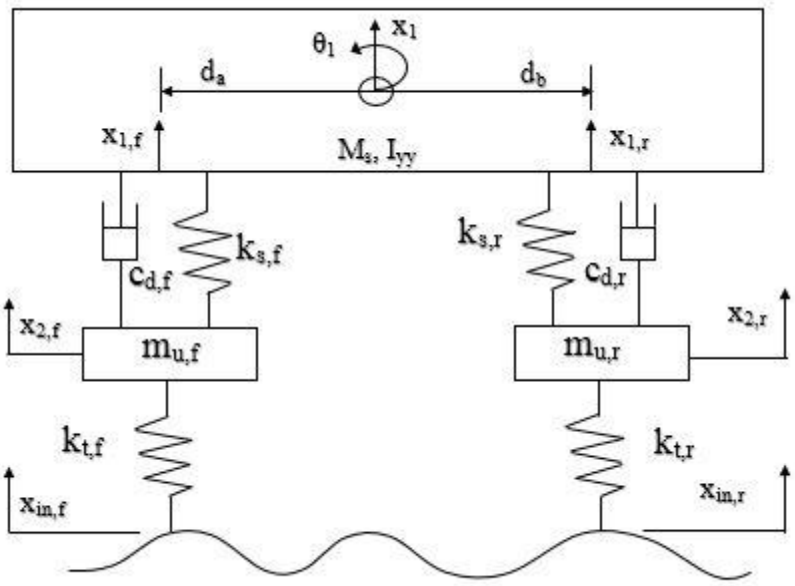

Fig. 2.3: 4-DOF half car model with passive suspension

The equations (2.8) to (2.11) can be represented in matrix form as:

$$M\,\ddot{x} + C\,\dot{x} + K\,x = f \tag{2.12}$$

where, M, C and K represent the mass, damping and stiffness matrices and f is the force vector, represented by:

$$M = diagonal\left[M_s, I_{yy}, M_{u,f}, M_{u,r}\right] \tag{2.13}$$

$$C = \begin{bmatrix} (c_{d,f} + c_{d,r}) & -c_{d,f} & -c_{d,r} & (-c_{d,f}d_a + c_{d,r}d_b) \\ (-c_{d,f}d_a + c_{d,r}d_b) & c_{d,f}d_a & -c_{d,r}d_b & (c_{d,f}d_a^2 + c_{d,r}d_b^2) \\ -c_{d,f} & c_{d,f} & 0 & c_{d,f}d_a \\ -c_{d,r} & 0 & c_{d,r} & -c_{d,r}d_b \end{bmatrix} \tag{2.14}$$

$$K = \begin{bmatrix} (k_{s,f} + k_{s,r}) & -k_{s,f} & -k_{s,r} & (-k_{s,f}d_a + k_{s,r}d_b) \\ (-k_{s,f}d_a + k_{s,r}d_b) & k_{s,f}d_a & -k_{s,r}d_b & (k_{s,f}d_a^2 + k_{s,r}d_b^2) \\ -k_{s,f} & (k_{s,f} + k_{t,f}) & 0 & k_{s,f}d_a \\ -k_{s,r} & 0 & (k_{s,r} + k_{t,r}) & -k_{s,r}d_b \end{bmatrix} \tag{2.15}$$

$$f = \begin{bmatrix} 0 \\ 0 \\ k_{t,f}x_{in,f} \\ k_{t,r}x_{in,r} \end{bmatrix} \tag{2.16}$$

2.5 Mathematical Model of 4-DOF Half Car with Semi-Active Suspension

A 4-DOF half vehicle model with semi-active dampers is shown in Fig. 2.4, where M_s is the vehicle body mass, $M_{u,f}$ is the unsprung mass or wheel mass of front suspension and $M_{u,r}$ is the same for rear suspension. $k_{s,f}$ and $k_{s,r}$ are the stiffnesses of the front and rear suspensions; $c_{d,f}$ and $c_{d,r}$ are the damping coefficients of the front and rear suspension controllable dampers and $k_{t,l}$ and $k_{t,r}$ are the stiffnesses of the front and the rear tires respectively. x_1 and θ_1 represent the heave and pitch motions of vehicle body; $x_{2,f}$ and $x_{2,r}$ represent the heave motions of the front and the rear wheels; $x_{in,l}$ and $x_{in,r}$ represent the road inputs to the front and the rear tires of the system.

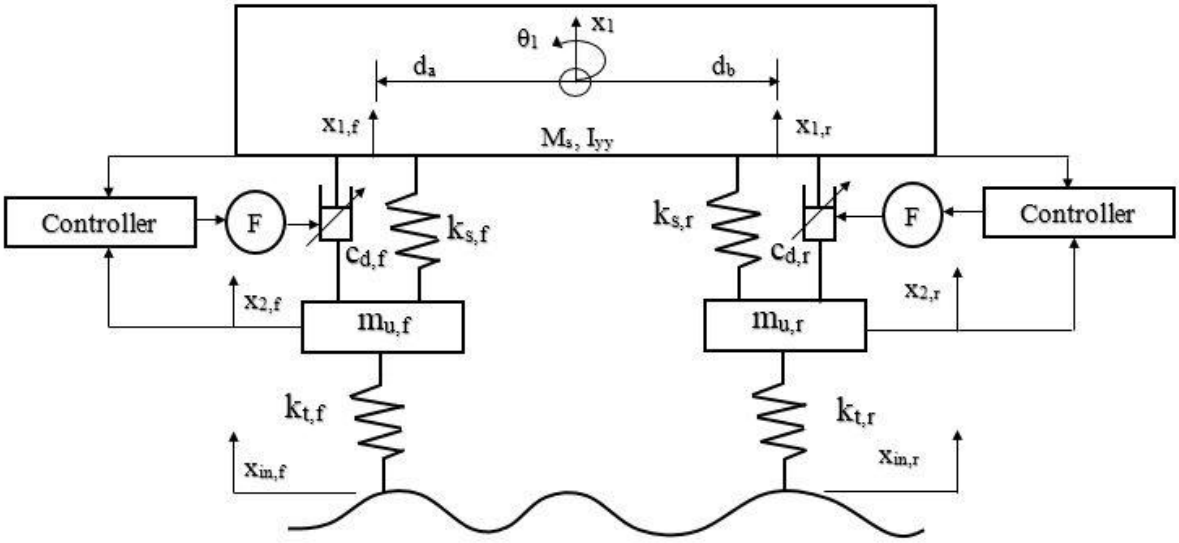

Fig. 2.4: 4-DOF half vehicle model with controllable damper

The dynamics of the model in Fig. 2.3 are described by:

$$M_s\ddot{x}_1 + F_{d,f} + F_{d,r} + k_{s,f}(x_1 - x_{2,f} - d_a\theta_1) + k_{s,r}(x_1 - x_{2,r} + d_b\theta_1) = 0 \tag{2.17}$$

$$I_{yy}\ddot{\theta}_1 - d_a F_{d,f} + d_b F_{d,r} - d_a k_{s,f}\left(x_1 - x_{2,f} - d_a\theta_1\right) + d_b k_{s,r}\left(x_1 - x_{2,r} + d_b\theta_1\right) = 0 \quad (2.18)$$

$$M_{u,f}\ddot{x}_{2,f} - F_{d,f} - k_{s,f}\left(x_1 - x_{2,f} - d_a\theta_1\right) + k_{t,f}\left(x_{2,f} - x_{in,f}\right) = 0 \quad (2.19)$$

$$M_{u,r}\ddot{x}_{2,r} - F_{d,r} - k_{s,r}\left(x_1 - x_{2,r} + d_b\theta_1\right) + k_{t,r}\left(x_{2,r} - x_{in,r}\right) = 0 \quad (2.20)$$

where, $F_{d,f}$and $F_{d,r}$ are the damping force of the controllable damper and can be given as,

$$F_{d,f} = c_{d,f}(\dot{x}_1 - \dot{x}_{2,f} - d_a\dot{\theta}_1) \quad (2.21)$$

$$F_{d,r} = c_{d,r}(\dot{x}_1 - \dot{x}_{2,r} + d_b\dot{\theta}_1) \quad (2.22)$$

The damping force can be controlled by controlling the damping coefficient of the semi-active damper with a suitable control strategy.

2.6 Summary of the chapter

In this chapter, mathematical models of 2-DOF quarter car model and 4-DOF half car model have been presented. Next chapter will present the computational model of the 2-DOF quarter vehicle and 4-DOF half vehicle using bond graph and Simulink module of MATLAB®.

CHAPTER 3

MODEL FORMULATION: COMPUTATIONAL MODEL

3.1 Introduction

In this chapter, computational model of the 2-DOF quarter car and 4-DOF half car model has been developed with the help of bond graph and Simulink module of MATLAB®.

3.2 Vehicle Modeling

In this section, quarter vehicle model and half vehicle model are considered. These models are equipped with semi-active suspensions to improve ride comfort and vibration isolation. Semi-active suspension is concerned with controlling the vertical movements of the vehicle in response to the road inputs to each of the wheels. This is achieved by controlling the damping force by adjusting the damping coefficient to counteract some of the effects of the road surface. As a result, the systems can be used to minimize vehicle vibrations and accelerations experienced by the passengers, and improve overall vehicle handling.

3.2.1 Modeling assumptions

The model of the vehicle is created with the following assumptions:

- The components of the vehicle body act as a rigid body.
- The springs and dampers of the suspension system elements have linear characteristics.
- The spring damper system is assumed to be mass less.
- The tire is assumed to provide stiffness and thus modeled as a spring.
- The vehicle is moving with constant velocity.
- The positions of the two ends of the spring connecting two rigid bodies or connecting one rigid body and one contact point are required as input data.
- Each rigid body is connected to each other by spring-damper system.
- Straight road is assumed.
- Bump type surface irregularity and random road inputs are assumed.

3.2.2 Vehicle structure

In this research, the body and base frame of the vehicle are treated as rigid bodies. The body (sprung mass) is modeled as the rigid body having a mass M_s with vertical movements (x_1) in case of quarter vehicle as shown in Fig. 2.2 (Chapter 2) or vertical (x_1) as well as pitching motion (θ_1) in case of half vehicle model as shown in Fig. 2.4 (Chapter 2). The spring and damper in the suspension system are characterized by the spring stiffness k_s and damping coefficient c_d respectively. The various displacements of the vehicle are described with respect to the equilibrium positions. As the vehicle is assumed to be rigid, thus its motion can be described by the vertical displacement (bounce or x_1) and the rotation about the transverse horizontal axis (pitch or θ_1) in case of half car only.

3.2.3 Detailed description of elements of suspension system

Suspension system can be teared down to the following parts, i) mass, ii) spring, and iii) damper. The next subsection will highlight these in details:

3.2.3.1 Mass

Mass of a vehicle is subdivided into two parts- a) sprung mass, and b) unsprung mass.

a) Sprung mass

Sprung mass is the portion of the vehicle's total mass that is supported above the suspension which also includes half of the weight of the suspension itself. Sprung weight typically includes the internal components, body, cargo, frame and passengers; but not the mass of the components that are suspended below the suspension components including the wheel bearings, wheels, calipers, brake rotors and continuous tracks (also called caterpillar tracks), if any.

b) Unsprung mass

Most of the vehicle's weight is supported by its suspension system, which suspends the body and associated parts so that they are insulated from vibrations and road shocks that would otherwise be transmitted to the vehicle and the passengers. However, the other parts of vehicle are not supported by the suspension system, such as tires, steering, brakes and suspension parts.

All these parts are called unsprung weight, which should be kept as low as possible in most of the applications.

3.2.3.3 Spring

Spring is an elastic object used to store mechanical energy, which is usually made of spring steel. Large springs are made from annealed steel and hardened after fabrication, whereas small springs can directly be wound from pre-hardened stock. Some non-ferrous metals are also used including titanium and phosphor bronze for springs requiring corrosion resistance and beryllium copper for the springs carrying electrical current (because of spring low electrical resistance).

When a spring is stretched or compressed, then the exerted force is proportional to its change in length. The rate or spring constant of a spring is the change in the force it exerts, which may be divided by the change in the deflection of spring. Basically, it is the gradient of force versus deflection curve. A compression or extension spring has unit of force divided by distance, for example N/m or lbf/in. Torsion springs has unit of force multiplied by distance divided by angle, for example ft·lbf/degree or N·m/rad. Inverse of spring rate is compliance, i.e. if the spring has a rate of 10 N/mm, then it has a compliance of 0.1 mm/N. The stiffness or rate of springs in parallel is additive, whereas the compliance of springs in series.

3.2.3.4 Damper

It is a mechanical device designed to smooth out or damp shock impulse, and dissipate kinetic energy. In a vehicle, it reduces the effect of traveling over rough ground leading to improved ride quality and increase in comfort. While it serves the purpose of limiting excessive suspension movement and their intended sole purpose is to dampen spring oscillations. It uses valving of oil and gasses to absorb excess energy from the springs. Spring rates are chosen by the manufacturer based on the weight of the vehicle, loaded and unloaded. Some people use shocks to modify spring rates but this is not the correct use. Along with hysteresis in the tire itself, they dampen the energy stored in the motion of the unsprung weight up and down. Effective wheel bounce damping may require tuning shocks to an optimal resistance. Spring-based dampers commonly use coil springs or leaf springs, whereas torsion bars are used in

torsional shocks as well. Ideal springs alone, however, are not dampers, as springs only store and do not dissipate or absorb energy in any form.

3.3 Dynamic Model of Road Vehicle

Dynamic models of quarter and half car are shown in Fig. 3.1 and Fig. 3.2.

3.3.1 Quarter vehicle model

This model consists of a single wheel and is a 2-DOF model. The labeled diagram is shown in Fig. 3.1.

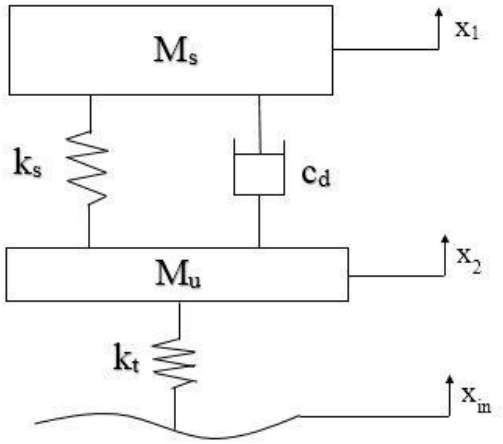

Fig. 3.1: Schematic diagram of quarter vehicle

3.3.2 Half car model

The vehicle model includes a suspension unit on both side of the vehicle, which consists of spring, controllable damper and controller unit as shown in Fig. 3.2. The body has mass M_s, and moments of inertia I_{yy} (pitch) about the transverse axis. The CG is located a distance 'd_a' from the front axle, 'd_b' from the rear axle. The suspension system has semi-active dampers implemented with controllable damping coefficient inputs to control the damping force. This will allow more flexibility once the control system has been designed for selecting the most appropriate damping coefficient.

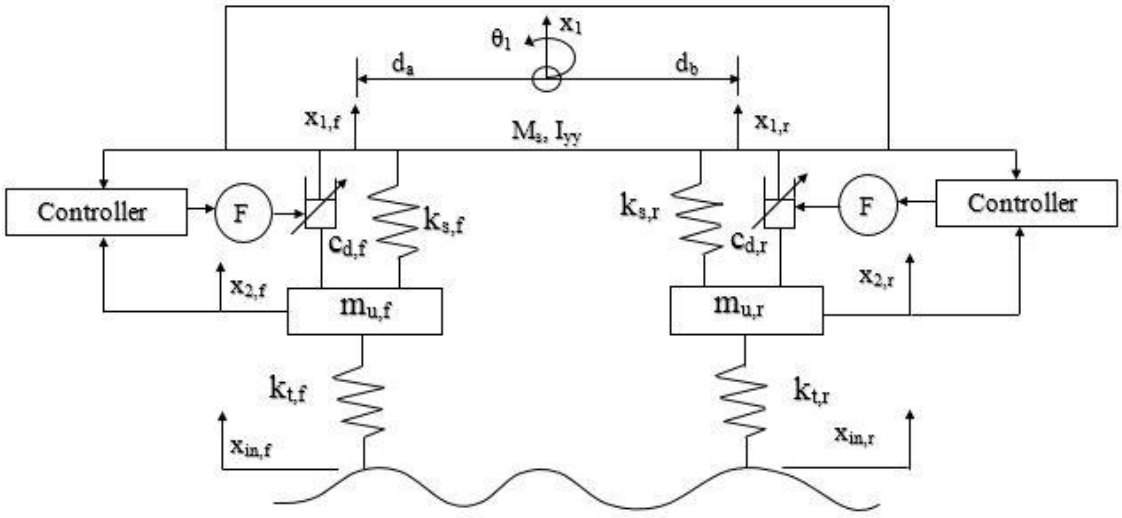

Fig. 3.2: Schematic diagram of half car model

3.4 Bond Graph Modeling

A road vehicle system comprises of different components such as sprung mass, springs, dampers, wheels or unspring mass and tires. When dynamic systems are put together from these components, one must interconnect translating and rotating inertial elements with axial and rotational springs, dampers and also suitably account for the kinematics of the system structure. Bond graphs are appropriate for this task.

Modeling the mentioned system started with the development of the "bond graph" of the system. Bond graphs are a brief pictorial representation of all types of interacting energy domains. It is an exceptional tool for representing vehicle dynamics with associated control hardware. Each bond portrays a pair of signals (effort and flow), the product of which gives the instantaneous power of the bond. In case of mechanical systems, effort transforms into force and flow transforms into velocity. The "half arrow" sign convention represents the direction of flow of energy. The energy storing elements of the system determine the number of state variables and using conventional methods in bond graph, state equations can directly be derived.

3.4.1 Bond graph model for 2-DOF quarter vehicle

Whole bond graph is divided into two parts- sprung and unsprung. M_s, k_s and c_d are the inertia, stiffness and resistance of sprung parts whereas M_u and k_t represent the inertia and stiffness of unsprung parts. SF is the source of flow which corresponds to the vertical velocity incurred to the tire due to road unevenness. The bond graph of the 2-DOF quarter vehicle is shown in Fig. 3.3.

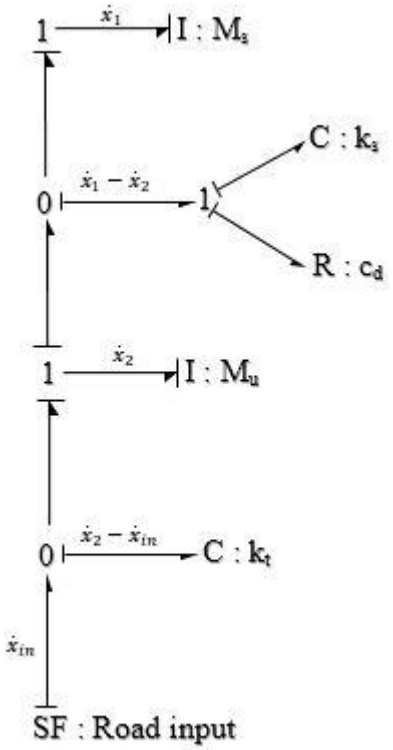

Fig. 3.3: Bond graph model of a 2-DOF quarter vehicle

3.4.2 Bond graph model of 4-DOF half vehicle

Similar to quarter vehicle model's nomenclature, a half car model can also be developed. The only difference is that in case of half car, there will be two wheels and so every part will be two times. M_s represents the mass of the half car whereas, I_{yy} represents the moment of inertia about transverse axis due to pitch motion of the vehicle. TF (transformers) is used for showing the distance from particular point. The remaining nomenclature is similar to quarter vehicle. The bond graph model for half car is shown in Fig. 3.4.

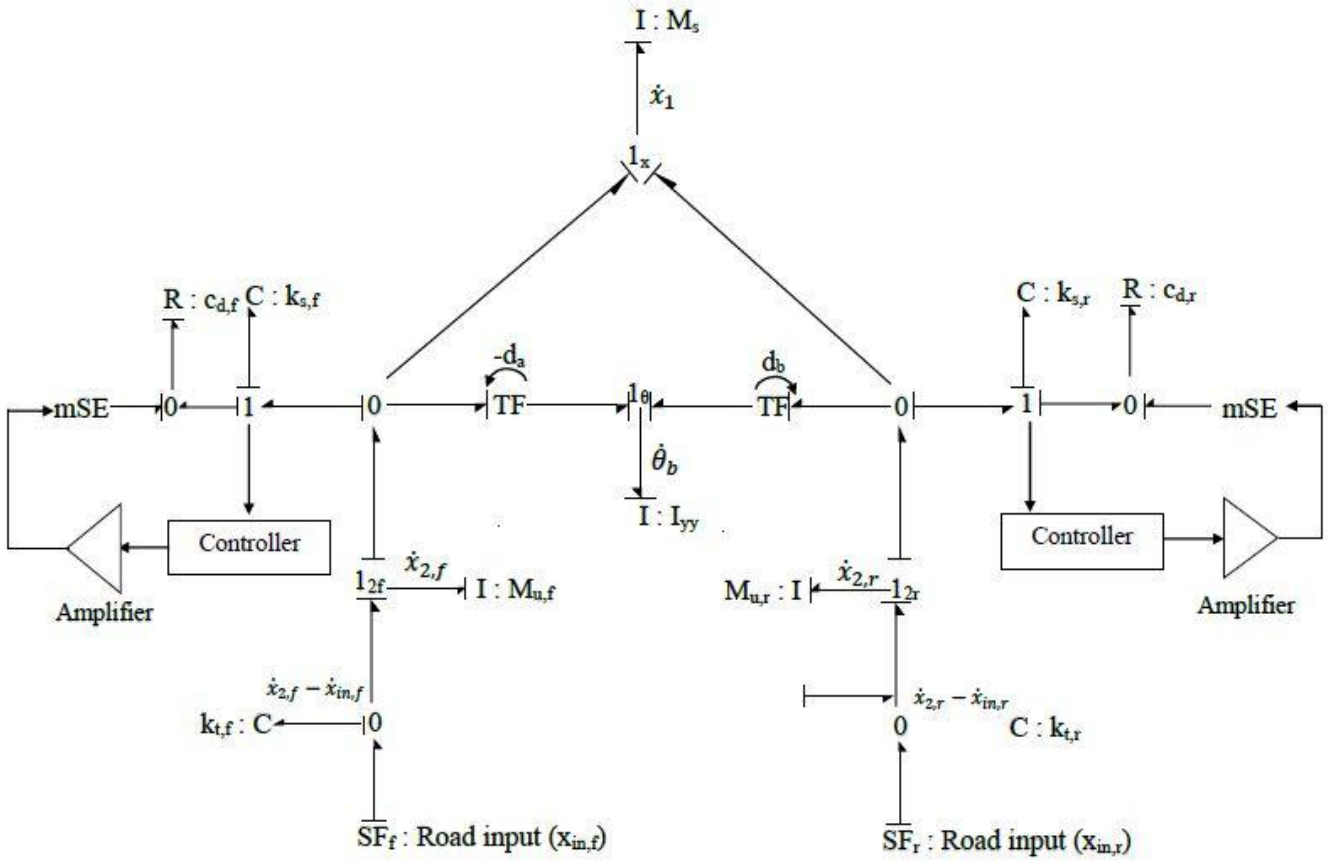

Fig. 3.4: Bond graph model for 4-DOF half car

3.5 MATLAB/Simulink modeling

The model for passive system and semi-active system has also been developed in the software environment of MATLAB/Simulink® for the performance analysis of quarter car and half car under random road excitation. The models are created in Simulink using the state-space representation of the quarter vehicle and half vehicle. Road excitation and damping force controlled with the help of different controller is fed as input to the system. Outputs of body acceleration, displacement and velocities have been considered. The model for passive system is shown in Fig. 3.5 below. The same for semi-active system is shown in Fig. 3.6. The controller in this case takes the input in the form of velocities or displacements according to the used control algorithm and thus controls the damping force. The different control strategies have been discussed thoroughly in the next chapter.

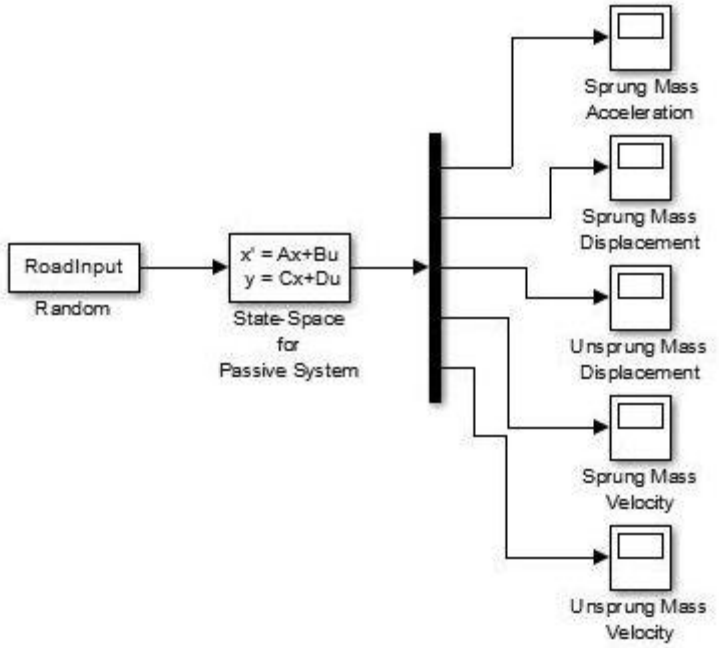

Fig. 3.5: MATLAB/Simulink model of passive suspension system

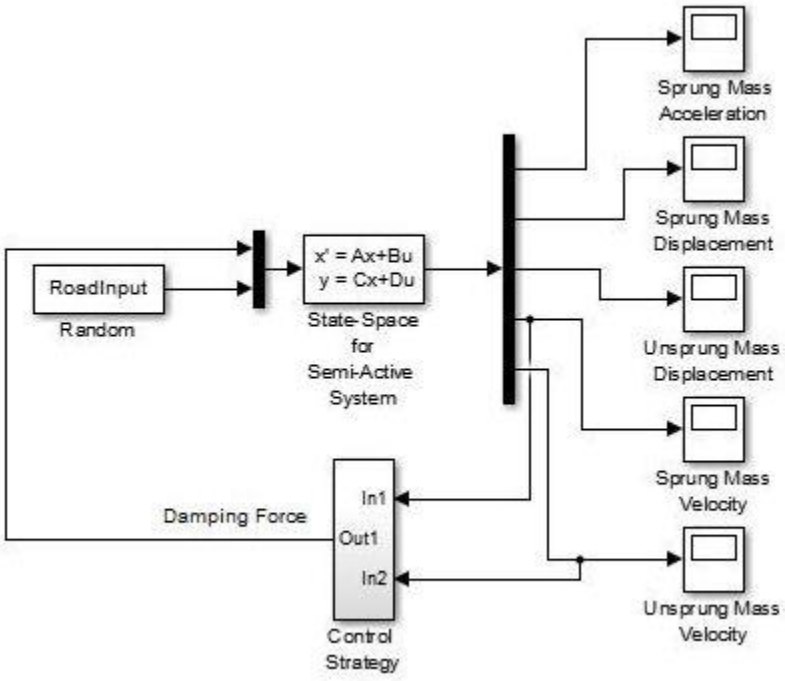

Fig. 3.6: MATLAB/Simulink model of semi-active suspension system

The state space representation for quarter car model can be given by the following equations:

$$\dot{X} = A \cdot X + B \cdot U \tag{3.1}$$

$$Y = C \cdot X + D \cdot U \tag{3.2}$$

where, Eq. (3.1) represents the input and Eq. (3.2) represents the output. A, B, C, D, X, Y and U can be represented by the following matrices for a quarter car system.

$$A = \begin{bmatrix} 0 & 1 & 0 & 0 \\ -\frac{k_s}{M_s} & 0 & \frac{k_s}{M_s} & 0 \\ 0 & 0 & 0 & 1 \\ \frac{k_s}{M_u} & 0 & -\frac{(k_s + k_t)}{M_u} & 0 \end{bmatrix} \tag{3.3}$$

$$B = \begin{bmatrix} 0 & 0 \\ -\frac{1}{M_s} & 0 \\ 0 & 0 \\ \frac{1}{M_u} & \frac{k_t}{M_u} \end{bmatrix} \tag{3.4}$$

$$C = \begin{bmatrix} -\frac{k_s}{M_s} & 0 & \frac{k_s}{M_s} & 0 \\ 0 & 1 & 0 & 0 \\ 0 & 0 & 0 & 1 \\ 1 & 0 & 0 & 0 \end{bmatrix} \tag{3.5}$$

$$D = \begin{bmatrix} -\frac{1}{M_s} & 0 \\ 0 & 0 \\ 0 & 0 \\ 0 & 0 \end{bmatrix} \tag{3.6}$$

$$X = [x_1;\ \dot{x}_1;\ x_2;\ \dot{x}_2] \tag{3.7}$$

$$U = [F_d;\ x_{in}] \tag{3.8}$$

$$Y = [\ddot{x}_1; \dot{x}_1;\ \dot{x}_2;\ x_1] \tag{3.9}$$

where, F_d is the damping force of the controllable damper or passive system that is used as input to the system. Similarly, for a half car model, the state space matrices may be presented as:

$$A = \begin{bmatrix} 0 & 1 & 0 & 0 & 0 & 0 & 0 & 0 \\ -\frac{(k_{s,f}+k_{s,r})}{M_s} & 0 & \frac{k_{s,f}}{M_s} & 0 & \frac{k_{s,r}}{M_s} & 0 & \frac{d_a \cdot k_{s,f} + d_b \cdot k_{s,r}}{M_s} & 0 \\ 0 & 0 & 0 & 1 & 0 & 0 & 0 & 0 \\ \frac{k_{s,f}}{M_{u,f}} & 0 & -\frac{(k_{s,f}+k_{t,f})}{M_{u,f}} & 0 & 0 & 0 & -\frac{d_a \cdot k_{s,f}}{M_{u,f}} & 0 \\ 0 & 0 & 0 & 0 & 0 & 1 & 0 & 0 \\ \frac{k_{s,r}}{M_{u,r}} & 0 & 0 & 0 & -\frac{(k_{s,r}+k_{t,r})}{M_{u,r}} & 0 & \frac{d_b \cdot k_{s,r}}{M_{u,r}} & 0 \\ 0 & 0 & 0 & 0 & 0 & 0 & 0 & 1 \\ \frac{d_a \cdot k_{s,f} - d_b \cdot k_{s,r}}{I_{yy}} & 0 & -\frac{d_a \cdot k_{s,f}}{I_{yy}} & 0 & \frac{d_b \cdot k_{s,r}}{I_{yy}} & 0 & -\frac{(d_a^2 \cdot k_{s,f} + d_b^2 \cdot k_{s,r})}{I_{yy}} & 0 \end{bmatrix} \quad (3.10)$$

$$B = \begin{bmatrix} 0 & 0 & 0 & 0 \\ -\frac{1}{M_s} & -\frac{1}{M_s} & 0 & 0 \\ 0 & 0 & 0 & 0 \\ \frac{1}{M_{u,f}} & 0 & \frac{k_{t,f}}{M_{u,f}} & 0 \\ 0 & 0 & 0 & 0 \\ 0 & \frac{1}{M_{u,r}} & 0 & \frac{k_{t,r}}{M_{u,r}} \\ 0 & 0 & 0 & 0 \\ \frac{d_a}{I_{yy}} & -\frac{d_b}{I_{yy}} & 0 & 0 \end{bmatrix} \quad (3.11)$$

$$C = \begin{bmatrix} -\frac{(k_{s,f}+k_{s,r})}{M_s} & 0 & \frac{k_{s,f}}{M_s} & 0 & \frac{k_{s,r}}{M_s} & 0 & \frac{d_a \cdot k_{s,f} + d_b \cdot k_{s,r}}{M_s} & 0 \\ 0 & 1 & 0 & 0 & 0 & 0 & 0 & -d_a \\ 0 & 0 & 0 & 1 & 0 & 0 & 0 & 0 \\ 0 & 1 & 0 & 0 & 0 & 0 & 0 & d_b \\ 0 & 0 & 0 & 0 & 0 & 1 & 0 & 0 \\ 1 & 0 & 0 & 0 & 0 & 0 & 0 & 0 \end{bmatrix} \quad (3.12)$$

$$D = \begin{bmatrix} -\frac{1}{M_s} & -\frac{1}{M_s} & 0 & 0 \\ 0 & 0 & 0 & 0 \\ 0 & 0 & 0 & 0 \\ 0 & 0 & 0 & 0 \\ 0 & 0 & 0 & 0 \end{bmatrix} \quad (3.13)$$

$$X = \left[x_1;\ \dot{x}_1;\ x_{2,f};\ \dot{x}_{2,f};\ x_{2,r};\ \dot{x}_{2,r};\ \theta_1;\ \dot{\theta}_1\right] \quad (3.14)$$

$$U = \left[F_{d,f};\ F_{d,r};\ x_{in,f};\ x_{in,r}\right] \quad (3.15)$$

$$Y = \left[\ddot{x}_1;\ (\dot{x}_1 - d_a \cdot \dot{\theta}_1);\ \dot{x}_{2,f};\ (\dot{x}_1 + d_b \cdot \dot{\theta}_1);\ \dot{x}_{2,r};\ x_1\right] \quad (3.16)$$

3.6 Summary

In this chapter, bond graph models are developed for both quarter car and half car models for passive and semi-active suspension systems. Simulink® models of quarter car and half car suspension system have been designed for the analysis of performance of vehicle subjected to random road input. Next chapter will present the different control strategies used for the control of the semi-active suspension system.

CHAPTER 4

CONTROL STRATEGIES FOR SEMI-ACTIVE SUSPENSION SYSTEM

4.1 Introduction

Semi-active damper can be of two types: on-off and continuously variable. An on-off damper is switched between "on" and "off" states of damping according to a suitable control algorithm. The on state damping coefficient is relatively high, while, the off state damping is low. Theoretically, the off state damping should be zero, but this is not possible practically. A continuously variable damper is also switched in between on and off states, but the on state damping coefficient is varied, thus varying the corresponding damping force. These concepts of semi-active damping are illustrated in Fig. 4.1(a) and 4.1(b), which show the force-velocity characteristics for on-off and continuous damper respectively [15].

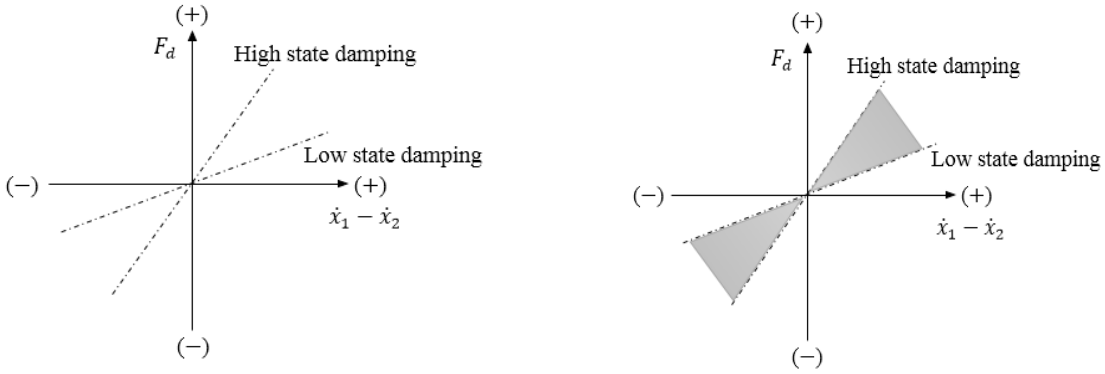

Fig. 4.1: Semi-active damper concepts: (a) On-off damper, (b) Continuous damper (the shadowed part in (b) shows the achievable range of damping coefficients)

The following section describes different control algorithms for semi-active damping control viz., skyhook, balance control and groundhook control with two variances of all control algorithms, viz. on-off and continuous. Hybrid control strategies are also presented which combines two or more of the said control algorithms. Control algorithms are developed for both quarter and half car models and are presented in details in the following sections.

4.2 Skyhook Control

The skyhook configuration shown in Fig. 4.2 consists of a damper connected to some inertial reference in the sky. With this configuration, the compromise between resonance control and high-frequency isolation, which is common in passive suspensions, is removed [27]. The skyhook control concentrates on the sprung mass; with the increase in c_{sky}, the sprung mass motion decreases. The isolation of the sprung mass from base excitations by skyhook control comes at the expense of heightened unsprung mass motion. The basic algorithm is given as,

$$F_d = F_{skyhook} = \begin{cases} c_{sky}\dot{x}_1, & \dot{x}_1(\dot{x}_1 - \dot{x}_2) \geq 0 \\ 0, & \dot{x}_1(\dot{x}_1 - \dot{x}_2) < 0 \end{cases} \tag{4.1}$$

where, F_d is the damping force, $F_{skyhook}$ is the required damping force of the skyhook damper and c_{sky} is the damping coefficient of the hypothetical skyhook damper. $\dot{x}_1$ is the sprung mass velocity and $\dot{x}_2$ is the unsprung mass velocity.

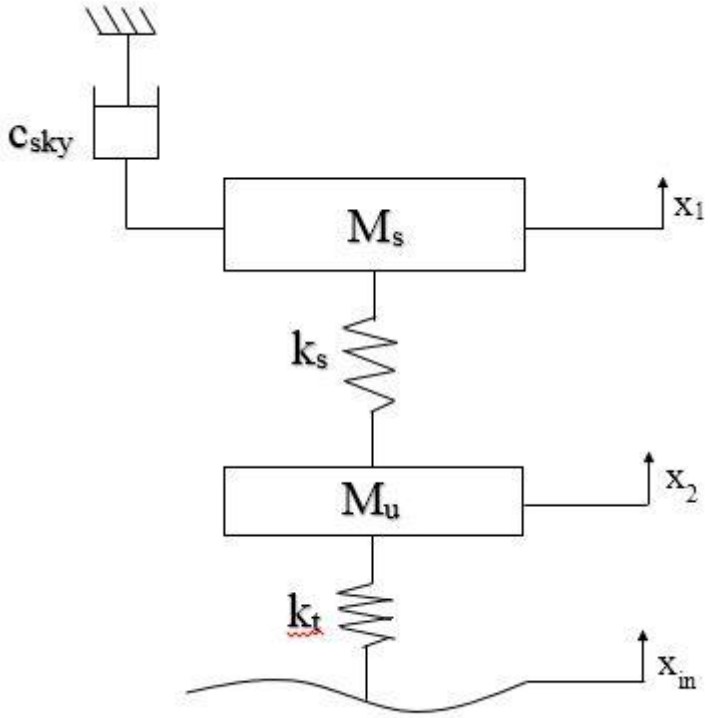

Fig. 4.2: Skyhook damper configuration

4.2.1 Continuous skyhook control for quarter vehicle

Considering a 2-DOF system with a skyhook damper as shown in Fig. 4.2, the damping force can be written as [15]

$$F_{skyhook} = c_{sky}\dot{x}_1, \tag{4.2}$$

where $F_{skyhook}$ is the skyhook damping force, $\dot{x}_1$ is the velocity of the vehicle body and c_{sky} is the damping coefficient of the skyhook damper. The aim is to imitate the skyhook damping force with a controllable damper mounted between the vehicle body and the wheel/unsprung mass as shown in Fig. 2.2 in Chapter 2. But, a passive damper can only absorb vibration energy. So the product of the damping force F_{sa}, and the relative velocity, $\dot{x}_1 - \dot{x}_2$, must satisfy the inequality

$$F_{sa}(\dot{x}_1 - \dot{x}_2) \geq 0. \tag{4.3}$$

The desired force is $c_{sky}\dot{x}_1$, but the semi-active damper can generate this force only when $\dot{x}_1$ and $\dot{x}_1 - \dot{x}_2$ have the same sign. When $\dot{x}_1$ and $\dot{x}_1 - \dot{x}_2$ are of opposite sign, the damper can give a force opposite the desired control force. It is better not to supply any force in this situation. Thus, the continuous skyhook control algorithm is given by

$$F_{sa} = \begin{cases} c_{sky}\dot{x}_1, & \dot{x}_1(\dot{x}_1 - \dot{x}_2) \geq 0, \\ 0, & \dot{x}_1(\dot{x}_1 - \dot{x}_2) < 0. \end{cases} \tag{4.4}$$

The switching of the damper is regulated by the term $\dot{x}_1(\dot{x}_1 - \dot{x}_2)$, which is the condition function. On state damping force can be written as

$$F_{sa} = c_d(\dot{x}_1 - \dot{x}_2), \tag{4.5}$$

where c_d is the semi-active damping coefficient. The value that c_d have to take to imitate a skyhook damper can be found by equating Eq. (4.4) to Eq. (4.5), which gives

$$c_d = \begin{cases} \dfrac{c_{sky}\dot{x}_1}{(\dot{x}_1 - \dot{x}_2)}, & \dot{x}_1(\dot{x}_1 - \dot{x}_2) \geq 0, \\ 0, & \dot{x}_1(\dot{x}_1 - \dot{x}_2) < 0. \end{cases} \tag{4.6}$$

It can be seen from Eq. (4.6) that when the relative velocity $(\dot{x}_1 - \dot{x}_2)$ is very small, the required damping coefficient increases abruptly and approaches infinity. In practice, the damping coefficient of a conventional damper is limited by its physical parameter, i.e., there

is an upper bound, c_{max} and a lower bound, c_{min}. Thus, the damping coefficient in Eq. (4.6) can be rewritten as

$$c_d = \begin{cases} max\left[c_{min}, min\left[\frac{c_{sky}\dot{x}_1}{(\dot{x}_1 - \dot{x}_2)}, c_{max}\right]\right], & \dot{x}_1(\dot{x}_1 - \dot{x}_2) \geq 0, \\ c_{min}, & \dot{x}_1(\dot{x}_1 - \dot{x}_2) < 0. \end{cases} \tag{4.7}$$

4.2.2 On-off skyhook control for quarter vehicle

In case of continuous skyhook, the damping coefficient requires to be varied continuously. To simplify the situation, an on-off scheme has been suggested [15]. The on-off damper acts as a conventional passive damper during the vibration depletion portion of the cycle, but the damping coefficient is assumed to be zero when the damping force generated is in opposite direction to that of an ideal skyhook damper. The damping force in case of on-off control is given by

$$F_{sa} = \begin{cases} c_{on}(\dot{x}_1 - \dot{x}_2), & \dot{x}_1(\dot{x}_1 - \dot{x}_2) \geq 0, \\ 0, & \dot{x}_1(\dot{x}_1 - \dot{x}_2) < 0, \end{cases} \tag{4.8}$$

where, c_{on} is the on-state damping coefficient of the on-off damper. In a real world situation, a zero damping coefficient is not possible in the off-state. So, the damping coefficient is switched between a maximum value, c_{max} and a minimum value, c_{min}. The control algorithm is changed accordingly as

$$c_d = \begin{cases} c_{max}, & \dot{x}_1(\dot{x}_1 - \dot{x}_2) \geq 0, \\ c_{min,} & \dot{x}_1(\dot{x}_1 - \dot{x}_2) < 0. \end{cases} \tag{4.9}$$

The on-state damping coefficient, c_{max} should be much greater than the off-state damping coefficient, c_{min}. The off-state damping constant should be as small as possible.

4.2.3 On-off skyhook control for half vehicle

The on-off skyhook control strategy for half vehicle model determines whether the damper should be adjusted to its maximum value or the minimum value based on the product of the absolute velocity of the vehicle sprung mass and the relative velocity across the suspension. The absolute velocity of the sprung mass for the half vehicle model as shown in Fig. 2.2 (Chapter 2) is given by,

$$V_{abs,f} = \dot{x}_1 - d_a \cdot \dot{\theta}_b \tag{4.10}$$

$$V_{abs,r} = \dot{x}_1 + d_b \cdot \dot{\theta}_b \tag{4.11}$$

The relative velocity across each of the suspension is given by the following expressions,

$$V_{rel,f} = \dot{x}_1 - \dot{x}_{2,f} - d_a \cdot \dot{\theta}_b \tag{4.12}$$

$$V_{rel,r} = \dot{x}_1 - \dot{x}_{2,r} + d_b \cdot \dot{\theta}_b \tag{4.13}$$

Hence, the on-off skyhook control strategy for a half vehicle model is formulated as given below,

Front Damper:

$$c_{d,f} = \begin{cases} c_{max,f}, & V_{abs,f} \cdot V_{rel,f} \geq 0, \\ c_{min,f}, & V_{abs,f} \cdot V_{rel,f} < 0, \end{cases} \tag{4.14}$$

Rear Damper:

$$c_{d,r} = \begin{cases} c_{max,r}, & V_{abs,r} \cdot V_{rel,r} \geq 0, \\ c_{min,r}, & V_{abs,r} \cdot V_{rel,r} < 0, \end{cases} \tag{4.15}$$

4.2.4 Continuous skyhook control for half vehicle

Continuous skyhook control is an extension of the on-off skyhook control policy. Let us consider the 4-DOF half vehicle model with a skyhook damper connected in between the body and an inertial reference point. The damping force can be given as,

$$F_{skyhook} = c_{sky} \cdot V_{abs,f} \tag{4.16}$$

where, $F_{skyhook}$ is the skyhook damping force, c_{sky} is the skyhook damping coefficient and $V_{abs,f}$ is the absolute velocity of the sprung mass. The motive is to imitate the skyhook damping force with a semi-active damper attached in between the sprung mass and the unsprung mass.

However, as the passive damper is capable of only absorbing energy, the semi-active damping force and the relative velocity across the damper must comply with the following inequality,

$$F_{sa} \cdot V_{rel,f} \geq 0 \tag{4.17}$$

The desired force $c_{sky} \cdot V_{abs,f}$ can only be produced if $V_{abs,f}$ and $V_{rel,f}$ have the same sign. When these two are of opposite sign, the semi-active damper can supply a force which is opposite to the desired force. In this condition, it is desirable to supply no force at all. Hence, the semi-active damping coefficient can be determined by the following relations,

Front Damper:

$$c_{d,f} = \begin{cases} c_{sky} \cdot V_{abs,f}/V_{rel,f}, & V_{abs,f} \cdot V_{rel,f} \geq 0, \\ 0, & V_{abs,f} \cdot V_{rel,f} < 0, \end{cases} \tag{4.18}$$

Rear Damper:

$$c_{d,r} = \begin{cases} c_{sky} \cdot V_{abs,r}/V_{rel,r}, & V_{abs,r} \cdot V_{rel,r} \geq 0, \\ 0, & V_{abs,r} \cdot V_{rel,r} < 0, \end{cases} \tag{4.19}$$

It can be observed from the Eq. 4.19 that for a very small value of the relative velocity, the required damping coefficient builds up unexpectedly and tends to infinity. But in real life situation, the semi-active damper constant is confined in between the physical boundary of the damper and has an upper limit, c_{max} and a lower limit, c_{min}. The control policy can be rewritten as,

Front Damper:

$$c_{d,f} = \begin{cases} \max\{c_{min,f}, \min\left[\left(c_{sky,f} \cdot V_{abs,f}/V_{rel,f}\right), c_{max,f}\right]\}, & V_{abs,f} \cdot V_{rel,f} \geq 0, \\ c_{min,f}, & V_{abs,f} \cdot V_{rel,f} < 0, \end{cases} \tag{4.20}$$

Rear Damper:

$$c_{d,r} = \begin{cases} \max\{c_{min,r}, \min\left[\left(c_{sky,r} \cdot V_{abs,r}/V_{rel,r}\right), c_{max,r}\right]\}, & V_{abs,r} \cdot V_{rel,r} \geq 0, \\ c_{min,r}, & V_{abs,r} \cdot V_{rel,r} < 0, \end{cases} \tag{4.21}$$

4.3 Balance Control

The fundamental concept of this semi-active control strategy is to balance the spring force by means of damping force for the instances when both the forces act in opposite directions and to set the damping force to a low value (possibly zero) otherwise. Therefore, the force transmitted through the system is significantly reduced or even cancelled out during the instances when the damper is acting and is slightly more than the spring force otherwise [28].

It is also referred to as "relative control" since the control variables are the relative displacement and the relative velocity between the vehicle body and the wheel.

4.3.1 On-off balance control for quarter vehicle

Considering the 2-DOF system shown in Fig. 2.2 (Chapter 2), the acceleration response of the vehicle mass can be expressed as

$$\ddot{x}_1 = -\frac{1}{m}(F_k + F_d), \tag{4.22}$$

where F_k and F_d are the spring force and damping force respectively. They are given by the following equations

$$F_k = k_s(x_1 - x_2) \tag{4.23}$$

and

$$F_d = c_d(\dot{x}_1 - \dot{x}_2), \tag{4.24}$$

where, k_s and c_d are the spring stiffness and the damping coefficient respectively. The amplitude of the acceleration of the vehicle body due to harmonic excitation can be expressed as [9]

$$|\ddot{x}_1| = \frac{|F_k| + |F_d|}{m} \begin{cases} t_0 < t < t_0 + \dfrac{\tau}{4}, \\ t_0 + \dfrac{\tau}{2} < t < t_0 + \dfrac{3\tau}{4}, \end{cases} \tag{4.25}$$

$$|\ddot{x}_1| = \frac{|F_k| - |F_d|}{m} \begin{cases} t_0 + \dfrac{\tau}{4} < t < t_0 + \dfrac{\tau}{2}, \\ t_0 + \dfrac{3\tau}{4} < t < t_0 + \tau, \end{cases} \tag{4.26}$$

where, t_0 is the time point at which $\ddot{x}_1 = 0$ and is increasing, and τ is the period of vibration. It can be seen from Eq. (4.25) that the damping force contributes to the increase in the acceleration for two quarters of the cycle, while in the remaining part of the cycle, it tends to decelerate the acceleration of the mass (Eq. (4.26)).

The acceleration will be increased whenever the spring and damper forces have the same sign, i.e., the relative velocity and relative displacement have the same sign. A control algorithm to ensure that this situation does not arise is [15]

$$F_{sa} = \begin{cases} c_{on}(\dot{x}_1 - \dot{x}_2), & (x_1 - x_2)(\dot{x}_1 - \dot{x}_2) \leq 0, \\ 0, & (x_1 - x_2)(\dot{x}_1 - \dot{x}_2) > 0, \end{cases} \quad (4.27)$$

where, c_{on} is the on state damping coefficient of the on-off damper. The corresponding algorithm for damping coefficient of the semi-active on-off damper is

$$c_d = \begin{cases} c_{max}, & (x_1 - x_2)(\dot{x}_1 - \dot{x}_2) \leq 0, \\ c_{min}, & (x_1 - x_2)(\dot{x}_1 - \dot{x}_2) > 0, \end{cases} \quad (4.28)$$

where, c_{max} and c_{min} are the maximum and the minimum damping coefficients of the on-off damper.

4.3.2 Continuous balance control for quarter vehicle

During the on-state, the instantaneous damping force is rarely equal to the instantaneous spring force in magnitude. The excess force will add to the acceleration of the vehicle body. In Ref. [15], a continuously variable control logic has been recommended. In this logic, the damping coefficient is continuously varied on the basis of relative displacement and relative velocity, such that the spring force and the damper force balance out completely during on-state. The required force is given by

$$F_{sa} = \begin{cases} -k_s(x_1 - x_2), & (x_1 - x_2)(\dot{x}_1 - \dot{x}_2) \leq 0, \\ 0, & (x_1 - x_2)(\dot{x}_1 - \dot{x}_2) > 0. \end{cases} \quad (4.29)$$

The damper here is attempting to behave like a spring with a negative stiffness during on-state. The damping force is regulated to balance the magnitude of the spring force such that zero acceleration is produced. The damping coefficient according to this control algorithm can be given by

$$c_d = \begin{cases} \dfrac{-k_s(x_1 - x_2)}{(\dot{x}_1 - \dot{x}_2)}, & (x_1 - x_2)(\dot{x}_1 - \dot{x}_2) \leq 0, \\ 0, & (x_1 - x_2)(\dot{x}_1 - \dot{x}_2) > 0. \end{cases} \quad (4.30)$$

In the Eq. (4.30), the damping coefficient will approach infinity when $(\dot{x}_1 - \dot{x}_2) \to 0$, which is practically not possible. The damping coefficient has an upper bound and a lower bound on the basis of the physical parameter of the damper. Taking into consideration the physical constraints, the damping coefficient is expressed as

$$c_d = \begin{cases} \max\left[c_{min}, min\left[\frac{-k_s(x_1 - x_2)}{(\dot{x}_1 - \dot{x}_2)}, c_{max}\right]\right], & (x_1 - x_2)(\dot{x}_1 - \dot{x}_2) \leq 0, \\ c_{min}, & (x_1 - x_2)(\dot{x}_1 - \dot{x}_2) > 0. \end{cases} \quad (4.31)$$

Both the on-off and continuous balance algorithm balance out the damping force and spring force to some extent, if both the forces have opposite signs. In on-state, the on-off logic can generate a damping force proportional to the relative velocity across the damper. Hence, it cannot assure that the damping force cancels out the spring force totally. The spring force can be partially balanced or may even be over-cancelled depending upon c_{min}, c_{max} and the frequency. In case of continuous balance control, the spring force can be balanced by the damping force partially or fully.

4.3.3 On-off balance control for half vehicle

The on-off balance control for half vehicle model regulates the damping coefficient of the semi-active damper. The damping coefficient is adjusted in between high state and low state depending upon the value of relative displacement and relative velocity across the damper. If the product is less than or equal to zero, the damper is allocated the high state value. If the product is greater than zero, the damper takes the low state value. The relative displacement for the half vehicle model as shown in Fig. 2.4 (Chapter 2) can be estimated as,

$$D_{rel,f} = x_1 - x_{2,f} - d_a \cdot \theta_b \quad (4.32)$$

$$D_{rel,r} = x_1 - x_{2,r} + d_b \cdot \theta_b \quad (4.33)$$

The relative velocity across the damper is given by the equations (4.12) and (4.13) as shown above. Hence, the on-off balance control logic can be represented as,

Front Damper:

$$c_{d,f} = \begin{cases} c_{max,f}, & D_{rel,f} \cdot V_{rel,f} \leq 0, \\ c_{min,f}, & D_{rel,f} \cdot V_{rel,f} > 0, \end{cases} \quad (4.34)$$

Rear Damper:

$$c_{d,r} = \begin{cases} c_{max,r}, & D_{rel,r} \cdot V_{rel,r} \leq 0, \\ c_{min,r}, & D_{rel,r} \cdot V_{rel,r} > 0, \end{cases} \quad (4.35)$$

4.3.4 Continuous balance control for half vehicle

In case of the continuous balance control for half car model, the damping coefficient is continuously varied on the basis of relative displacement and relative velocity across the damper. The semi-active damper here acts as a spring with a negative stiffness such that the spring force and the damper force can be cancelled out completely. The required force can be written as,

$$F_{sa} = \begin{cases} -k_{s,f} D_{rel,f}, & D_{rel,f} \cdot V_{rel,f} \leq 0, \\ 0, & D_{rel,f} \cdot V_{rel,f} > 0. \end{cases} \tag{4.36}$$

The damping force is regulated to balance the magnitude of the spring force such that zero acceleration is produced. The damping coefficient according to this control algorithm can be given by

$$c_{d,f} = \begin{cases} \dfrac{-k_{s,f} D_{rel,f}}{V_{rel,f}}, & D_{rel,f} \cdot V_{rel,f} \leq 0, \\ 0, & D_{rel,f} \cdot V_{rel,f} > 0. \end{cases} \tag{4.37}$$

In the Eq. (4.37), the damping coefficient will approach infinity when $V_{rel,f} \to 0$, which is practically not possible. The damping coefficient has an upper bound, c_{max} and a lower bound, c_{min} on the basis of the physical parameter of the damper. Taking into consideration the physical constraints, the damping coefficient is expressed as

Front Damper:

$$c_{d,f} = \begin{cases} \max\left[c_{min,f}, min\left[\dfrac{-k_{s,f} D_{rel,f}}{V_{rel,f}}, c_{max,f}\right]\right], & D_{rel,f} \cdot V_{rel,f} \leq 0, \\ c_{min,f}, & D_{rel,f} \cdot V_{rel,f} > 0. \end{cases} \tag{4.38}$$

Rear Damper:

$$c_{d,r} = \begin{cases} \max\left[c_{min,r}, min\left[\dfrac{-k_{s,r} D_{rel,r}}{V_{rel,r}}, c_{max,r}\right]\right], & D_{rel,r} \cdot V_{rel,r} \leq 0, \\ c_{min,r}, & D_{rel,r} \cdot V_{rel,r} > 0. \end{cases} \tag{4.39}$$

4.4 Groundhook Control

Groundhook logic aims at reducing dynamic tire force, and hence leads to better handling as well as less road damage. Similar to skyhook damper, the groundhook damper is assumed to

be hooked to a fixed point, in this case the ground. Schematic diagram of a groundhook damper is shown in Fig. 4.2. Here, the damping force is given by [29]:

$$F_d = F_{groundhook} = \begin{cases} c_{gnd}\dot{x}_2, & -\dot{x}_2(\dot{x}_1 - \dot{x}_2) \geq 0 \\ 0, & -\dot{x}_2(\dot{x}_1 - \dot{x}_2) < 0 \end{cases} \quad (4.40)$$

where, F_d is the damping force, $F_{groundhook}$ is the required damping force of the groundhook damper and c_{gnd} is the damping coefficient of the groundhook damper.

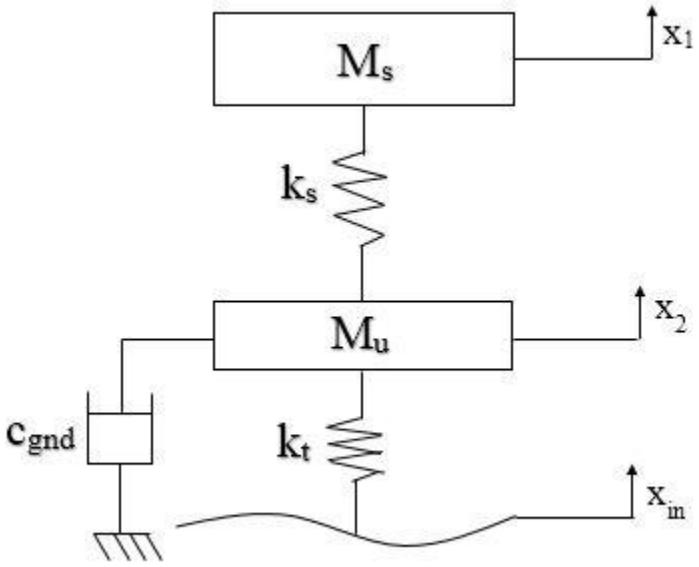

Fig. 4.3: Groundhook damper configuration

4.4.1 Continuous groundhook control for quarter vehicle

Considering a 2-DOF system with a groundhook damper as shown in Fig. 4.3, the damping force can be written as

$$F_{groundhook} = c_{gnd}\dot{x}_2, \quad (4.41)$$

where $F_{groundhook}$ is the groundhook damping force, $\dot{x}_2$ is the velocity of the unsprung mass and c_{gnd} is the damping coefficient of the groundhook damper. The aim is to imitate the groundhook damping force with a controllable damper mounted between the vehicle body and the wheel/unsprung mass as shown in Fig. 2.2 in Chapter 2. But, a passive damper can only

absorb vibration energy. So the product of the damping force F_{sa}, and the relative velocity, $\dot{x}_1 - \dot{x}_2$, must satisfy the inequality

$$F_{sa}(\dot{x}_1 - \dot{x}_2) \geq 0. \tag{4.42}$$

The desired force is $c_{gnd}\dot{x}_2$, but the semi-active damper can generate this force only when $\dot{x}_2$ and $\dot{x}_1 - \dot{x}_2$ have the opposite sign. When $\dot{x}_2$ and $\dot{x}_1 - \dot{x}_2$ are of same sign, the damper can give a force opposite the desired control force. It is better not to supply any force in this situation. Thus, the continuous skyhook control algorithm is given by

$$F_{sa} = \begin{cases} c_{gnd}\dot{x}_2, & -\dot{x}_2(\dot{x}_1 - \dot{x}_2) \geq 0, \\ 0, & -\dot{x}_2(\dot{x}_1 - \dot{x}_2) < 0. \end{cases} \tag{4.43}$$

The switching of the damper is regulated by the term $-\dot{x}_2(\dot{x}_1 - \dot{x}_2)$, which is the condition function. On state damping force can be written as

$$F_{sa} = c_d(\dot{x}_1 - \dot{x}_2), \tag{4.44}$$

where c_d is the semi-active damping coefficient. The value that c_d have to take to imitate a groundhook damper can be found by equating Eq. (4.43) to Eq. (4.44), which gives

$$c_d = \begin{cases} \dfrac{c_{gnd}\dot{x}_2}{(\dot{x}_1 - \dot{x}_2)}, & -\dot{x}_2(\dot{x}_1 - \dot{x}_2) \geq 0, \\ 0, & -\dot{x}_2(\dot{x}_1 - \dot{x}_2) < 0. \end{cases} \tag{4.45}$$

It can be seen from Eq. (4.45) that when the relative velocity $(\dot{x}_1 - \dot{x}_2)$ is very small, the required damping coefficient increases abruptly and approaches infinity. In practice, the damping coefficient of a conventional damper is limited by its physical parameter, i.e., there is an upper bound, c_{max} and a lower bound, c_{min}. Thus, the damping coefficient in Eq. (4.45) can be rewritten as

$$c_d = \begin{cases} max\left[c_{min}, min\left[\dfrac{c_{gnd}\dot{x}_2}{(\dot{x}_1 - \dot{x}_2)}, c_{max}\right]\right], & -\dot{x}_2(\dot{x}_1 - \dot{x}_2) \geq 0, \\ c_{min}, & -\dot{x}_2(\dot{x}_1 - \dot{x}_2) < 0. \end{cases} \tag{4.46}$$

4.4.2 On-off groundhook control for quarter vehicle

The on-off damper acts as a conventional passive damper during the vibration depletion portion of the cycle, but the damping coefficient is assumed to be zero when the damping force

generated is in opposite direction to that of an ideal groundhook damper. The damping force in case of on-off control is given by

$$F_{sa} = \begin{cases} c_{on}(\dot{x}_1 - \dot{x}_2), & -\dot{x}_2(\dot{x}_1 - \dot{x}_2) \geq 0, \\ 0, & -\dot{x}_2(\dot{x}_1 - \dot{x}_2) < 0, \end{cases} \tag{4.47}$$

where, c_{on} is the on-state damping coefficient of the on-off damper. In a real world situation, a zero damping coefficient is not possible in the off-state. So, the damping coefficient is switched between a maximum value, c_{max} and a minimum value, c_{min}. The control algorithm is changed accordingly as

$$c_d = \begin{cases} c_{max}, & -\dot{x}_2(\dot{x}_1 - \dot{x}_2) \geq 0, \\ c_{min}, & -\dot{x}_2(\dot{x}_1 - \dot{x}_2) < 0. \end{cases} \tag{4.48}$$

The on-state damping coefficient, c_{max} should be much greater than the off-state damping coefficient, c_{min}. The off-state damping constant should be as small as possible.

4.4.3 On-off groundhook control for half vehicle

The on-off groundhook control strategy for half vehicle model determines whether the damper should be adjusted to its maximum value or the minimum value based on the product of the absolute velocity of the unsprung mass and the relative velocity across the suspension. The absolute velocity of the unsprung mass for the half vehicle model as shown in Fig. 2.2 (Chapter 2) is given by $\dot{x}_{2,f}$ and $\dot{x}_{2,r}$ for front and rear suspensions respectively. The relative velocities across each of the suspension are given in Eq. (4.12) and Eq. (4.13). Hence, the on-off skyhook control strategy for a half vehicle model is formulated as given below,

Front Damper:

$$c_{d,f} = \begin{cases} c_{max,f}, & -\dot{x}_{2,f} \cdot V_{rel,f} \geq 0, \\ c_{min,f}, & -\dot{x}_{2,f} \cdot V_{rel,f} < 0, \end{cases} \tag{4.49}$$

Rear Damper:

$$c_{d,r} = \begin{cases} c_{max,r}, & -\dot{x}_{2,r} \cdot V_{rel,r} \geq 0, \\ c_{min,r}, & -\dot{x}_{2,r} \cdot V_{rel,r} < 0, \end{cases} \tag{4.50}$$

4.4.4 Continuous groundhook control for half vehicle

Let us consider the 4-DOF half vehicle model with groundhook dampers connected in between the body and an inertial reference point on the ground. The damping force can be given as,

$$F_{groundhook} = c_{gnd} \cdot \dot{x}_{2,f} \tag{4.51}$$

where, $F_{groundhook}$ is the groundhook damping force, c_{gnd} is the groundhook damping coefficient and $\dot{x}_{2,f}$ is the absolute velocity of the unsprung mass. The motive is to imitate the groundhook damping force with a semi-active damper attached in between the sprung mass and the unsprung mass.

However, as the passive damper is capable of only absorbing energy, the semi-active damping force and the relative velocity across the damper must comply with the following inequality,

$$F_{sa} \cdot V_{rel,f} \geq 0 \tag{4.52}$$

The desired force $c_{gnd} \cdot \dot{x}_{2,f}$ can only be produced if $\dot{x}_{2,f}$ and $V_{rel,f}$ have the opposite sign. When these two are of same sign, the semi-active damper can supply a force which is opposite to the desired force. In this condition, it is desirable to supply no force at all. Hence, the semi-active damping coefficient can be determined by the following relations,

Front Damper:

$$c_{d,f} = \begin{cases} c_{gnd} \cdot \dot{x}_{2,f}/V_{rel,f}, & -\dot{x}_{2,f} \cdot V_{rel,f} \geq 0, \\ 0, & -\dot{x}_{2,f} \cdot V_{rel,f} < 0, \end{cases} \tag{4.53}$$

Rear Damper:

$$c_{d,r} = \begin{cases} c_{gnd} \cdot \dot{x}_{2,r}/V_{rel,r}, & -\dot{x}_{2,r} \cdot V_{rel,r} \geq 0, \\ 0, & -\dot{x}_{2,r} \cdot V_{rel,r} < 0, \end{cases} \tag{4.54}$$

It can be observed from the Eq. 4.54 that for a very small value of the relative velocity, the required damping coefficient builds up unexpectedly and tends to infinity. But in real life situation, the semi-active damper constant is confined in between the physical boundary of the damper and has an upper limit, c_{max} and a lower limit, c_{min}. The control policy can be rewritten as,

Front Damper:

$$c_{d,f} = \begin{cases} \max\{c_{min,f}, \min\left[\left(c_{gnd,f} \cdot \dot{x}_{2,f}/V_{rel,f}\right), c_{max,f}\right]\}, & -\dot{x}_{2,f} \cdot V_{rel,f} \geq 0, \\ c_{min,f}, & -\dot{x}_{2,f} \cdot V_{rel,f} < 0, \end{cases} \quad (4.55)$$

Rear Damper:

$$c_{d,r} = \begin{cases} \max\{c_{min,r}, \min\left[\left(c_{gnd,r} \cdot \dot{x}_{2,r}/V_{rel,r}\right), c_{max,r}\right]\}, & -\dot{x}_{2,r} \cdot V_{rel,r} \geq 0, \\ c_{min,r}, & -\dot{x}_{2,r} \cdot V_{rel,r} < 0, \end{cases} \quad (4.56)$$

4.5 Hybrid Control Strategy

Hybrid control strategies can be developed by combining two or more of the above control strategies. They can provide the benefit of both the control strategies and hence may provide better performance in terms of vibration isolation as well as vehicle handling.

4.5.1 Hybrid skyhook-groundhook control

This logic is intended at reducing both the body acceleration and the dynamic tire force. The sprung mass here is considered to be linked to a hypothetical damper which is connected to an inertial reference in sky, whereas the unsprung mass has a damper which is connected to a reference point in ground as shown in Fig. 4.4.

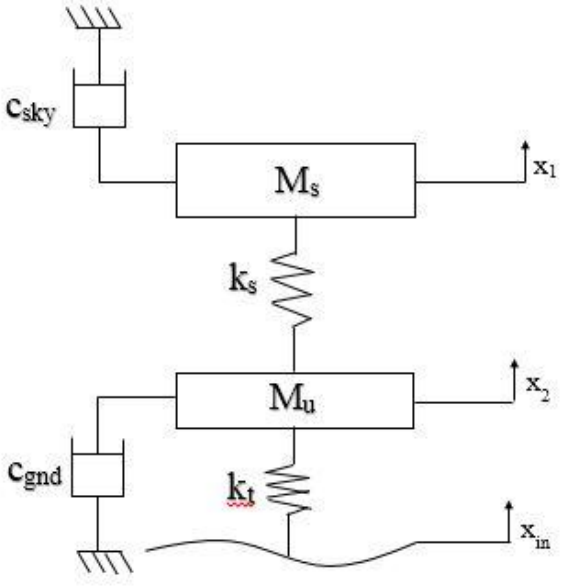

Fig. 4.4: Hybrid skyhook-groundhook damper configuration

The control algorithm is obtained by combining both skyhook and groundhook control algorithms [22,26].

$$F_{hybrid-SH-GH} = \alpha F_{skyhook} + (1-\alpha)F_{groundhook} \quad (4.57)$$

where, $F_{hybrid-SH-GH}$ is the damping force of the hybrid controller, $F_{skyhook}$ is the skyhook damping force, $F_{groundhook}$ is the groundhook damping force and α is the weighing factor to adjust comfort or handling, $\alpha \in (0,1)$ [23]. The skyhook damping force is controlled with the on-off skyhook strategy as discussed before and the groundhook force is controlled by the on-off groundhook logic respectively.

4.5.2 Hybrid skyhook-balance control

Similar to above hybrid logic, other hybrid strategies can be developed by combining two or more control strategies. We can combine skyhook and balance logic to give the hybrid control logic as shown below,

$$F_{hybrid-SH-B} = \beta F_{skyhook} + (1-\beta)F_{balance} \quad (4.58)$$

where, $F_{hybrid-SH-B}$ is the damping force of hybrid controller, $F_{balance}$ is the balance control force and β is the weighing factor to adjust the level of skyhook control or balance control. If β is set to 1, the control will be purely skyhook control, whereas, if β is set to 0, it will be a pure balance control. Similar as before, the skyhook and balance damping forces are controlled by the on-off skyhook and on-off balance control algorithms.

4.5.3 Hybrid groundhook-balance control

Groundhook and balance control logics were fused together to achieve a hybrid control strategy as shown below,

$$F_{hybrid-GH-B} = \gamma F_{groundhook} + (1-\gamma)F_{balance} \quad (4.59)$$

where, $F_{hybrid-GH-B}$ is the damping force of hybrid controller and γ is the weighing factor to adjust the level of groundhook control or balance control. If γ is set to 1, the control will be purely groundhook control, whereas, if γ is set to 0, it will be a pure balance control. Here, the groundhook damping force is regulated by the on-off groundhook logic whereas, balance damping force is controlled with on-off balance logic.

4.5.4 Hybrid skyhook-groundhook-balance control

All the three control strategies are integrated to get a hybrid control strategy which will have the advantages of all the three strategies. The contribution of different control strategies have been decided by the weighing factors δ and μ as shown in the following expression.

$$F_{hybrid-SH-GH-B} = \delta F_{skyhook} - \mu F_{groundhook} + (1 - \delta - \mu) F_{balance} \quad (4.60)$$

4.6 Summary

Different control strategies for semi-active suspension control have been discussed in this chapter. Different variance of skyhook, balance and groundhook control logics such as on-off and continuous algorithms have been described in detail. Hybrid control strategies have also been presented by combining two or more of the presented semi-active control logics. Logics are developed for both quarter vehicle model and half vehicle model so that same can be implemented in the bond graph modeling of these vehicle models.

CHAPTER 5

SIMULATION STUDY

5.1 Numerical Simulation

Computer simulation can compress the performance of a system over years into a few minutes of computer running time. Simulation models are relatively flexible and can be modified to accommodate the changing environment to the real situation. There is no area, where the technique of system simulation cannot be applied as the complexities of the problem increase the scope of application of simulation equations. At present, most of the simulation models are made by means of differential equations. In this research, quarter vehicle and half vehicle model suspension systems are investigated at different operating speed on different road profile inputs using bond graphs technique and simulator of SYMBOLS-Sonata® and MATLAB/Simulink® softwares are used.

5.2 Simulation Environment

The Simulator of Symbols sonata, which is the base post-processing module of SYMBOLS-Sonata®, is used for the simulation quarter and full car model on different road inputs at different operating speed.

5.2.1 SYMBOLS-Sonata® software

SYMBOLS-Sonata® is the next generation of SYMBOLS software (System Modeling by Bond graph Language and Simulation) running in Microsoft Windows 95/98/XP/7/NT 4.0 environment. It is a modeling, simulation and control systems software for a variety of scientific and engineering applications. Being a powerful research tool, it can help avoid unaffordable, sophisticated fabrications. Yet, one may know precisely the response characteristics of the simulated system. A model in SYMBOLS-Sonata® may be created using combination of bond graphic elements, block diagram elements in capsulated forms or others capsules. Even model can be created purely using capsules. Sub-model capsules can be imported from the huge capsules library or can even be created by the modeler. The pre-cast

capsules are not Pandora's boxes. They can be opened using the Bond pad editor and customized according to modeler need. Modeler may personalize and organize capsules created by them to separate their capsule group from other users.

Key Features of SYMBOLS Sonata Software is as follows

- Drawing a Bond graph model.
- Augmenting the model by numbering the bonds, assigning power direction.
- Causality, module of 2-port elements, bond activation etc.
- Validation of the Bond graph. Bond graph's integrity is validated after the model is created.
- Creation of non-integrated observers in form of detectors.
- Equations can be generated and displayed on single pallets.
- Creation of expressions.
- Generation of program code.
- Creation of sub-system models henceforth called as Capsules and incorporation of Capsules in a Bond graph model.
- Fault diagnosis.
- Preparing models for simulator and control modules.
- Export of sub-system and system models to MATLAB/Simulink environment.
- Integrated simulation environment.
- Easy to access control panels.
- Multiple and intelligent entry mode.
- Online plotting, pause, stop and resume option.
- Online parameter variation through slider during simulation.
- Continuous run simulation, multiple simulations of different systems at the same time.
- Simulation extension facility.

- Advance post simulation plotting facilities.
- Online code editing and compilation.
- Different integration methods for stiff equations.
- Multi-run facility with interpolated or discrete parameter values.
- Event handlers and notification messages.
- Direct debugging and variable tracking.
- Improved external date and chart interpolation routines.
- Export routines for Microsoft Excel Datasheet.

5.3 Simulation Properties

The bond graph model of the vehicle is simulated for 10 sec to obtain different output responses. Total 1024 records are used in the simulation and error is kept in the order of 5.0×10^{-4}. Runge-Kutta Gill method of fifth order is used in present work to solve the differential equations generated through bond graph model.

5.3.1 Runge-Kutta method

Runge-Kutta methods propagate a solution over an interval by combining the information from several Euler-style steps (each involving one evaluation of the state equations), and then using the information obtained to match a Taylor series expansion up to some higher order. This method treats every step in a sequence of steps in an identical manner. This is mathematically correct, since any point along the trajectory of an ordinary differential equation can serve as an initial point. Fifth-order Runge-Kutta method is used in present simulation work.

5.4 Simulation Parameters

Bond graph models for the 2-DOF quarter vehicle and 4-DOF half vehicle models are developed. In the expression window, the control algorithms are incorporated in the expression of the damping coefficient. The model is now subjected to base excitation of single half sine bump or random road disturbance for performance evaluation. The disturbance in the form of velocity is also fed into the expression of the source of flow (SF) of the bond graph model. The

parameters used for the simulation of the bond graph models of quarter vehicle and half vehicle are presented below.

5.4.1 Parameters for quarter vehicle model

The parameters for the simulation of the 2-DOF quarter car model are shown in Table 5.1. The parameters used by Blanchard [29] for a full car model are used in this work. The sprung mass or the mass of the full car has been scaled down to one forth for the quarter car model and other parameters for the front suspension are used.

Table 5.1: Model Parameter for 2-DOF quarter car model [29]

Parameter	Value	Unit	Parameter	Value	Unit
M_s	365	kg	c_{min}	258	Ns/m
M_u	40	kg	c_{max}	2838	Ns/m
k_s	19960	N/m	c_{sky}	1290	Ns/m
k_t	175500	N/m	c_{gnd}	1290	Ns/m

5.4.2 Parameters for half vehicle model

The parameters for the simulation of the 4-DOF half vehicle model are shown in Table 5.2. The parameters used by Blanchard [29] for a full car model are used in this work. For the half vehicle model, the sprung mass and pitch moment of inertia of the full car model in [29] have been reduced to half and other parameters are kept same for front suspension and rear suspension as shown below.

Table 5.2: Model Parameter for 4-DOF half vehicle model [29]

Parameter	Value	Unit	Parameter	Value	Unit
M_s	730	kg	$c_{max,f}$	2838	Ns/m
$M_{u,f}$	40	kg	$c_{sky,f}$	1290	Ns/m
$M_{u,r}$	35.5	kg	$c_{gnd,f}$	1290	Ns/m
I_{yy}	1230	kg.m^2	$c_{min,r}$	324	Ns/m
$k_{s,f}$	19960	N/m	$c_{max,r}$	3564	Ns/m
$k_{s,r}$	17500	N/m	$c_{sky,r}$	1620	Ns/m
$k_{t,f}$	175500	N/m	$c_{gnd,r}$	1620	Ns/m

$k_{t,r}$	175500	N/m	d_a	1.011	m
$c_{min,f}$	258	Ns/m	d_b	1.803	m

5.5 Road input

Two types of road profile inputs are used for the simulation of the quarter vehicle model, viz. half sine bump and random road inputs.

5.5.1 Half sine bump

The transient input chosen is a half sine bump, may be represented as [30]

$$y = \begin{cases} h * \sin\left(PI * \frac{V}{L} * t\right), & for\ 0 \le t \le \frac{L}{V} \\ 0, & otherwise \end{cases} \quad (5.1)$$

where, h is the height of the bump, which is 0.1m; L is the length of the bump, which is 0.3m; t is the time and V is the velocity of the vehicle. We have considered three condition for velocity, i.e., 60kmph, 80kmph and 100kmph. The bump profile is shown in Fig. 5.1.

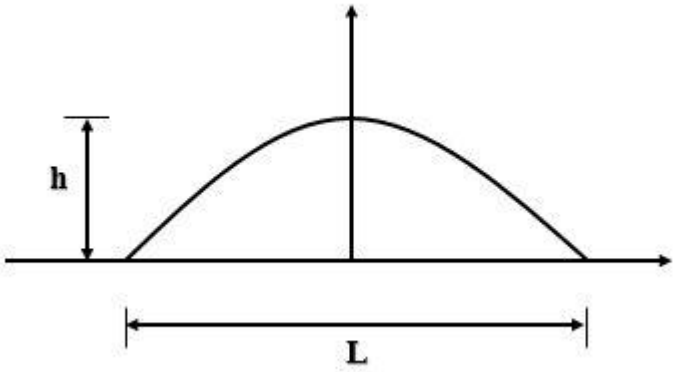

Fig. 5.1: Bump type surface irregularity

The expressions for $\frac{dy}{dt}$ with a switch function is used as an input in the expression of SF: Road input in bond graph model as shown in Fig. 3.3 (Chapter 3), which can be written as

$$SF = PI * h * \frac{V}{L} * \cos\left(PI * \frac{V}{L} * t\right) * swi(t, 0) * swi\left(\frac{L}{V}, t\right) \quad (5.2)$$

For the half vehicle model, the road input in the form of velocity or source of flow (SF) has been used as shown below,

Front Suspension:

$$SF_f = PI * h * \frac{V}{L} * \cos\left(PI * \frac{V}{L} * t\right) * swi(t, 0) * swi\left(\frac{L}{V}, t\right) \quad (5.3)$$

Rear Suspension:

$$SF_r = PI * h * \frac{V}{L} * \cos\left(PI * \frac{V}{L} * (t - \frac{d}{V})\right) * swi\left(t, \frac{d}{V}\right) * swi\left(\frac{(L+d)}{V}, t\right) \quad (5.4)$$

where, d is the distance between the front and the rear suspensions.

5.5.2 Random road input

A random road profile is generated according to the International Organization for Standardization (ISO 8608). It gives a depiction of the road profile through estimation of the PSD of the vertical displacements G_d, as a function of spatial frequency n ($n = \Omega/2\pi\ cycles/m$) and also of angular spatial frequency Ω. ISO 8608 introduces a classification which is evaluated in accordance with conventional values of spatial frequency $n_0 = 0.1\ cycles/m$ and angular spatial frequency $\Omega_0 = 1\ rad/m$. Eight classes of roads are identified; from class A to class H according to the values of $G_d(n_0)$ and $G_d(\Omega_0)$ established in ISO 8608 and are shown in Table 5.3 [31].

Table 5.3: ISO 8608 values of $G_d(n_0)$ and $G_d(\Omega_0)$

Road Class	$G_d(n_0)$ (10^{-6} m^3)		$G_d(\Omega_0)$ (10^{-6} m^3)	
	Lower Limit	Upper Limit	Lower Limit	Upper Limit
A	-	32	-	2
B	32	128	2	8
C	128	512	8	32
D	512	2048	32	128
E	2048	8192	128	512
F	8192	32768	512	2048
G	32768	131072	2048	8192

H	131072	-	8192	-
	$n_0 = 0.1\ cycles/m$		$\Omega_0 = 1\ rad/m$	

In simulation, ISO 8608 gives that the roughness of the road surface profile can be defined using the equations:

$$G_d(n) = G_d(n_0) \cdot \left(\frac{n}{n_0}\right)^{-w} \tag{5.5}$$

$$G_d(\Omega) = G_d(\Omega_0) \cdot \left(\frac{n}{n_0}\right)^{-w} \tag{5.6}$$

where, w is the waviness and taken to be 2 in this case. In this research, random road inputs have been developed by taking into consideration the PSD of vertical displacement G_d as a function of spatial frequency n. Beginning from a continuous road profile, for a specified value of spatial frequency n, loped within a frequency band Δn, the value of the PSD function is represented through the following expression:

$$G_d(n) = \lim_{\Delta n \to 0} \left(\frac{\Psi_x^2}{\Delta n}\right) \tag{5.7}$$

where, Ψ_x^2 is the mean square value of the component of the signal for the spatial frequency n, within the frequency band Δn. Accordingly, the road profile signal is discretized and therefore it is characterized by a sequence of elevation points evenly spaced. If L is the length of road profile and B is the sampling interval, then the maximum theoretical sampling spatial frequency is $n_{max} = 1/B$ and the maximum effective sampling spatial frequency is $n_{eff} = n_{max}/2$ and, the discretized spatial frequency values n_i are equally spaced within the frequency domain, with an interval of $\Delta n = 1/L$. The generic spatial frequency value n_i can be regarded as $i \cdot \Delta n$ and (5.7) can be written in the discrete form:

$$G_d(n_i) = \frac{\Psi_x^2(n_i, \Delta n)}{\Delta n} = \frac{\Psi_x^2(i \cdot \Delta n, \Delta n)}{\Delta n} \tag{5.8}$$

where, i varying from 0 to $N = n_{max}/\Delta n$. If the road profile can be defined through a simple harmonic function as:

$$h(x) = A_i \cos(2\pi \cdot n_i \cdot x + \varphi) = A_i \cos(2\pi \cdot i \cdot \Delta n \cdot x + \varphi) \tag{5.9}$$

where, A_i is the amplitude, n_i is the spatial frequency and φ is the phase angle. It can be shown that mean square value of this harmonic signal is

$$\Psi_x^2 = \frac{A_i^2}{2} \tag{5.10}$$

Therefore,

$$G_d(n_i) = \frac{\Psi_x^2(n_i)}{\Delta n} = \frac{A_i^2}{2 \cdot \Delta n} \tag{5.11}$$

It has been shown in several works that if the PSD function of vertical displacements is known, it is possible to develop an artificial road profile using the expression (5.11) and presuming a random phase angle φ_i following a uniform probabilistic distribution within the $0 - 2\pi$ range. The artificial profile can be given as:

$$h(x) = \sum_{i=0}^{N} A_i \cos(2\pi \cdot n_i \cdot x + \varphi_i) = \sum_{i=0}^{N} \sqrt{2 \cdot \Delta n \cdot G_d(i \cdot \Delta n)} \cdot \cos(2\pi \cdot i \cdot \Delta n \cdot x + \varphi_i) \tag{5.12}$$

Using Eq. (5.5) in Eq. (5.12), a random road profile can be generated according to ISO classification by the following equation,

$$h(x) = \sum_{i=0}^{N} \sqrt{\Delta n} \cdot 2^k \cdot 10^{-3} \cdot \left(\frac{n_0}{i \cdot \Delta n}\right) \cdot \cos(2\pi \cdot i \cdot \Delta n \cdot x + \varphi_i) \tag{5.13}$$

where, x is the abscissa variable from 0 to L; $\Delta n = 1/L$; $n_{max} = 1/B$; $N = n_{max}/\Delta n = L/B$; where L=250, N=100; k is a constant value depending from ISO road profile classification. In this work, k is a constant value depending from ISO road profile classification, it assumes integers increasing from 3 to 9, corresponding to the profiles from class A to class H (as shown in Table 5.4); here k is assumed to take the value 3 corresponding to the class A road profile and $G_d(n_0)$ is taken to be 32. $n_0 = 0.1\, cycles/m$; φ_i random phase angle following an uniform probabilistic distribution within the $0 - 2\pi$ range. The random road profile thus generated is shown in Fig. 5.2.

Table 5.4: k values for ISO road roughness classification

Road Class		k
Lower Limit	Upper Limit	
A	B	3
B	C	4
C	D	5
D	E	6

E	F	7
F	G	8
G	H	9

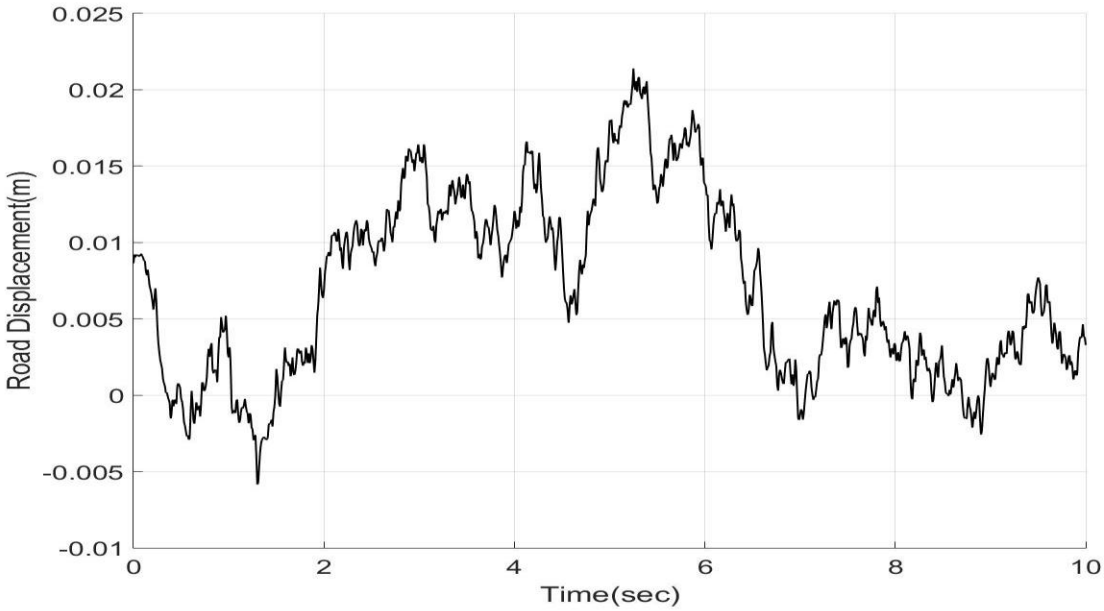

Fig. 5.2: Random road input to the vehicle suspension system

Fig. 5.2 represents the profile obtained by the MATLAB programming of the previously discussed ISO 8608 random road input. The profile shows a continuous unevenness of the random type road with maximum magnitude of 0.02m in upward direction from the neutral position and 0.005m in downward direction as can be evident from the figure.

5.6 Summary of the chapter

Parameters for simulation and road profile inputs are described in this chapter. Simulations were performed for both quarter vehicle and half vehicle models with bump and random road inputs for different velocities of the vehicle and results are obtained for sprung mass acceleration, sprung mass displacement and tire deflection to evaluate the performance of different control strategies incorporated in the semi-active suspension design. The detailed results are presented in the next chapter with discussions.

CHAPTER 6
RESULTS AND DISCUSSIONS

6.1 Introduction

The previous chapters have discussed the numerical and computational models for semi-active suspension systems of quarter car and half car models, different semi-active control strategies available and considered in this work and the parameters and road profile inputs for the study of the performance of the semi-active suspension systems. Different basic semi-active control logics have been considered such as skyhook, balance and groundhook control. Hybrid control strategies by combining any two or all three of the mentioned strategies are also presented.

In this chapter, the numerical investigation of the performance of the different semi-active control strategies are described. A 2-DOF quarter car and a 4-DOF half car models are used to study the vibration isolation efficiency and road holding performance. Different parameters such as body acceleration, unsprung mass acceleration, body displacement, tire deflection and transmissibility of acceleration are considered to evaluate the performance. The parameters of the semi-active systems are compared with those of a traditional passive suspension system.

6.2 Performance of Quarter Car Model for Bump Type Profile Input

A quarter car model has been subjected to a road input of half sine bump as discussed in the previous chapter. Simulations have been carried out for the bond graph model of the quarter car model in the software environment of SYMBOLS Sonata®. The results have been presented in three sections- i) On-off strategies, ii) Continuous strategies and iii) Hybrid strategies.

6.2.1 Performance of on-off control strategies

The performance of the different on-off control algorithms as discussed in chapter 2 are presented in this section. The 2-DOF quarter car model has been subjected to a half sine bump road input and different on-off logics such as skyhook, balance and groundhook strategies have been applied to control the damping force of the suspension system. The results were obtained

in terms of body acceleration, unsprung mass acceleration, body displacement and transmissibility, both in time and frequency domain.

6.2.1.1 Body acceleration

Fig. 6.1 shows the body acceleration vs time plot for the passive suspension system and semi-active system controlled with different on-off strategies.

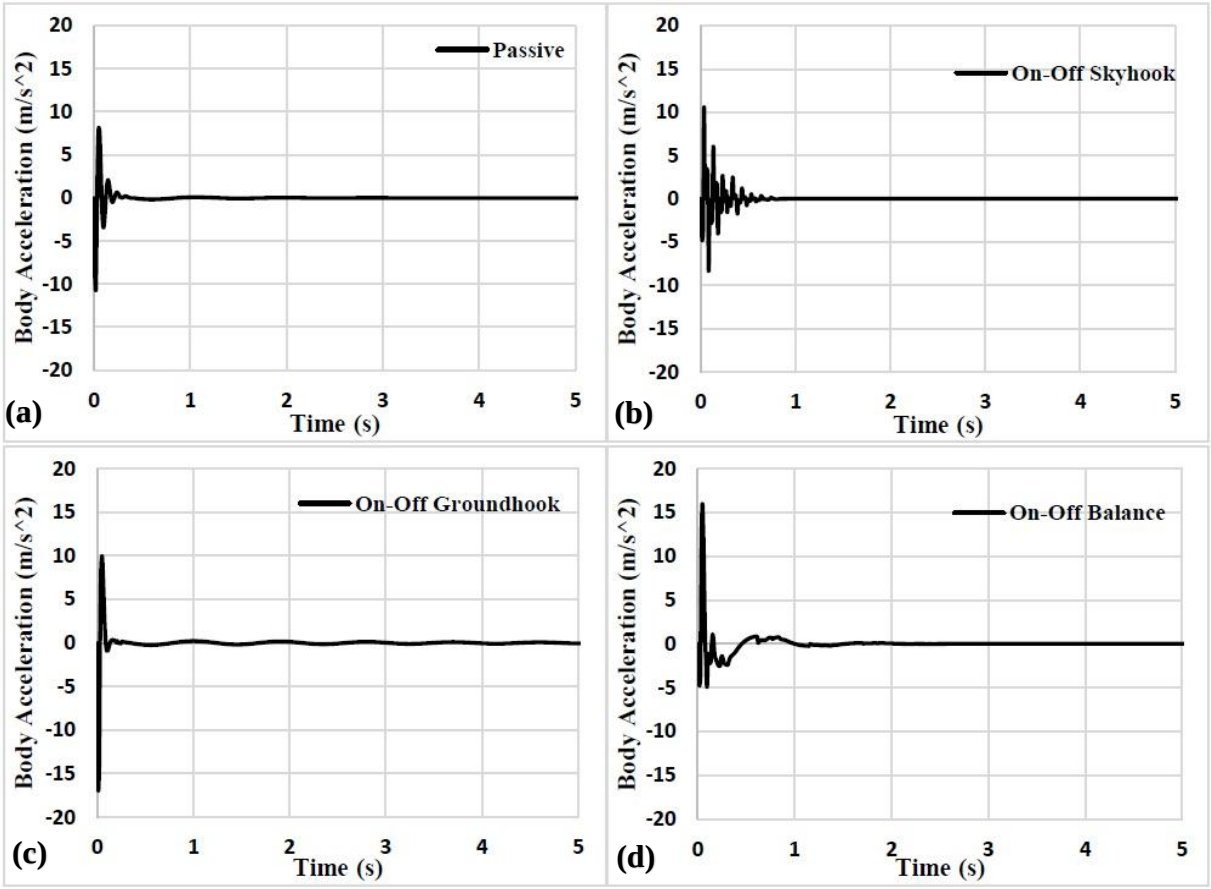

Fig. 6.1: Body acceleration vs time plot of quarter car at 60 kmph for (a) passive suspension system (b) on-off skyhook control (c) on-off groundhook control and (d) on-off balance control

Fig. 6.1 (a) shows the acceleration for the passive system. The maximum amplitude of body acceleration reached with all on-off control strategies is more than that of a passive suspension system, which is clearly depicted from Fig 6.1 (b-d). However, the settling time for the passive suspension system is approximately 2.5 seconds whereas, that of an on-off skyhook logic is found to be approximately 1 second. The settling time has been reduced by 60% approximately. But there is an added disadvantage of the on-off skyhook control. Whenever

the condition function i.e., the product of the absolute velocity of the sprung mass and the relative velocity across the suspension, changes sign, the damper is switched between the on and the off states. Hence, there is a sudden rise in the amplitude of body acceleration and the passenger or the driver will feel a sudden jerk, which can be considered uncomfortable. The on-off groundhook logic does not show such sudden jerks as shown in Fig. 6.1 (c). But the settling time for this logic is very large and hence, the vibration can be felt for a longer duration. In case of on-off balance logic, there is significant reduction in the sudden jerks, but the settling time is almost same as that for a passive system as depicted in Fig. 6.1 (d).

6.2.1.2 Unsprung mass acceleration

Fig. 6.2 demonstrates the response of the system's un-sprung mass acceleration in time domain.

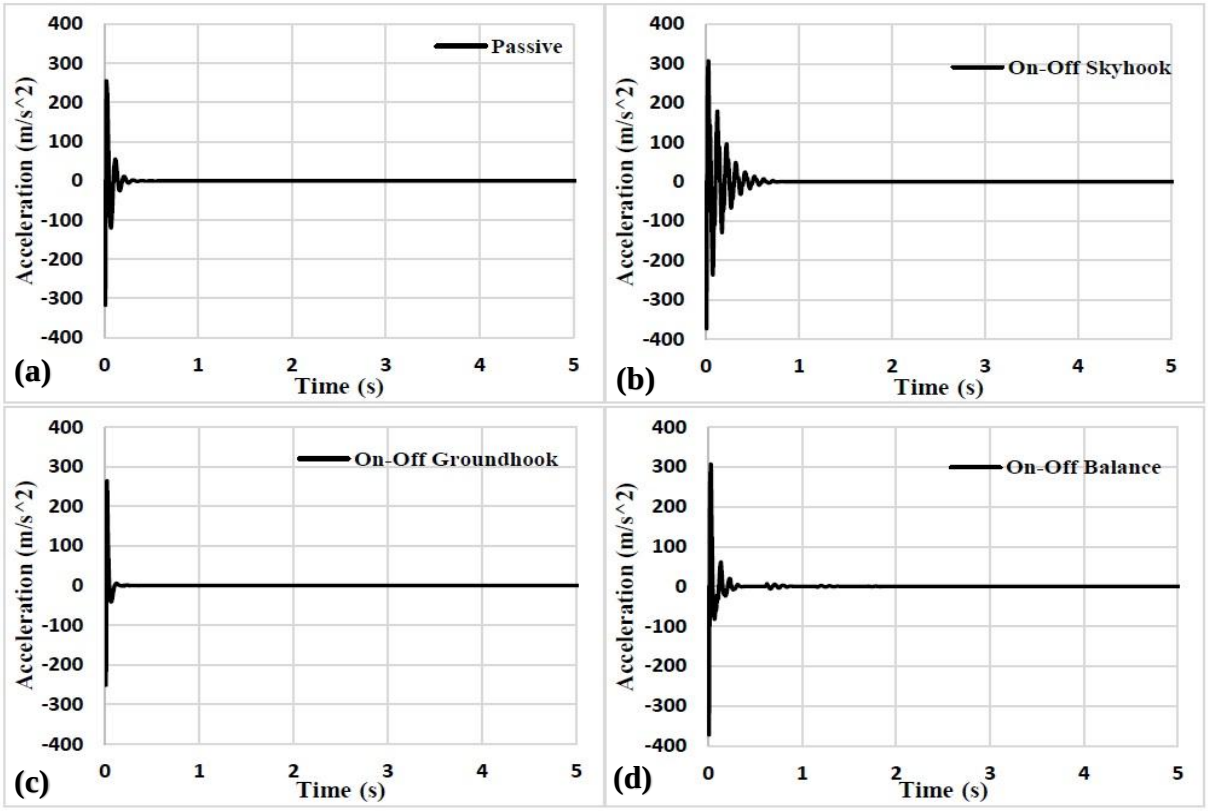

Fig. 6.2: Unsprung mass acceleration vs time plot of quarter car at 60 kmph for (a) passive suspension system (b) on-off skyhook control (c) on-off groundhook control and (d) on-off balance control

Un-sprung acceleration of passive system is shown in Fig 6.2 (a). It can be shown from Fig. 6.2 (b) that the on-off skyhook logic has increased magnitude of the unsprung mass acceleration as well as more settling time. The groundhook logic gives better performance in this regard. The magnitude is less than that of a passive system or the other two control strategies as can be seen in Fig. 6.2 (c). The settling time is also less in case of on-off groundhook control and is approximately 0.25 seconds, whereas the settling time for passive system is about 0.5 seconds. This is due to the inherent nature of groundhook logic, which gives better road holding as compared to other logics. In Fig. 6.2 (d), on-off balance logic has also increased magnitude at the beginning but immediately dampens out to small values. But the settling time is more in this case.

6.2.1.3 Body displacement

Fig. 6.3 exhibits the body displacement vs time plot for the passive as well as semi-active suspension systems controlled with different on-off strategies.

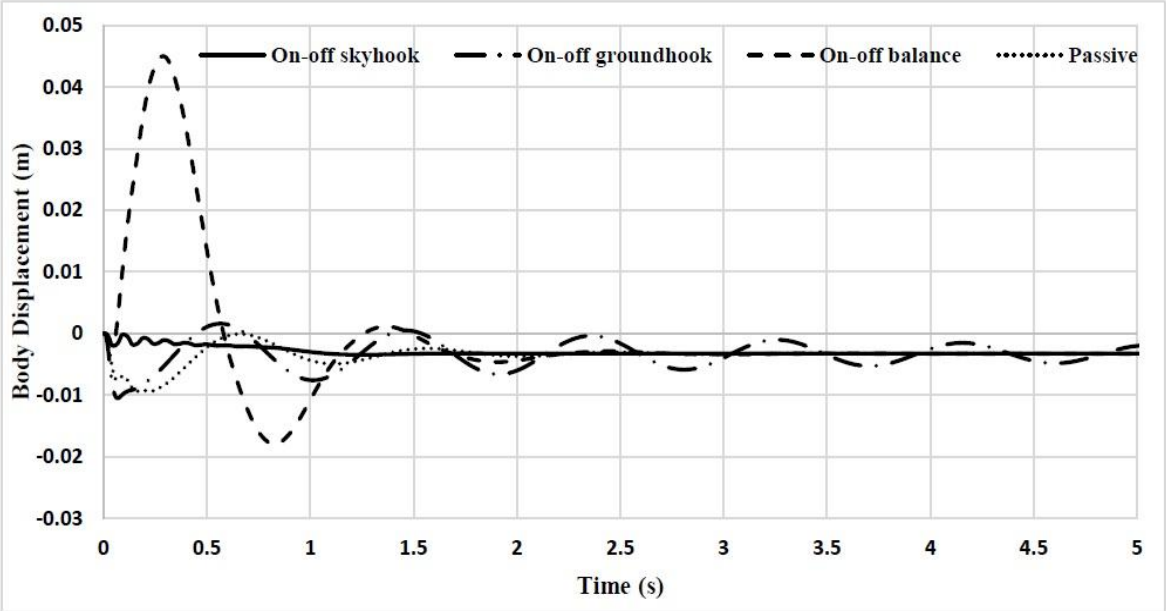

Fig. 6.3: Body displacement vs time of quarter car at 60kmph for on-off logics

It can be seen from the Fig. 6.3 that the magnitude of displacement is considerably less for on-off skyhook control as compared to any other system. The balance logic exhibits a drastic increase in magnitude of displacement as can be seen in Fig. 6.3. Groundhook logic has

the maximum settling time as it continues to vibrate in a periodic manner as shown in figure. The maximum value of displacement achieved by passive system is approximaltely 0.009m whereas, the same has been reduced drastically to 0.0035m in case of on-off skyhook control which is approximately 60% less. The settling time for passive system is approximately 4.5 seconds. The same has been reduced to 2.5 seconds in case of on-off skyhook logic which is almost 45% less than that of passive system. The displacement response of the on-off skyhook control strategy is better in both aspects.

6.2.1.4 Transmissibility

Fig. 6.4 represents the transmissibility of acceleration in between sprung mass and unsprung mass in frequency domain. From figure, it is obvious that the on-off skyhook logic has shown extreme performance regarding reducing transmissibility of vibration from unsprung to sprung mass. However, the transmissibility is found to be more for groundhook and balance logics. Maximum value of transmissibility achieved by passive system is approximately 0.22 whereas, the same for skyhook is less than 0.1. On the contrary, groundhook and balance logics have maximum value of transmissibility at 0.6 and 0.75 respectively.

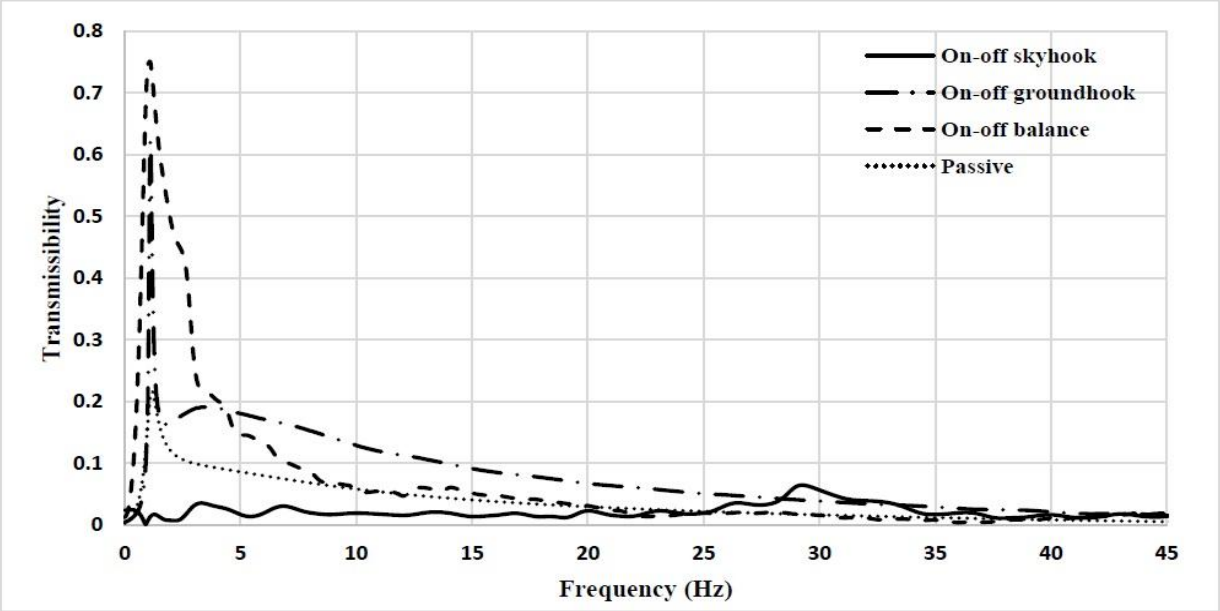

Fig. 6.4: Transmissibility of acceleration of quarter car at 60 kmph for on-off logics

6.2.2 Performance of continuous control strategies

The results for continuous control algorithms have been presented in this section.

6.2.2.1 Body acceleration

The body acceleration response of different continuous control strategies in time domain, which is shown in Fig 6.5. It can be observed from Fig. 6.5 that for all the three continuous strategies, the maximum magnitude of acceleration has been reduced to almost half of that of a passive suspension system. However, the settling time has been compromised in the case of continuous strategies and a continuous vibration reducing in magnitude over time can be felt. The settling time for continuous skyhook and continuous balance logics have been found to be in between 3-3.5 seconds as can be seen in Fig. 6.5 (b) and (d) respectively, whereas that for passive system is 2.5 seconds (Fig. 6.5 (a)). Groundhook logic has poor settling time, a periodic disturbance is present for a prolonged duration in case of continuous groundhook logic (Fig. 6.5 (c)).

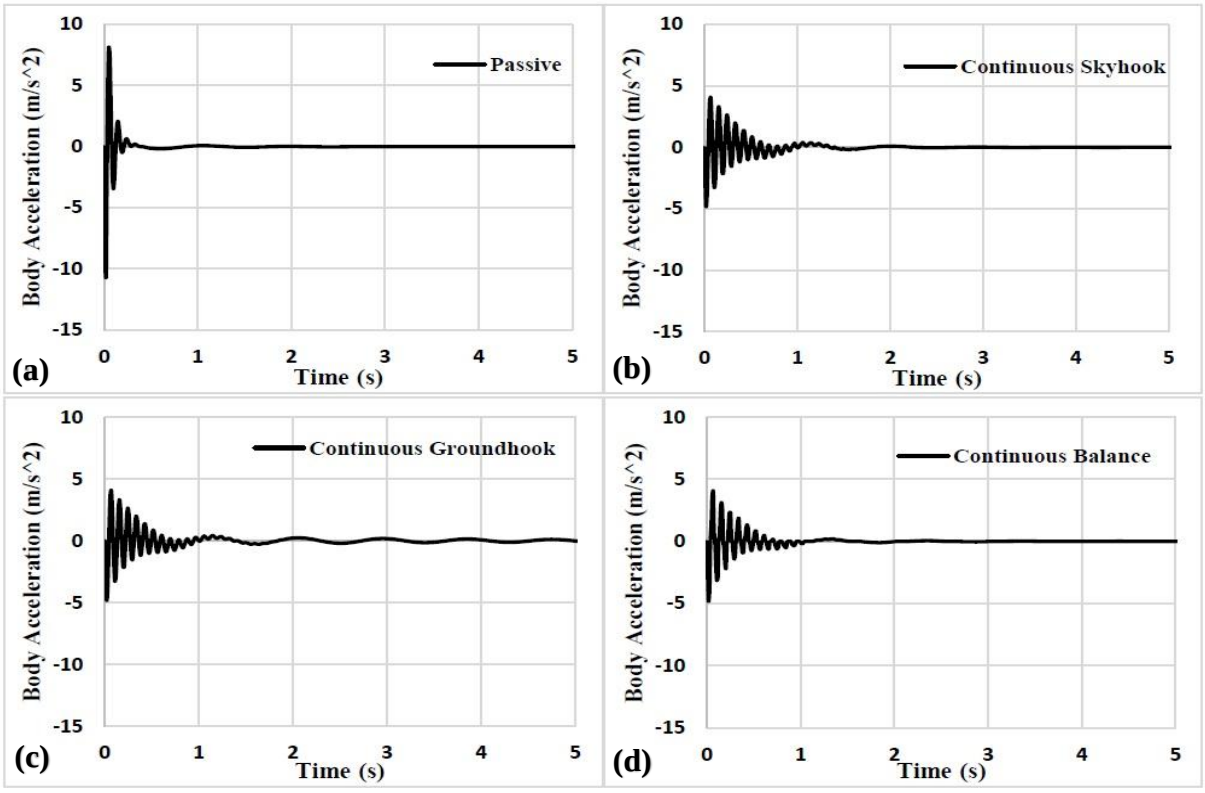

Fig. 6.5: Body acceleration vs time plot of quarter car at 60 kmph for (a) passive suspension system (b) continuous skyhook control (c) continuous groundhook control and (d) continuous balance control

6.2.2.2 Unsprung mass acceleration

Fig. 6.6 displays the acceleration response of the un-sprung mass of the vehicle model in time domain. It can be seen from figure that for all the three continuous control strategies, the magnitude as well as the settling time has been compromised for the unsprung mass acceleration. Whereas the amplitude is slightly higher in each case, the settling time is more. The wheel of the vehicle has to undergo a prolonged vibration before coming to a steady state.

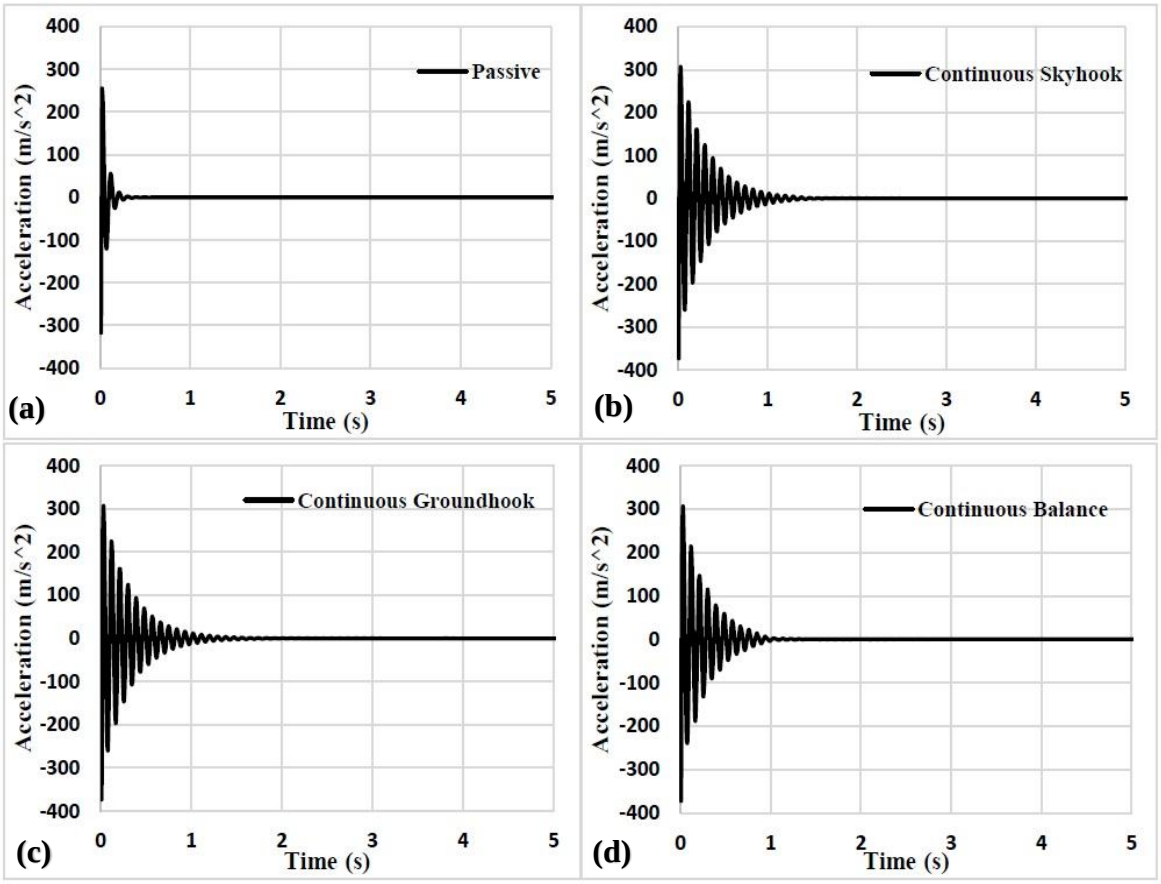

Fig. 6.6: Unsprung mass acceleration vs time plot of quarter car at 60 kmph for (a) passive suspension system (b) continuous skyhook control (c) continuous groundhook control and (d) continuous balance control

6.2.2.3 Body displacement

Fig. 6.7 demonstrates the body displacement vs time plot for all three strategies. The maximum magnitude of displacement is found more for all three strategies as compared to passive system. Settling time for continuous skyhook logic is at per with the passive system. Continuous

balance and continuous groundhook logics have more settling time. A prolonged periodic oscillation of the displacement response can be seen for continuous groundhook.

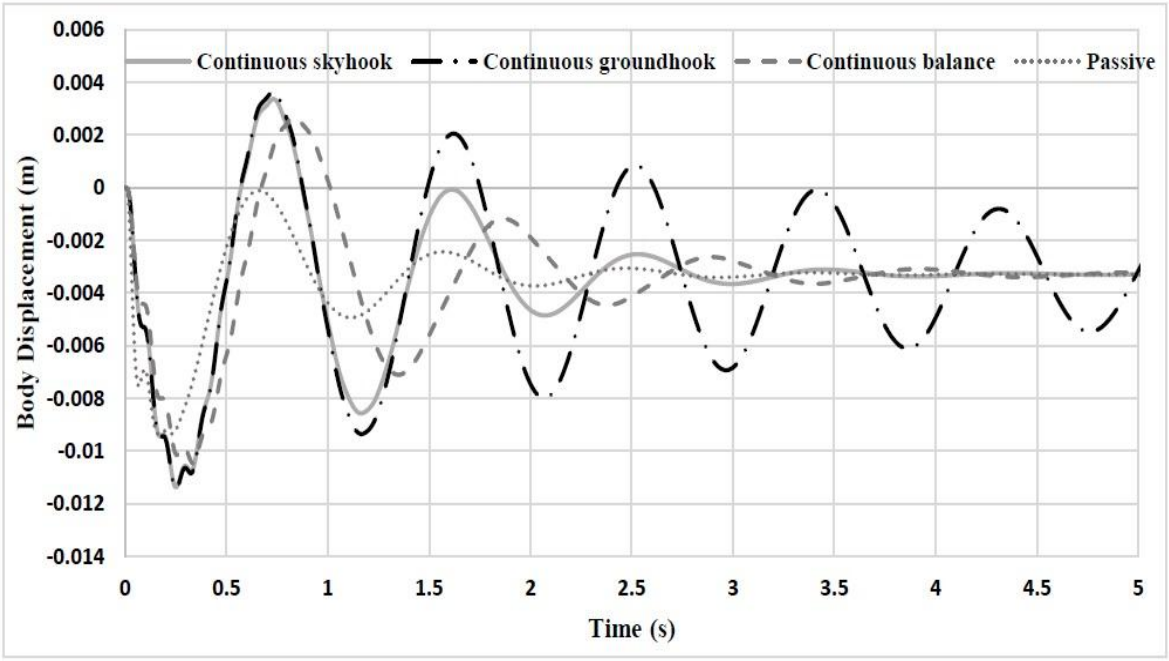

Fig. 6.7: Body displacement vs time of quarter car at 60kmph for continuous logics

6.2.2.4 Transmissibility

The transmissibility of acceleration at 60kmph has been shown in Fig. 6.8.

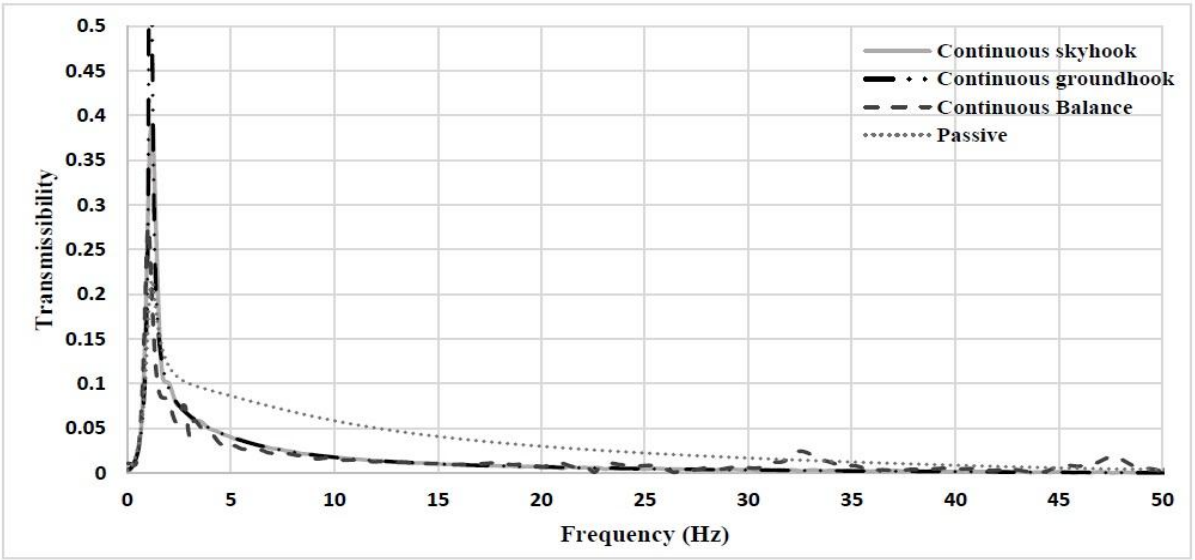

Fig. 6.8: Transmissibility of acceleration of quarter car at 60 kmph for continuous logics

It can be observed that the transmissibility of acceleration is more for all the three continuous strategies. Maximum transmissibility for continuous balance is found to be comparatively less than skyhook and groundhook logics and is approximately 0.25. For continuous skyhook logic, the value of maximum transmissibility is found to be approximately 0.4 whereas, for continuous groundhook, it's even more.

6.2.3 Performance of hybrid control strategies

The performance of the quarter car model has been carried out for four different hybrid combinations, which are follows; - i) Hybrid skyhook-groundhook (HY-SH-GH), ii) Hybrid skyhook-balance (HY-SH-B), iii) Hybrid groundhook-balance (HY-GH-B) and iv) Hybrid skyhook-groundhook-balance (HY-SH-GH-B). The response of semi active suspension with different control strategies has been presented in this research work.

6.2.3.1 Body acceleration

Fig. 6.9 demonstrates the acceleration response of the sprung mass of the quarter vehicle controlled by different hybrid strategies. The weighing factors for all four hybrid logics have been optimized by hit and trial method and final values are presented in Table 6.1 below.

Table 6.1: Optimized value of weighing factors for hybrid logic

Hybrid logic	α	β	γ	δ	μ
HY-SH-GH	0.85	---	---	---	---
HY-SH-B	---	0.4	---	---	---
HY-GH-B	---	---	0.45	---	---
HY-SH-GH-B	---	---	---	0.65	0.15

It can be observed from Fig. 6.9 (a) and (d) that the responses of HY-SH-GH and HY-SH-GH-B logics are better in case of both magnitude and settling time respectively. However, the magnitude of acceleration is maximum for the HY-GH-B combination. The settling time is almost better for HY-SH-GH and HY-SH-GH-B logics than HY-SH-B and HY-GH-B logics, which can be seen in Fig. 6.9 (b) and (c). The comparable study of HY-SH-GH and HY-SH-GH-B logics shows that HY-SH-GH-B logic have a slightly lower value of acceleration. The sudden jerks due to uneven road in on-off skyhook logic has been

significantly reduced in case of hybrid strategies. HY-SH-GH-B logic has less severe sudden jerks when the condition functions have changed their sign as compared to HY-SH-GH logic, which is shown in Fig 6.10. The settling time for both the logics have been found to be approximately 0.5 seconds which is 80% less than the passive suspension system and 50% less than simple on-off skyhook logic.

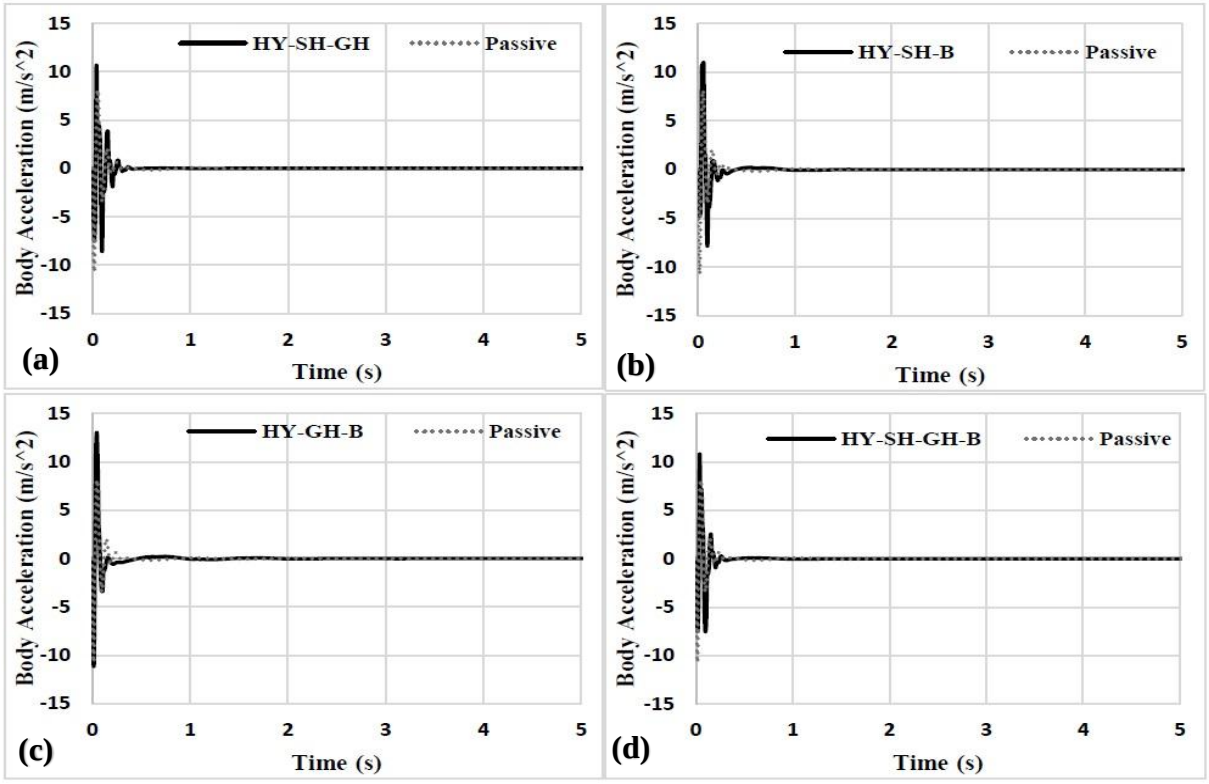

Fig. 6.9: Body acceleration vs time plot of quarter car at 60 kmph for (a) HY-SH-GH (b) HY-SH-B (c) HY-GH-B and (d) HY-SH-GH-B control

In Fig. 6.10, it can be observed that the magnitude of acceleration for sprung mass is less for the HY-SH-GH-B logic (Fig. 6.10 (a)) as compared to HY-SH-GH logic (Fig. 6.10 (b)). Moreover, the sudden jerks caused by the switching of the damper in between the on and the off state as the condition functions change their direction is less severe in case of the former strategy. The severity of the jerks is directly related to passenger's comfort. HY-SH-GH-B logic can thus provide a better comfort as compared to HY-SH-GH logic. Both the logics have better performance as compared to conventional on-off strategies, especially on-off skyhook logic, which provides numerous jerks before coming to a steady state position.

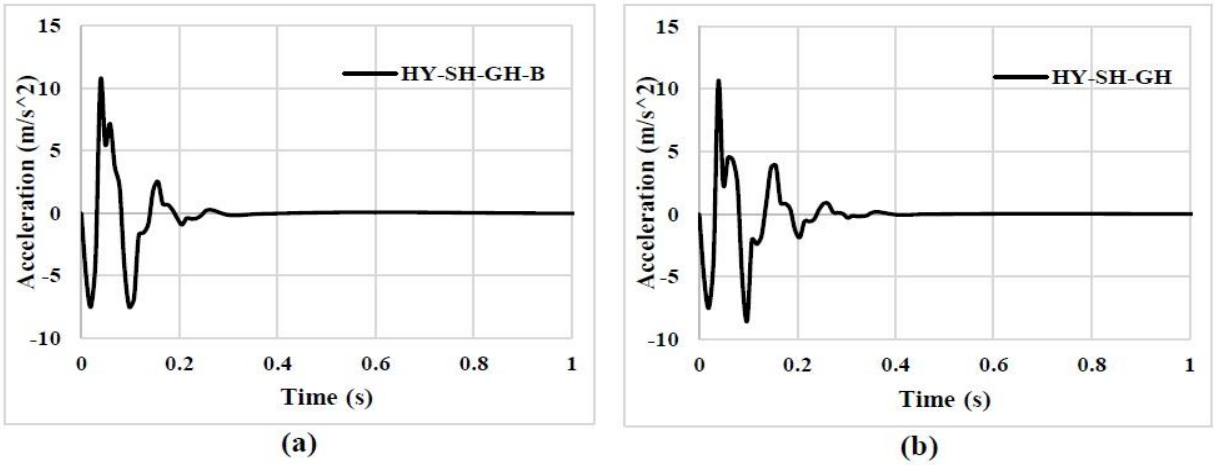

Fig. 6.10: Acceleration response of sprung mass of quarter car for (a) HY-SH-GH-B and (b) HY-SH-GH

6.2.3.2 Unsprung mass acceleration

Acceleration response of un-sprung mass in time domain has been displayed in Fig. 6.11.

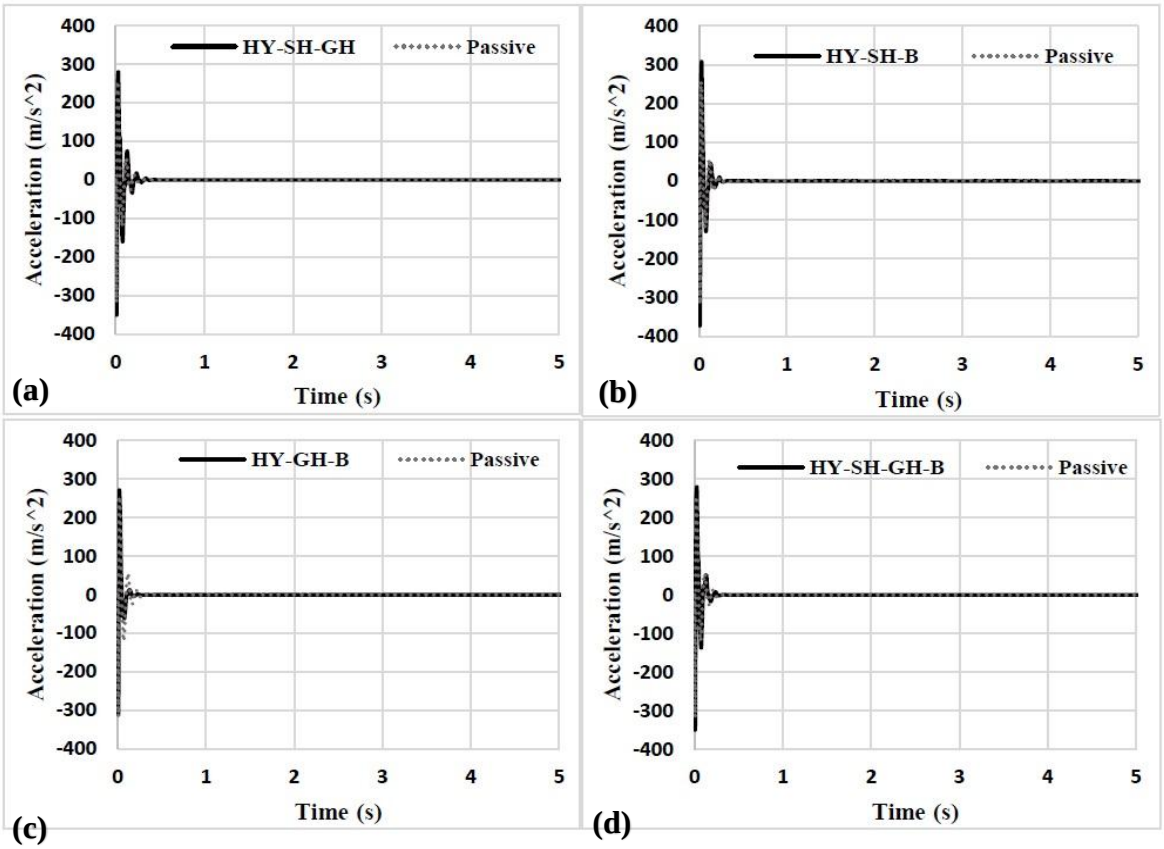

Fig. 6.11: Unsprung acceleration vs time plot of quarter car at 60 kmph for (a) HY-SH-GH (b) HY-SH-B (c) HY-GH-B and (d) HY-SH-GH-B control

Results have shown that the acceleration response of the un-sprung mass is best for the hybrid combination of groundhook and balance logic (Fig. 6.11 (c)). The magnitude as well as the settling time is minimum for this strategy. Other strategies have a slightly higher settling time and the magnitude of acceleration is also comparatively more than HY-GH-B as well as passive system. The settling time is approximately 0.5 seconds for passive systems and also for all hybrid strategies except for HY-GH-B, for which the settling time is 0.25 seconds which is 50% less. The magnitude is maximum for the HY-SH-B logic as can be seen in Fig. 6.11 (b).

6.2.3.3 Body displacement

Body displacement vs time for speed of 60kmph has been plotted and shown in Fig. 6.12.

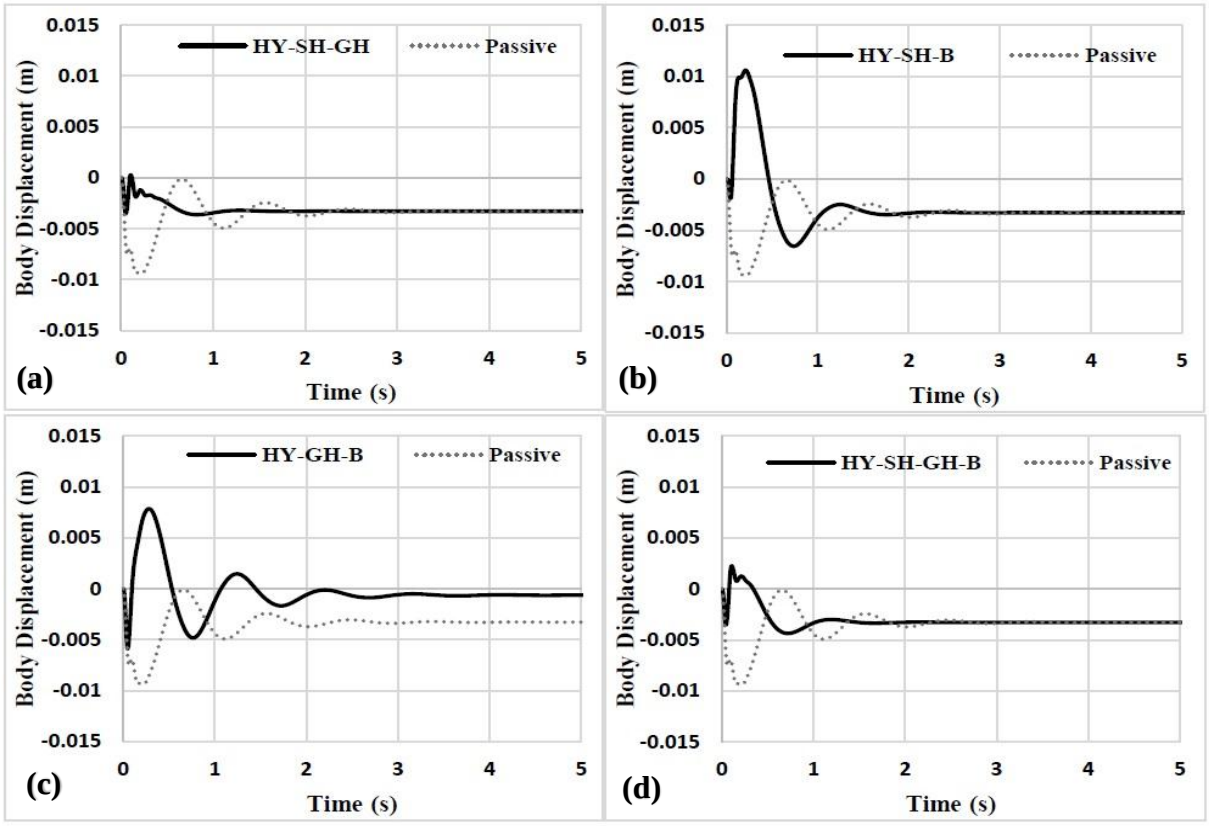

Fig. 6.12: Body displacement vs time plot of quarter car at 60 kmph for (a) HY-SH-GH (b) HY-SH-B (c) HY-GH-B and (d) HY-SH-GH-B control

It can be observed from Fig. 6.12 (a) that the HY-SH-GH logic has the best performance regarding displacement response as the maximum amplitude achieved is less for

this logic. HY-SH-GH-B logic gives a comparable result with a slightly higher amplitude of displacement (Fig. 6.12 (d)). Other two logics have more magnitude of body displacement as well as the settling time. The combination of skyhook-groundhook and skyhook-groundhook-balance has less settling time as well.

6.2.3.4 Transmissibility

Fig. 6.13 presents the transmissibility of acceleration between sprung and unsprung masses for all hybrid control logics. It is found that the HY-SH-GH and HY-SH-GH-B logics have better performance in terms of transmissibility of acceleration. The maximum transmissibility achieved is much less than that of a passive system. For both the logics, the maximum transmissibility is found to be approximately about 0.07 whereas, for a passive system, maximum transmissibility is found to be around 0.22. For HY-SH-B and HY-GH-B logics, maximum transmissibility is found to be approximately 0.25 which is even more than the passive system.

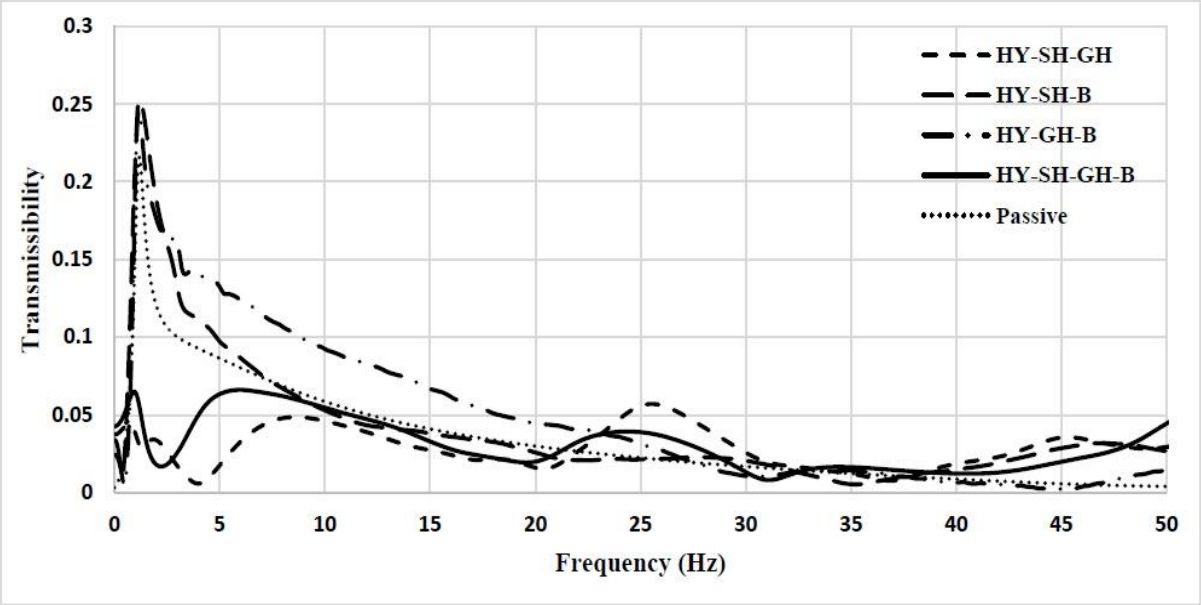

Fig. 6.13: Transmissibility of acceleration of quarter car at 60 kmph for hybrid logics

6.3 Performance of Half Car Model for Bump Type Profile Input

A half car model has been subjected to a road input of half sine bump as discussed in the previous chapter. Simulations have been carried out for the bond graph model of the half car

model in the software environment of SYMBOLS Sonata®. The results have been presented in three sections- i) On-off strategies, ii) Continuous strategies and iii) Hybrid strategies.

6.3.1 Performance of on-off control strategies

The performance of the different on-off control algorithms for semi active suspension system in a 4-DOF half car model as discussed in chapter 2 are presented in this section. The half car model has been subjected to a bump type road input of half sine nature and different on-off logics such as skyhook, balance and groundhook strategies have been applied to control the damping force of the suspension system. The results were obtained in terms of body acceleration, pitch acceleration, unsprung mass acceleration, body displacement, pitch angle and transmissibility, both in time and frequency domain.

6.3.1.1 Body acceleration

Fig. 6.14 shows the body acceleration vs time plot for the passive suspension system and semi-active system controlled with different on-off strategies. In Fig. 6.14 (a), the response of passive suspension system has been plotted. It is found that the maximum amplitude of acceleration achieved is in the range of 7.5 m/s^2 and the settling time is found to be approximately 4 seconds. In case of on-off skyhook logic (Fig. 6.14 (b)), the maximum magnitude has been found to be 7 m/s^2 which is almost same as passive system. But there are sudden increase or decrease of the amplitude of acceleration at numerous times when the condition function has changed its direction and hence, the damper is switched in between on and off states. This is because of the sudden rise or fall of the damping force as the damper is switched. This will lead to sudden jerks which may be bothersome to the passengers. The settling time is however reduced to 1.5 seconds with a decrement of 62.5% approximately than passive system. Fig. 6.14 (c) shows the response of on-off groundhook logic which has a maximum amplitude of 10 m/s^2 and also the settling time has been increased. But there are no sudden jerks developed in this case. The on-off balance logic (Fig. 6.14 (d)) has a maximum amplitude of 8.5 m/s^2 approximately and the settling time is also at per with passive system. However, there are less jerks in this case.

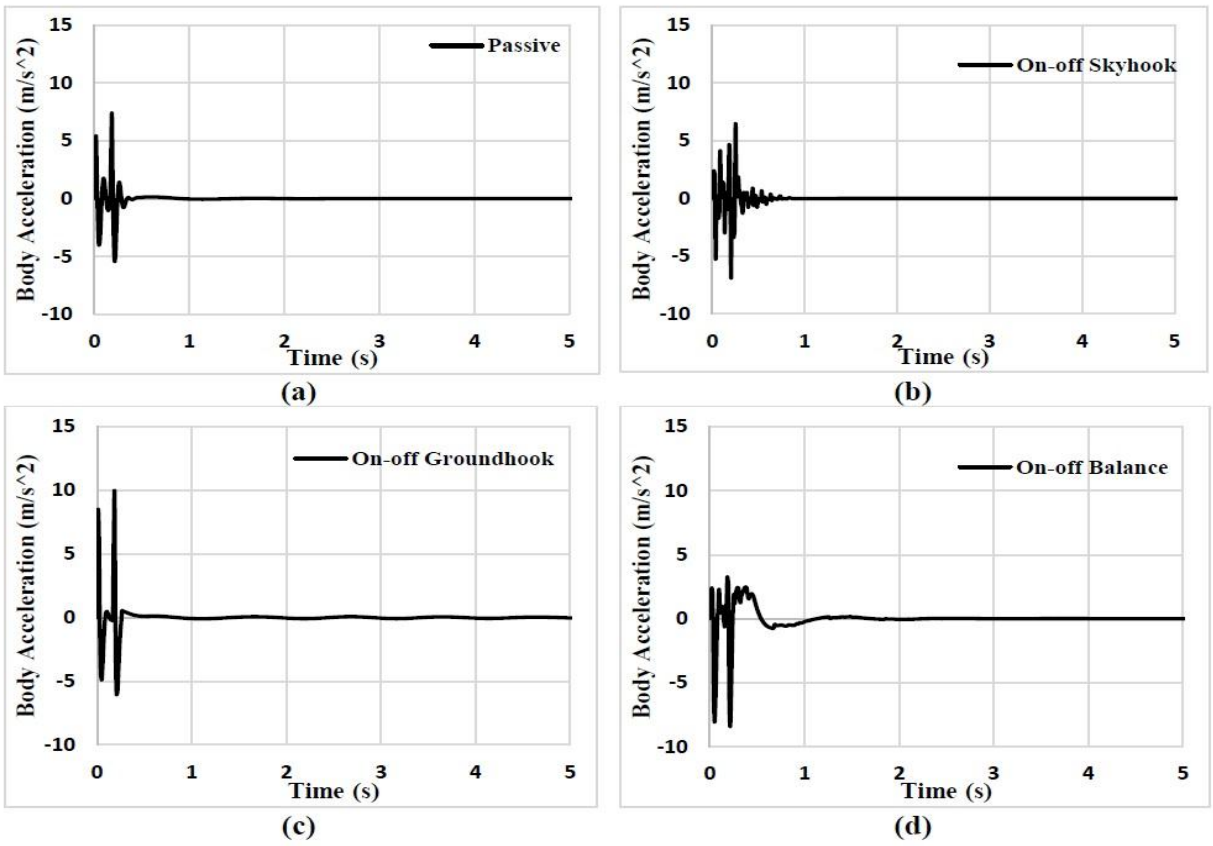

Fig. 6.14: Body acceleration vs time plot of half car at 60 kmph for (a) passive suspension system (b) on-off skyhook control (c) on-off groundhook control and (d) on-off balance control

6.3.1.2 Pitch acceleration

Fig. 6.15 represents the response of the system in terms of pitch acceleration. The response of passive system has been shown in Fig. 6.15 (a) where, the maximum amplitude has been found to be around 8 rad/s^2 and the settling time is approximately 4 seconds. In case of on-off skyhook logic, the amplitude is slightly more than 8 rad/s^2 but the settling time is reduced to 1.5 seconds (Fig. 6.15 (b)). But similar to body acceleration response, there are sudden jerks that can be felt. On-off groundhook logic (Fig. 6.15 (c)) has a maximum pitch acceleration of magnitude 11 rad/s^2 and the settling time is also increased with a prolonged periodic disturbance. Fig. 6.15 (d) shows the response of on-off balance logic. Here the maximum amplitude achieved is 11 rad/s^2 and the settling time is at per with passive system. On-off skyhook logic has better performance in terms of settling time but the sudden jerks generated may be unacceptable to the passengers.

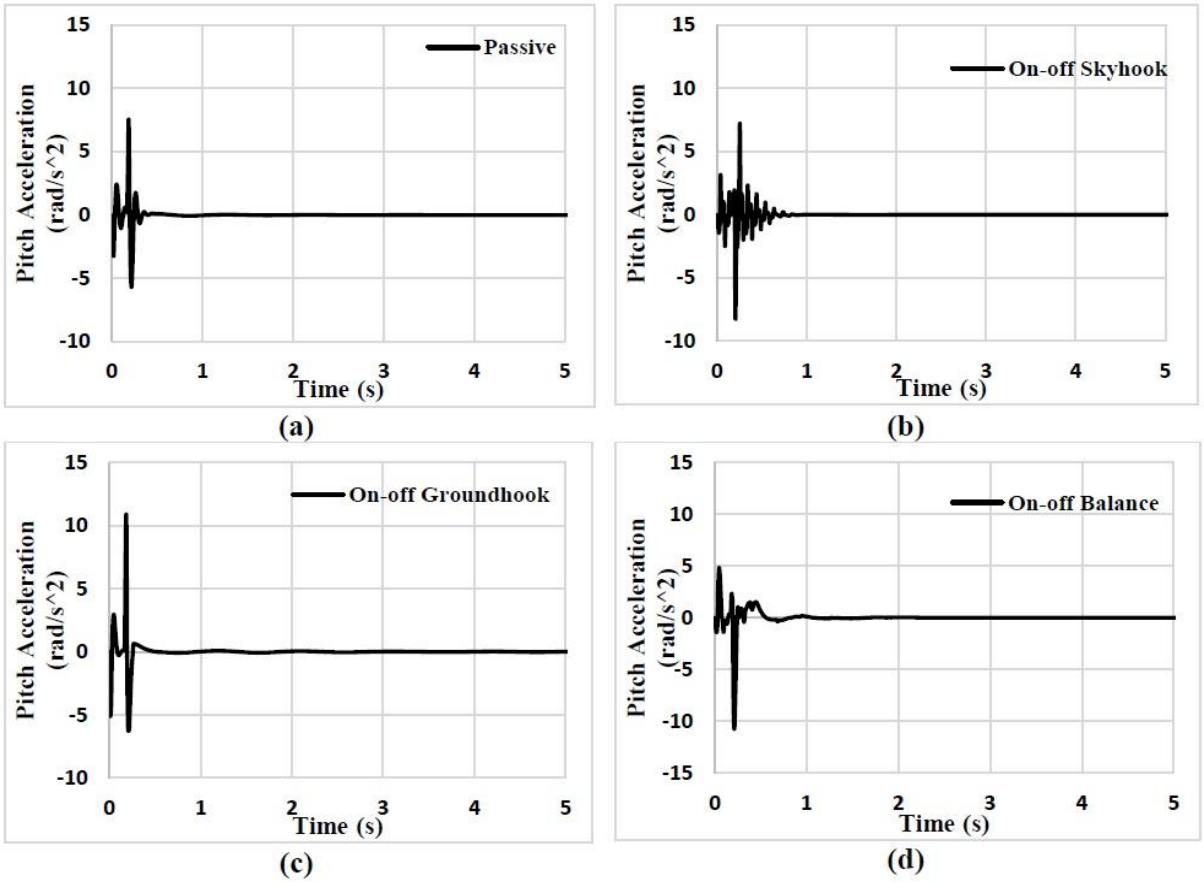

Fig. 6.15: Pitch acceleration vs time plot of half car at 60 kmph for (a) passive suspension system (b) on-off skyhook control (c) on-off groundhook control and (d) on-off balance control

6.3.1.3 Unsprung mass acceleration

Acceleration response of the unsprung mass of the front suspension has been demonstrated in Fig. 6.16. It can be seen in Fig. 6.16 (a) that the unsprung acceleration has a maximum amplitude of 320 m/s^2 approximately and settling time of 0.5 seconds for passive system. However, for on-off skyhook logic (Fig. 6.16 (b)), the amplitude is around 380 m/s^2 and settling time is slightly increased to 0.75 seconds. In Fig. 6.16 (c), for on-off groundhook logic the amplitude has been reduced to 270 m/s^2 which is the minimum of all. On-off groundhook logic has achieved the best performance in terms of unsprung mass acceleration. For on-off balance logic, the magnitude is found to be around 380 m/s^2 and settling time is also increased as can be seen in Fig. 6.16 (d). Comparable performance for the rear suspension has also been observed.

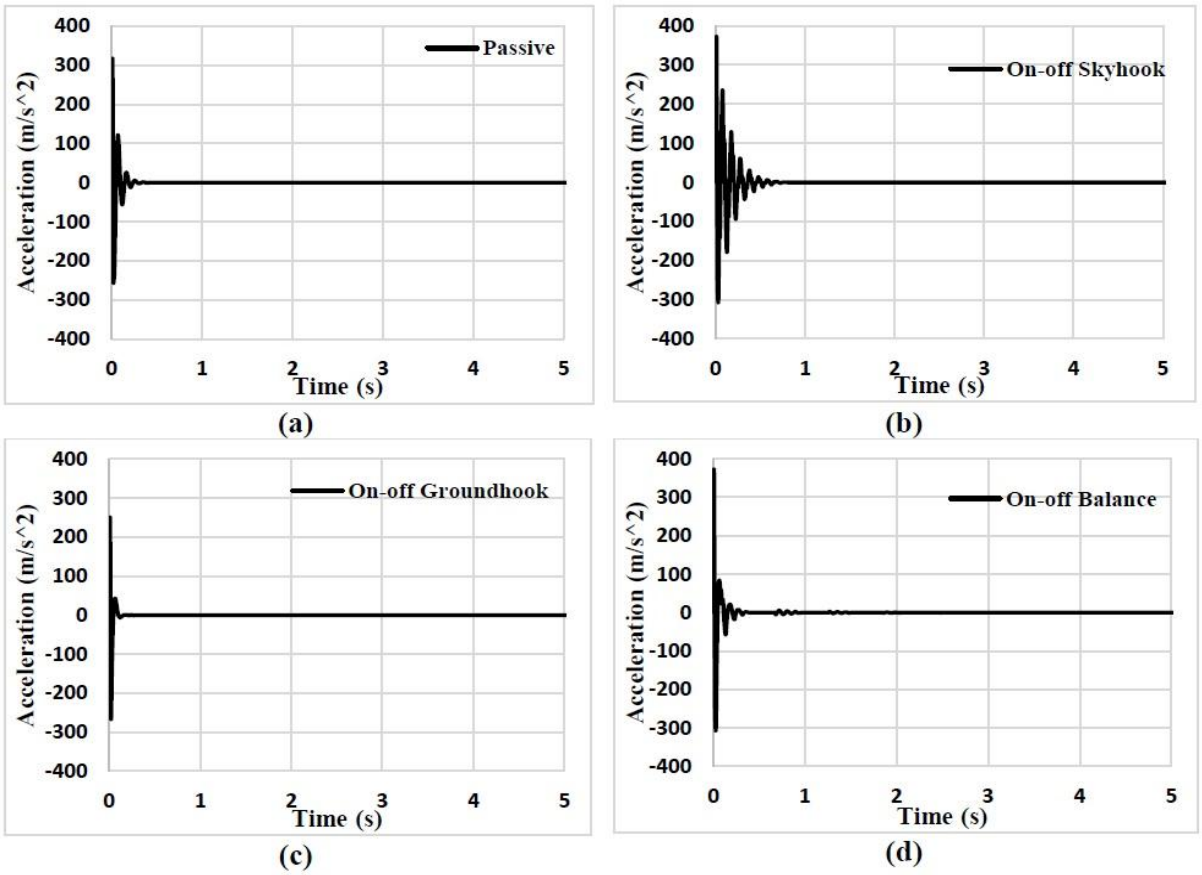

Fig. 6.16: Unsprung mass acceleration of front suspension vs time plot of half car at 60 kmph for (a) passive suspension system (b) on-off skyhook control (c) on-off groundhook control and (d) on-off balance control

6.3.1.4 Body displacement

Body displacement in time domain has been presented in Fig. 6.17. It is observed that for on-off skyhook logic, the displacement has been minimum and reaches the steady position in the shortest possible time. The maximum displacement reached in case of on-off skyhook logic has been found to be 0.0014m. The time to reach steady position is approximate 4 seconds for on-off skyhook logic. For passive system, the maximum displacement is approximately 0.009m and the settling time is around 8 seconds. There is almost 85% reduction in displacement magnitude for on-off skyhook than passive system and around 50% reduction in settling time. For on-off groundhook logic, the displacement is slightly more than 0.009m. However, there is a prolonged period of oscillation in case of displacement and time to reach steady state is increase beyond 10 seconds. In case of on-off balance, the maximum

displacement has been drastically increased to 0.049m. The settling time is at per with that of a passive system for on-off balance.

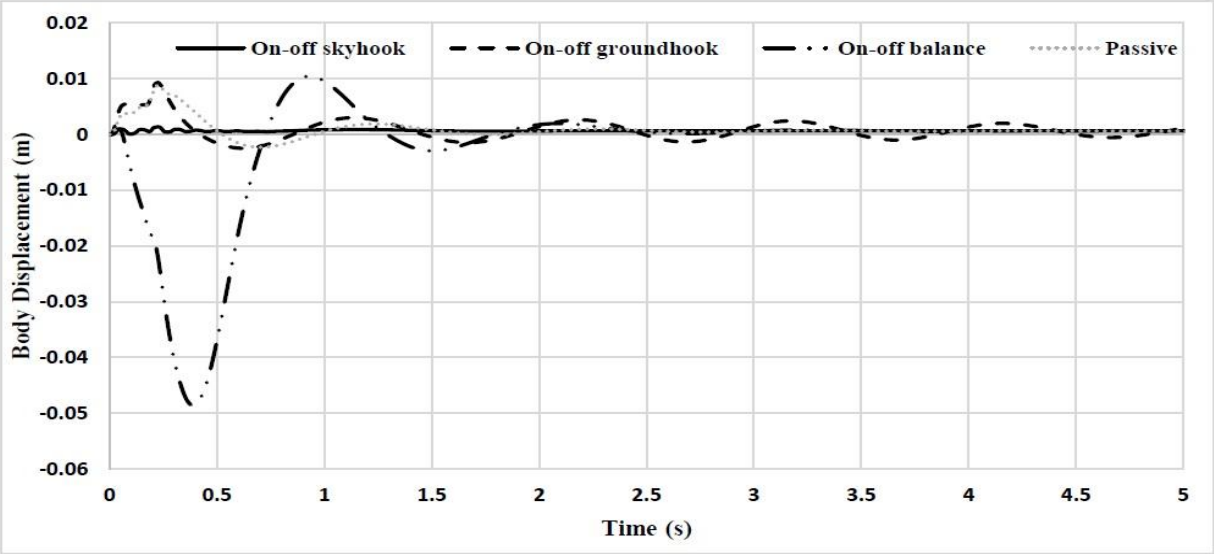

Fig. 6.17: Body displacement vs time of half car at 60kmph for on-off logics

6.3.1.5 Transmissibility

Fig. 6.18 shows the transmissibility of acceleration for the rear suspension in frequency domain.

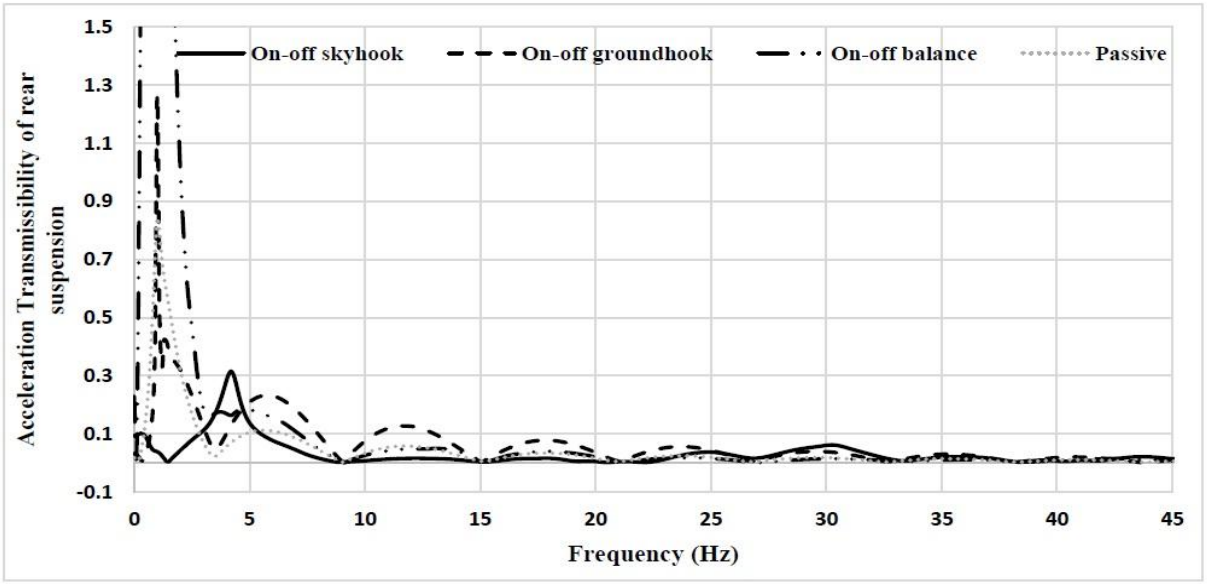

Fig. 6.18: Transmissibility of acceleration for rear suspension of half car at 60kmph for on-off logics

It can be observed that the maximum transmissibility of acceleration is about 0.8 for passive suspension system whereas it is found to be about 0.3 for on-off skyhook logic. There is a 67% reduction in transmissibility for skyhook system than passive system. However, on-off balance and on-off groundhook logics have more transmissibility as can be seen in Fig. 6.18. Comparable performance is observed in case of front suspension as well.

6.3.2 Performance of continuous control strategies

The results for continuous control algorithms have been presented in this section.

6.3.2.1 Body acceleration

In Fig. 6.19, the body acceleration response of different continuous control strategies in time domain has been shown.

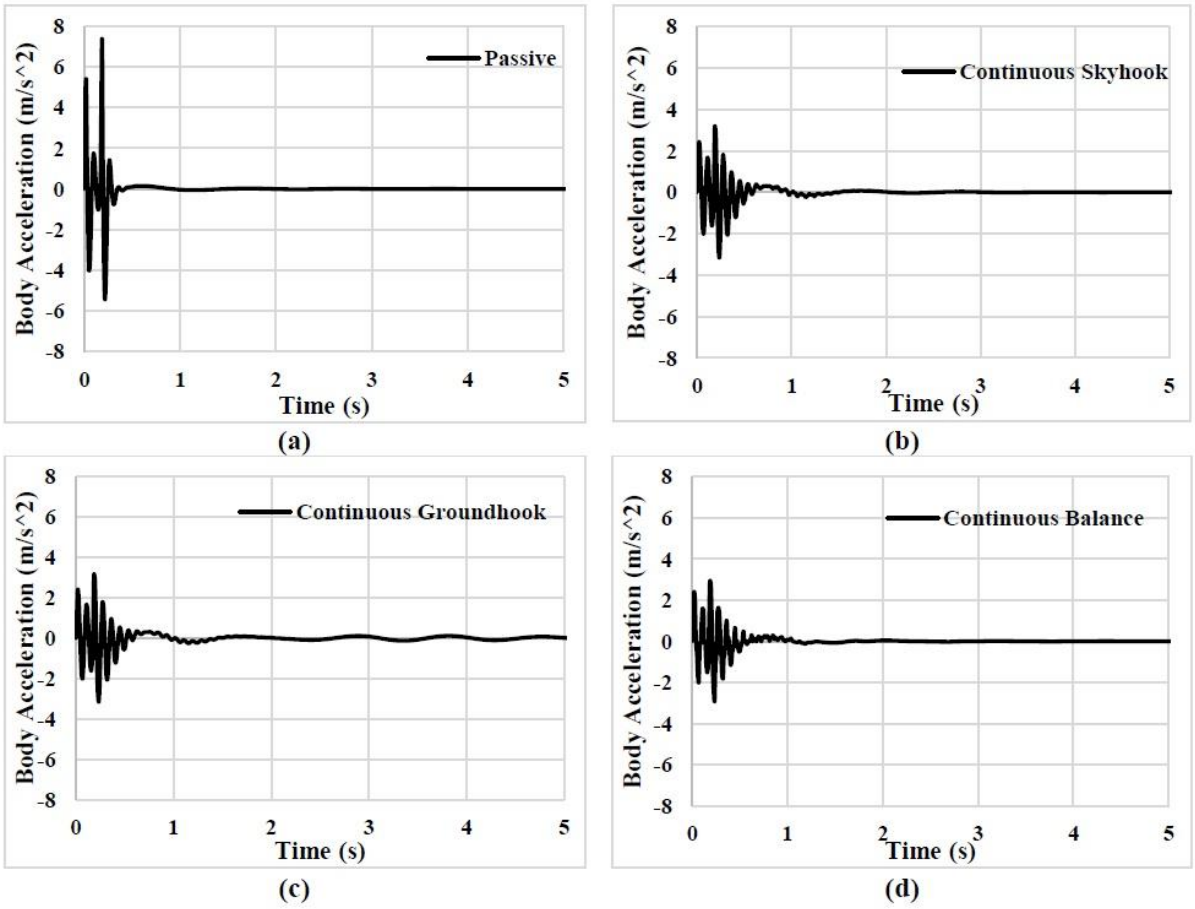

Fig. 6.19: Body acceleration vs time plot of half car at 60 kmph for (a) passive suspension system (b) continuous skyhook control (c) continuous groundhook control and (d) continuous balance control

It can be observed from Fig. 6.19 that for all the three continuous strategies, the maximum magnitude of acceleration has been reduced to almost half of that of a passive suspension system. However, the settling time has been compromised in the case of continuous strategies and a continuous vibration reducing in magnitude over time can be felt. The settling time for continuous skyhook and continuous balance logics have been found to be in between 6-7 seconds as can be seen in Fig. 6.19 (b) and (d) respectively, whereas that for passive system is 4 seconds (Fig. 6.19 (a)). Continuous groundhook logic has poor settling time, a periodic disturbance is present for a prolonged duration in case of continuous groundhook logic (Fig. 6.19 (c)).

6.3.2.2 Pitch acceleration

In Fig. 6.20, the pitch acceleration response of the half car model for different continuous control algorithms has been presented.

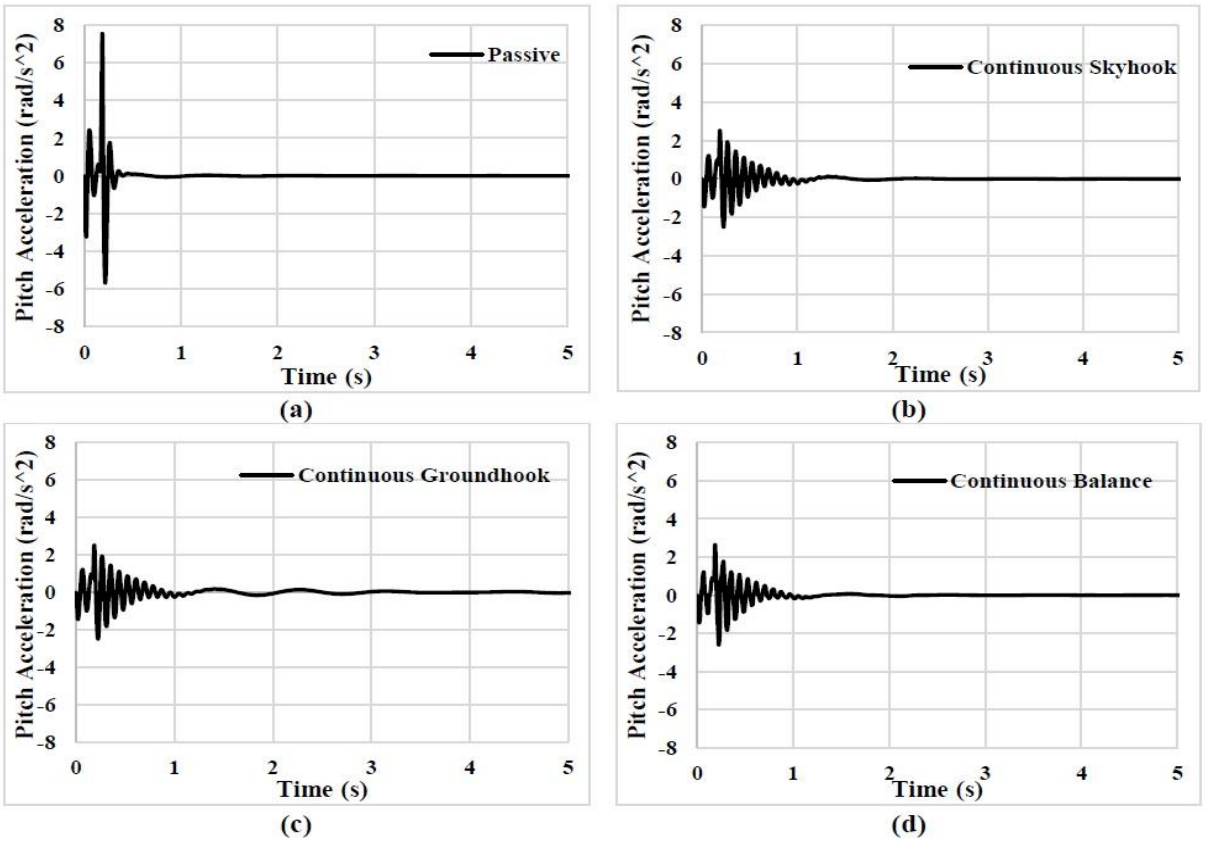

Fig. 6.20: Pitch acceleration vs time plot of half car at 60 kmph for (a) passive suspension system (b) continuous skyhook control (c) continuous groundhook control and (d) continuous balance control

It can be observed that for passive suspension system, the maximum value of pitch acceleration achieved is approximately about 8 rad/s^2 and the settling time is about 4 seconds. For all the three continuous strategies shown in Fig. 6.20 (b), (c) and (d), the maximum value of pitch acceleration is less than 3 rad/s^2. The settling time is however more for the continuous strategies. The settling time for continuous skyhook and continuous balance logic has been found to be in between 5-6 seconds. However, for continuous groundhook control, the settling time is much large and even more than 10 seconds. The vehicle in this case will undergo a prolonged periodic vibration declining in magnitude with time.

6.3.2.3 Unsprung mass acceleration

Fig. 6.21 represents the acceleration response of the unsprung mass of the front suspension of the half car system in time domain.

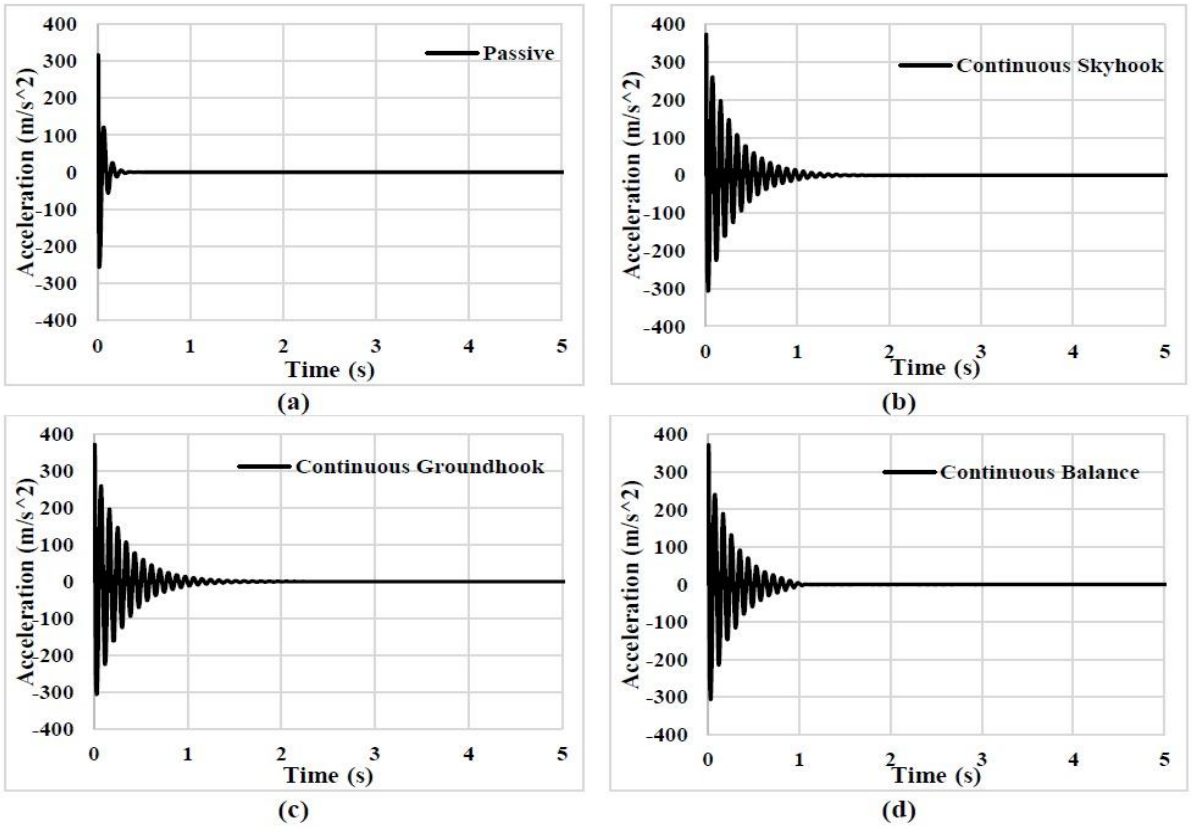

Fig. 6.21: Unsprung mass acceleration of front suspension vs time plot of half car at 60 kmph for (a) passive suspension system (b) continuous skyhook control (c) continuous groundhook control and (d) continuous balance control

The passive system has a maximum amplitude of 320 m/s^2 and a settling time of about 0.5 seconds as can be seen in Fig. 6.21 (a). Whereas, for continuous skyhook, groundhook and balance logics, the maximum acceleration is found to be about 380 m/s^2 as shown in Fig. 6.21 (b), (c) and (d). In case of continuous skyhook and balance logics, the settling time is found to be in between 6-7 seconds. However, in case of continuous groundhook logic, a periodic disturbance of very small magnitude can be observed for a prolonged duration after the initial high amplitude disturbance for about 1 second. Comparable results are observed for the rear suspension of the half car model.

6.3.2.4 Body displacement

The body displacement vs time plot has been displayed in Fig. 6.22. The maximum amplitude for passive system is 0.009m and the settling time is about 8 seconds. For continuous skyhook logic, the maximum displacement is found to be about 0.009m and the settling time is in between 8-9 seconds. But the decrement of the amplitude is less in case of continuous skyhook logic than passive system. In case of continuous balance logic, the maximum displacement achieved is slightly less than passive system and is about 0.008m. However, the settling time is more. For continuous groundhook logic, the maximum displacement is about 0.009m and there can be seen a prolonged periodic oscillation of the displacement of the vehicle body for a very low amplitude as can be seen in Fig. 6.22.

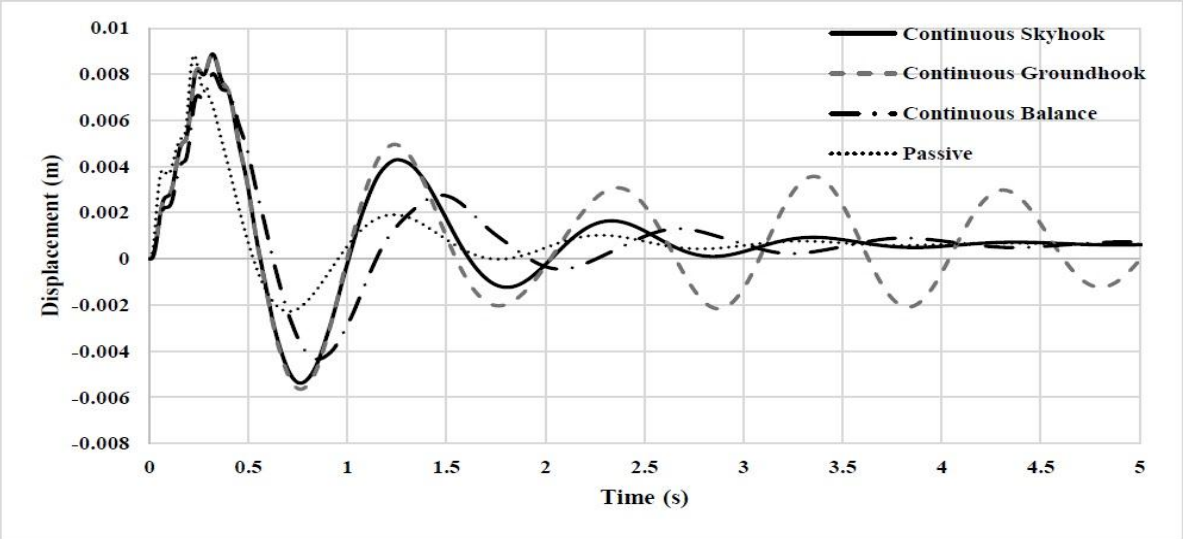

Fig. 6.22: Body displacement vs time of half car model at 60 kmph for continuous control

6.3.2.5 Transmissibility

Fig. 6.23 illustrates the transmissibility of acceleration between the sprung and the unsprung mass for the rear suspension. It can be observed that the passive system has a maximum transmissibility of 0.8. Continuous skyhook logic has a much larger transmissibility of about 2.3 and continuous groundhook logic has even more. However, for continuous balance logic, the maximum transmissibility is found to be about 0.6. This is 25% less than that of a passive suspension system. Comparable results have been observed for transmissibility of acceleration for the front suspension system.

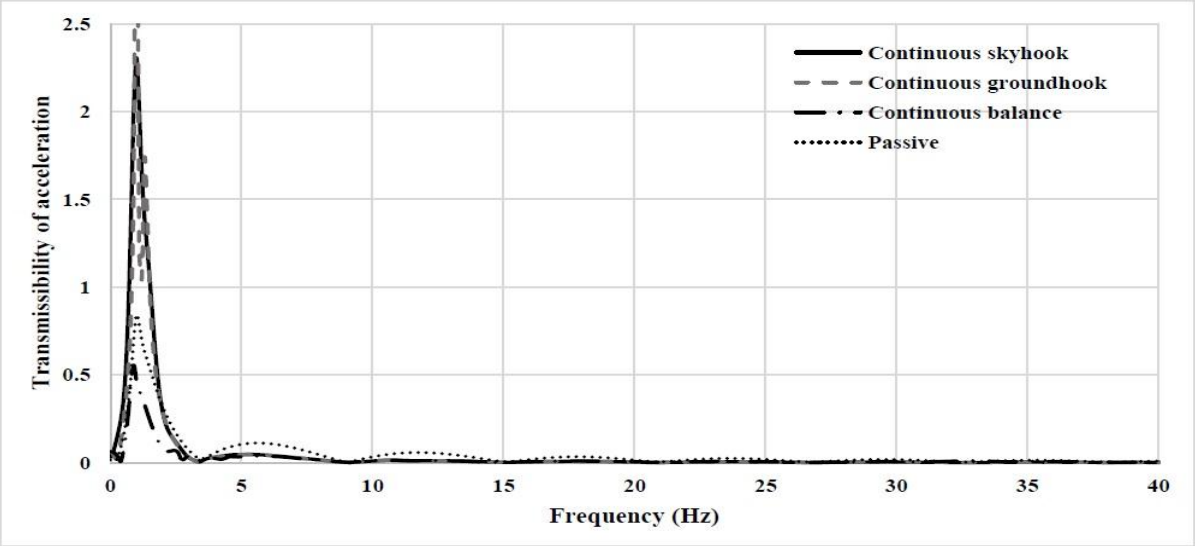

Fig. 6.23: Transmissibility of acceleration for rear suspension at 60kmph for continuous control

6.3.3 Performance of hybrid control strategies

The performance analysis has been carried out for four different hybrid combinations of the three on-off control strategies and they are- i) Hybrid skyhook-groundhook (HY-SH-GH), ii) Hybrid skyhook-balance (HY-SH-B), iii) Hybrid groundhook-balance (HY-GH-B) and iv) Hybrid skyhook-groundhook-balance (HY-SH-GH-B). The results are discussed in this section.

6.3.3.1 Body acceleration

Fig. 6.24 demonstrates the acceleration response of the sprung mass of the half car controlled by different hybrid strategies. The value of weighing factors are as presented in Table 6.1. It

can be observed from Fig. 6.24 (a) and (d) that the responses of HY-SH-GH and HY-SH-GH-B logics are better in case of both magnitude and settling time respectively. However, the magnitude of acceleration is maximum for the HY-GH-B combination and settling time is also more for both HY-SH-B and HY-GH-B logics as can be seen in Fig. 6.24 (b) and (c). HY-SH-GH and HY-SH-GH-B logics show comparable results. HY-SH-GH-B logic has achieved a slightly higher value of acceleration that HY-SH-GH. However, the sudden jerks observed in on-off skyhook logic has been significantly reduced in case of hybrid strategies. HY-SH-GH-B logic has less severe sudden jerks when the condition functions have changed their directions as compared to HY-SH-GH logic. The comparison is shown in Fig 6.25. The settling time for both the logics have been found to be approximately 2.5 seconds which is almost 37.5% less than the passive suspension.

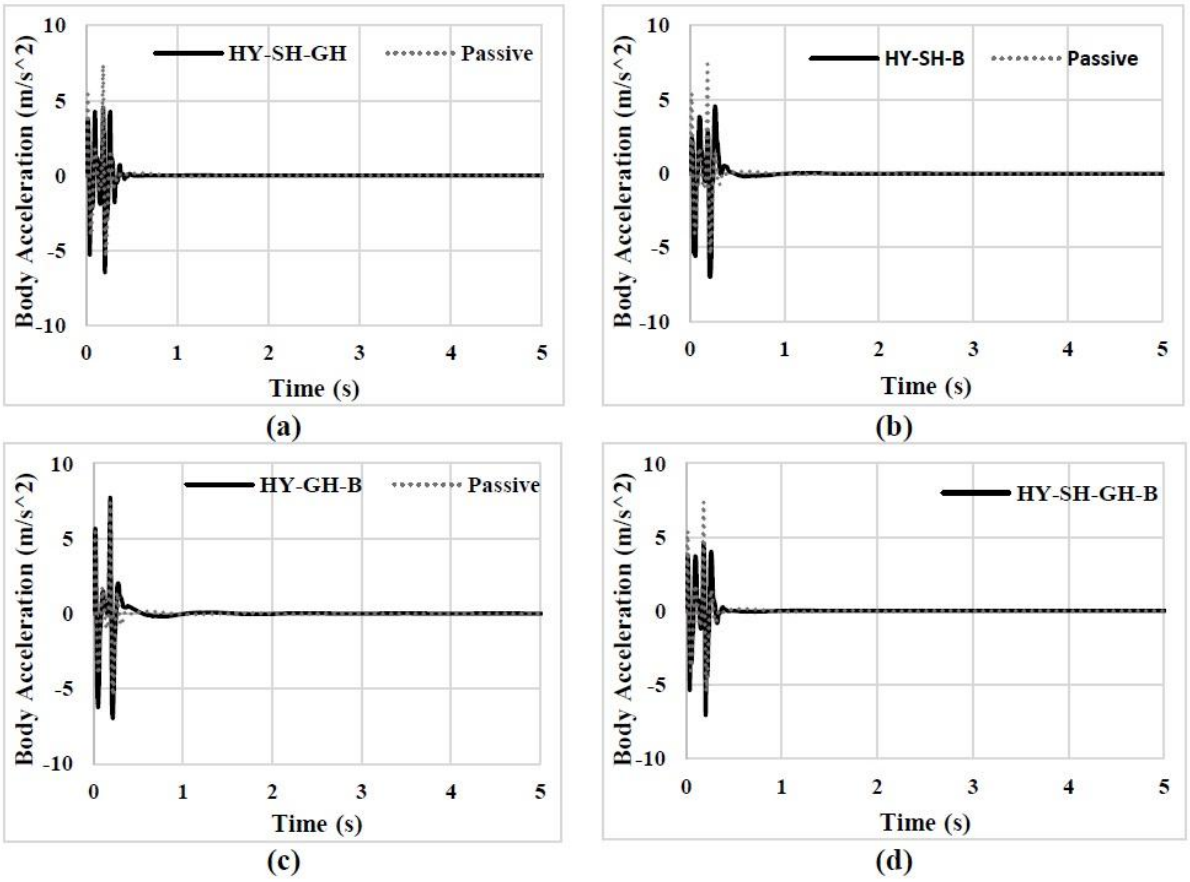

Fig. 6.24: Body acceleration vs time plot of half car at 60 kmph for (a) HY-SH-GH (b) HY-SH-B (c) HY-GH-B and (d) HY-SH-GH-B control

In Fig. 6.25, it can be observed that the magnitude of acceleration for sprung mass is slightly more for the HY-SH-GH-B logic (Fig. 6.25 (b)) as compared to HY-SH-GH logic (Fig. 6.25 (a)). However, the sudden jerks caused by the switching of the damper in between the on and the off state as the condition functions change their direction is less severe in case of the former strategy. The severity of the jerks is directly related to passenger's comfort. HY-SH-GH-B logic can thus provide better comfort as compared to HY-SH-GH logic. Both the logics have better performance as compared to conventional on-off strategies, especially on-off skyhook logic, which provides numerous jerks before coming to a steady state position.

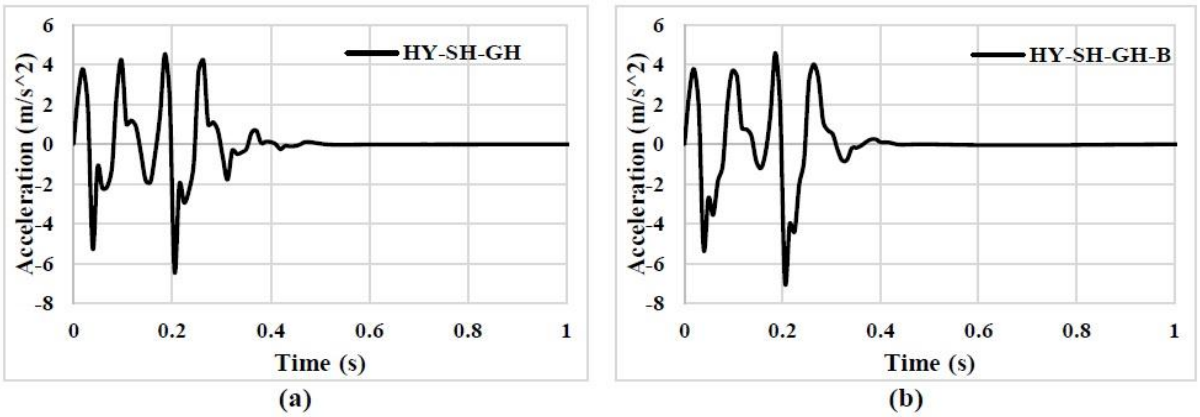

Fig. 6.25: Acceleration response of sprung mass of half car for (a) HY-SH-GH and (b) HY-SH-GH-B

6.3.3.2 Pitch acceleration

Pitch acceleration response of the sprung mass in time domain has been presented in Fig. 6.26. It can be observed in Fig. 6.26 (a) that the maximum amplitude of HY-SH-GH logic is about 8.5 rad/s^2 in downward direction whereas that for passive system is about 8 rad/s^2. However, the settling time is found to be 2 seconds which is 50% less than passive system. In case of HY-SH-B, the maximum value of pitch acceleration is found to be slightly more than 8 rad/s^2 as can be seen in Fig. 6.26 (b), but the settling time is found to be in between 3-4 seconds. For HY-GH-B, the magnitude is 8 rad/s^2 in both directions as shown in Fig. 6.26 (c). Moreover, the settling time is more for this case and is in between 5-6 seconds. The HY-SH-GH-B logic has given better results in terms of pitch acceleration isolation. The maximum value reached is around 8 rad/s^2 and the settling time is around 2 seconds.

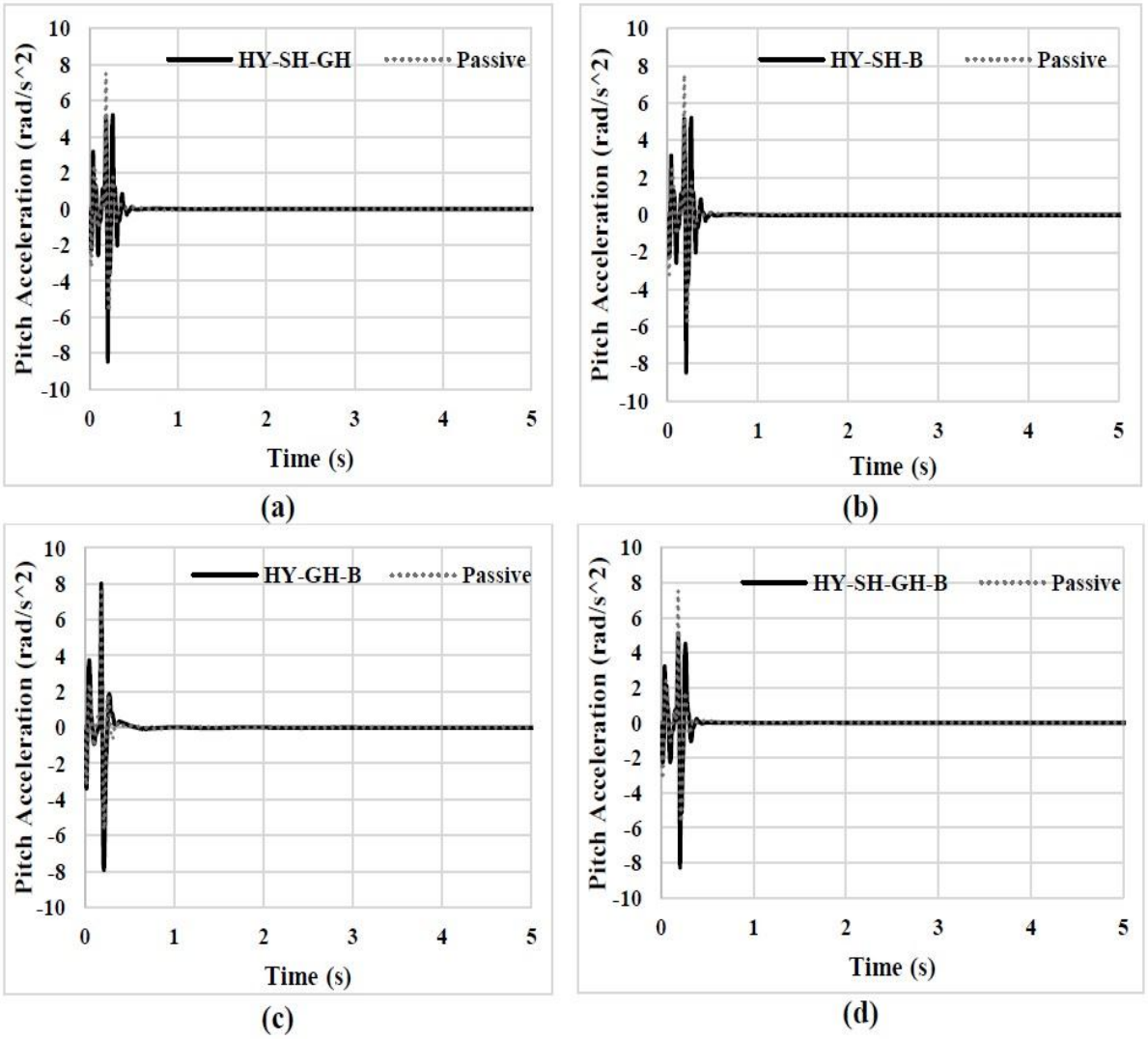

Fig. 6.26: Pitch acceleration vs time plot of half car at 60 kmph for (a) HY-SH-GH (b) HY-SH-B (c) HY-GH-B and (d) HY-SH-GH-B control

HY-SH-GH-B and HY-SH-GH logics show comparable results. Both logics significantly reduce the jerks that can be seen in case of on-off skyhook control strategy. However, the magnitude of acceleration is slightly less in case of HY-SH-GH-B logic than that of HY-SH-GH logic and is demonstrated in Fig. 6.27. The severity of the jerks is also less for the former strategy as shown in Fig. 6.27 (b). It can also be observed that the magnitude of pitch acceleration for HY-SH-GH-B logic has reduced to smaller values more quickly than HY-SH-GH logic.

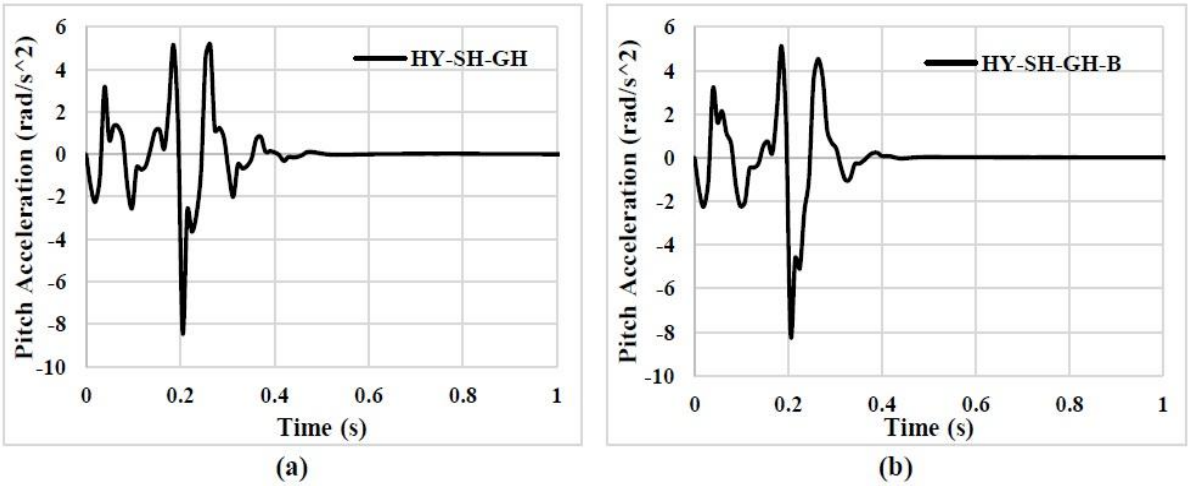

Fig. 6.27: Pitch acceleration response of sprung mass of half car for (a) HY-SH-GH and (b) HY-SH-GH-B

6.3.3.3 Unsprung mass acceleration

Acceleration response of unsprung mass in time domain has been displayed in Fig. 6.28.

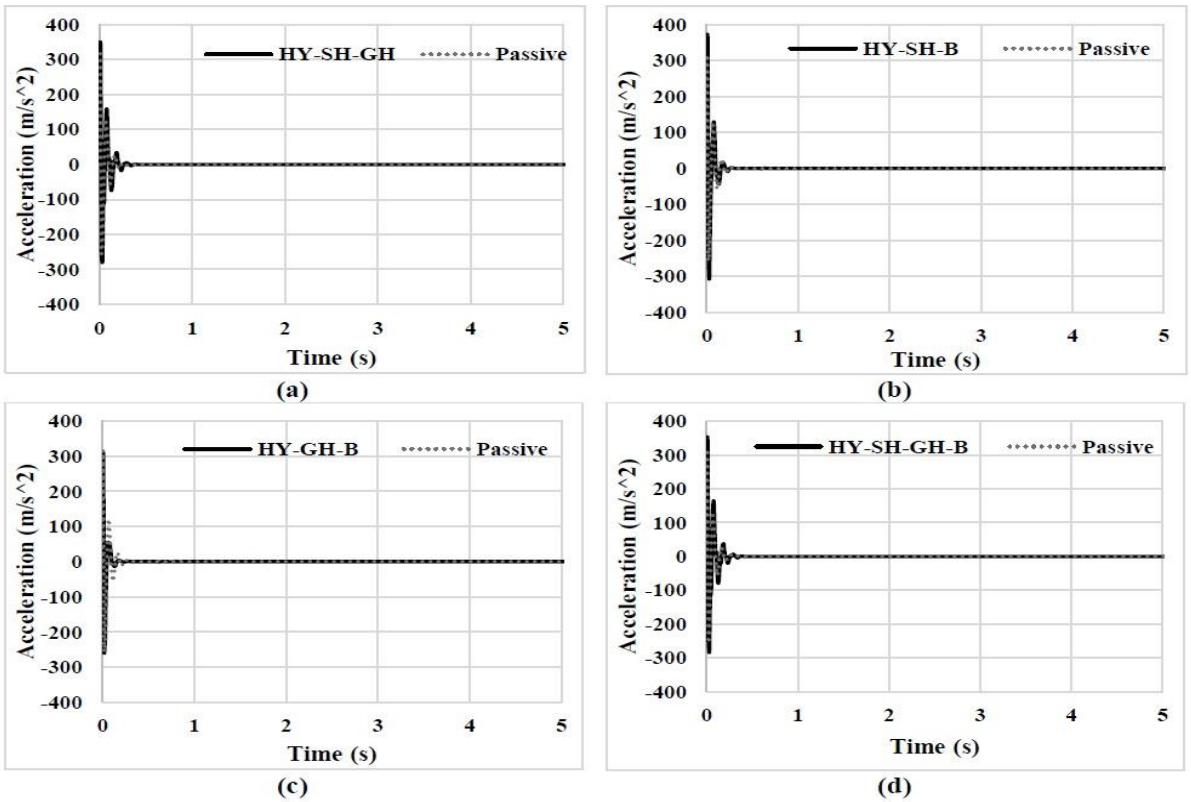

Fig. 6.28: Unsprung mass acceleration of front suspension vs time plot of half car at 60 kmph for (a) HY-SH-GH (b) HY-SH-B (c) HY-GH-B and (d) HY-SH-GH-B control

Results have shown that the acceleration response of the unsprung mass is best for the hybrid combination of groundhook and balance logic (Fig. 6.28 (c)). The magnitude as well as the settling time is minimum for this strategy. Other strategies have a slightly higher settling time and the magnitude of acceleration is also comparatively more than HY-GH-B as well as passive system. The settling time is approximately 0.5 seconds for passive systems and also for all hybrid strategies except for HY-GH-B, for which the settling time is 0.25 seconds which is 50% less. The magnitude is maximum for the HY-SH-B logic as can be seen in Fig. 6.28 (b) and its found out to be 380 m/s^2. The magnitude is found to be 350 m/s^2 for HY-SH-GH and HY-SH-GH-B logics.

6.3.3.4 Body displacement

Body displacement vs time for speed of 60kmph has been plotted and shown in Fig. 6.29.

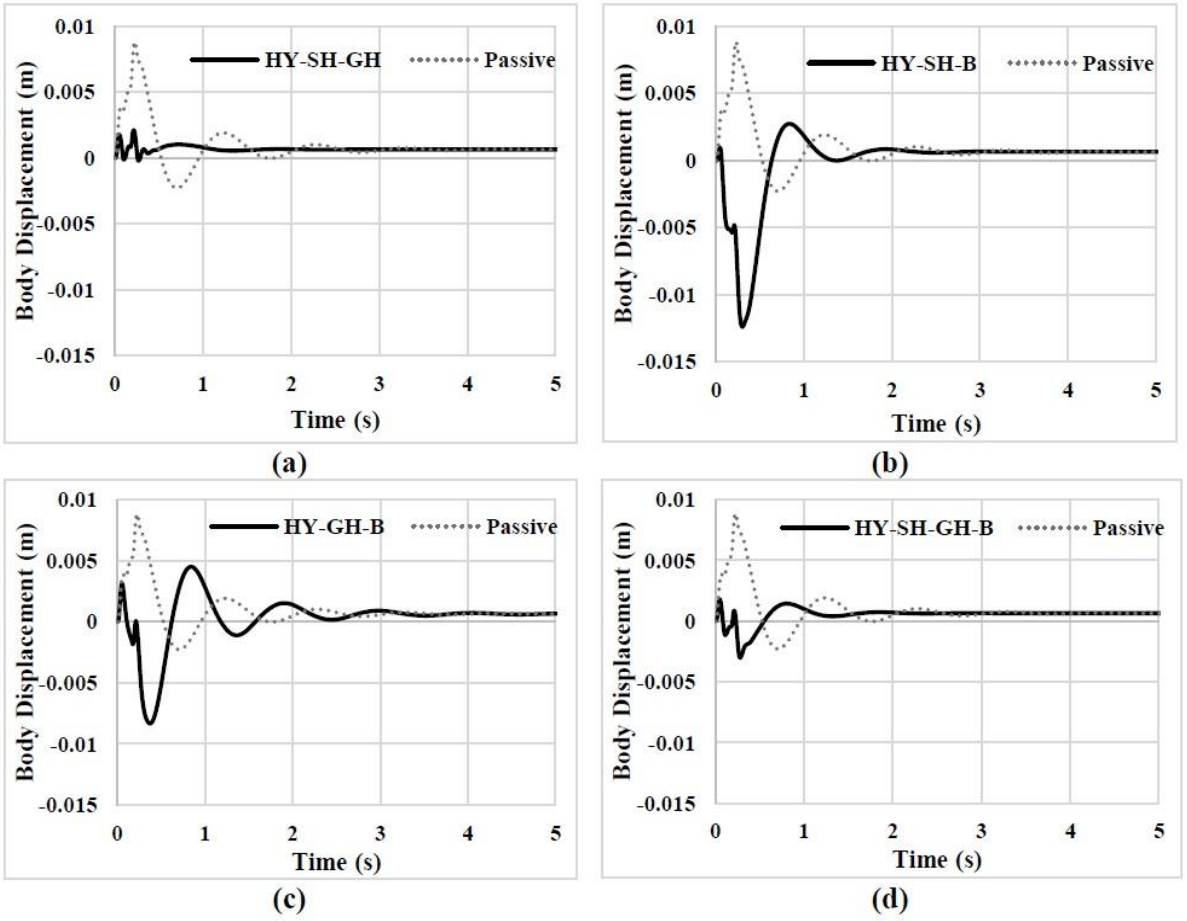

Fig. 6.29: Body displacement vs time plot of half car at 60 kmph for (a) HY-SH-GH (b) HY-SH-B (c) HY-GH-B and (d) HY-SH-GH-B control strategies

It can be observed from Fig. 6.29 (a) that the HY-SH-GH logic has the best performance regarding displacement response as the maximum amplitude achieved is less for this logic. HY-SH-GH-B logic gives a comparable result with a slightly higher amplitude of displacement (Fig. 6.29 (d)). The other two logics demonstrates more value of amplitude of displacement as well as more settling time. The combination of skyhook and balance logic has shown the maximum magnitude of displacement as shown in Fig. 6.29 (b). The combination of skyhook-groundhook and skyhook-groundhook-balance has less settling time as well.

6.3.3.5 Transmissibility

Fig. 6.30 presents the transmissibility of acceleration between sprung and unsprung masses for rear suspension for all hybrid control logics. It is found that the HY-SH-GH and HY-SH-GH-B logics have better performance in terms of transmissibility of acceleration. The maximum transmissibility achieved is much less than that of a passive system. For both the logics, the maximum transmissibility is found to be less than 0.2 for these two hybrid combinations whereas, for a passive system, maximum transmissibility is found to be around 0.8. For HY-GH-B logic, maximum transmissibility is found to be approximately 1, whereas, for HY-SH-B logic, the maximum transmissibility is even more than 1.

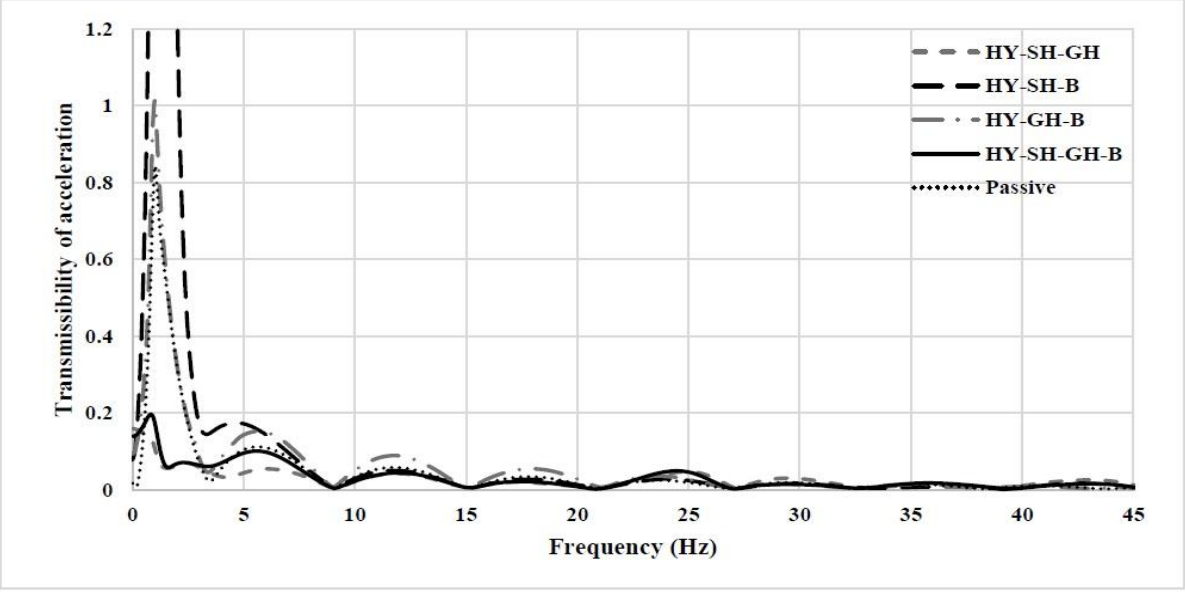

Fig. 6.30: Transmissibility of acceleration for rear suspension at 60kmph for hybrid control

6.4 Performance of Quarter Car Model for Random Road Input

A quarter car model has been subjected to a random road input as discussed in the previous chapter. Simulations have been carried out for the Simulink model of the quarter car model in the software environment of MATLab/Simulink®. The results have been presented in three sections- i) On-off strategies, ii) Continuous strategies and iii) Hybrid strategies.

6.4.1 Performance of on-off control strategies

The performance of the different on-off control algorithms as discussed in chapter 2 are presented in this section. The 2-DOF quarter car model has been subjected to a random road input and different on-off logics such as skyhook, balance and groundhook strategies have been applied to control the damping force of the suspension system. The results were obtained in terms of body acceleration and body displacement.

6.4.1.1 Body acceleration

Fig. 6.31 shows the body acceleration vs time plot for the passive suspension system and semi-active system controlled with on-off skyhook strategy.

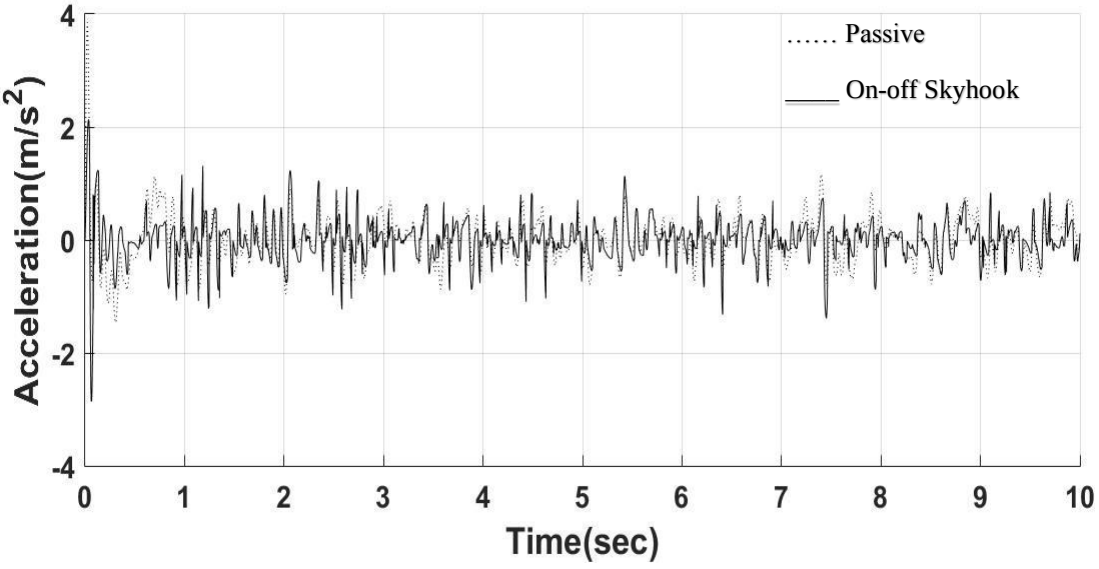

Fig. 6.31: Body acceleration response of quarter car on-off skyhook for random road input

It can be observed from figure that the maximum value of acceleration achieved by passive system is about 4m/s^2, whereas, the same for on-off skyhook is found to be about 3m/s^2.

The pattern also shows reduction in the value of acceleration. However, when the condition function changes its direction, there will be sudden change in the damping force due to the switching of the damper in between on and off states. So there will be sudden jerks shown by the sharp peaks in case of on-off skyhook logic.

For on-off groundhook logic as shown in Fig. 6.32, it is observed that the logic almost follows the response of passive system. However, the initial magnitude of acceleration is found to be more than 5m/s^2 which is almost 20% more than passive system.

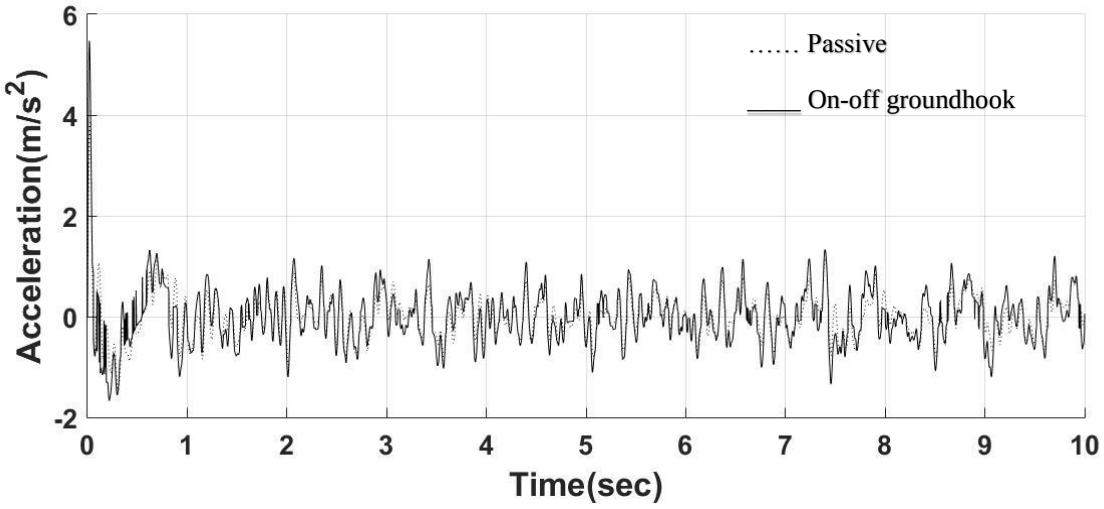

Fig. 6.32: Body acceleration response of quarter car on-off groundhook for random road input

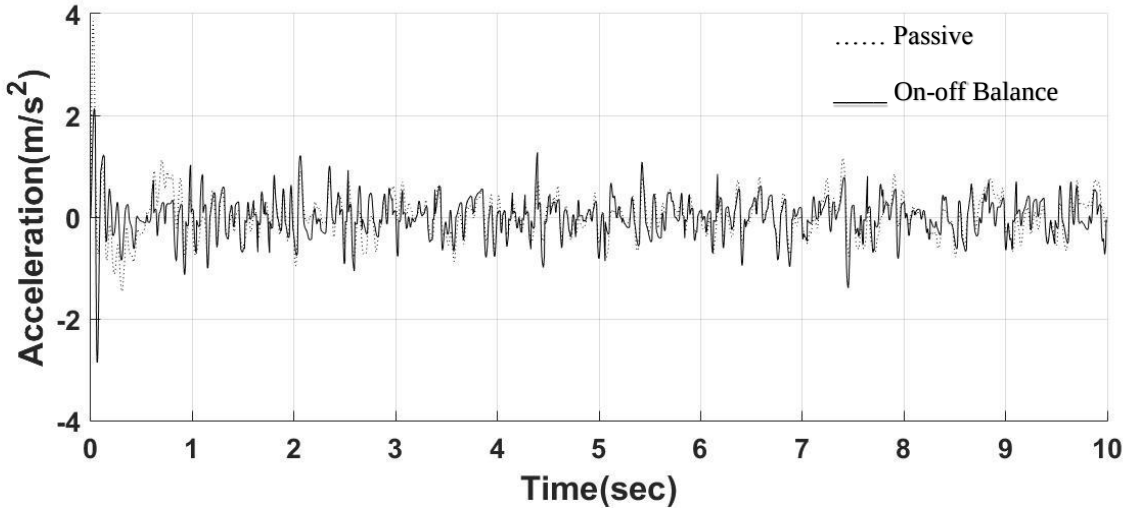

Fig. 6.33: Body acceleration response of quarter car on-off balance for random road input

The response of on-off balance logic has been presented in Fig. 6.33, where it is found that the initial acceleration is reduced to almost 3m/s^2. The overall response of the balance logic is also found satisfactory in terms of acceleration as the number of sharp peaks or sudden jerks is comparatively less for this case.

6.4.1.2 Body displacement

The displacement response of all on-off logics has been shown in Fig. 6.34. The trend shows that the on-off skyhook logic has the best performance as it has almost brought down the oscillating nature of response of the passive system to a neutral position throughout. On-off balance logic also gives comparable performance with a little bit of disturbance here and there. However, on-off gorundhook logic has comparatively more value of body displacement than other two strategies.

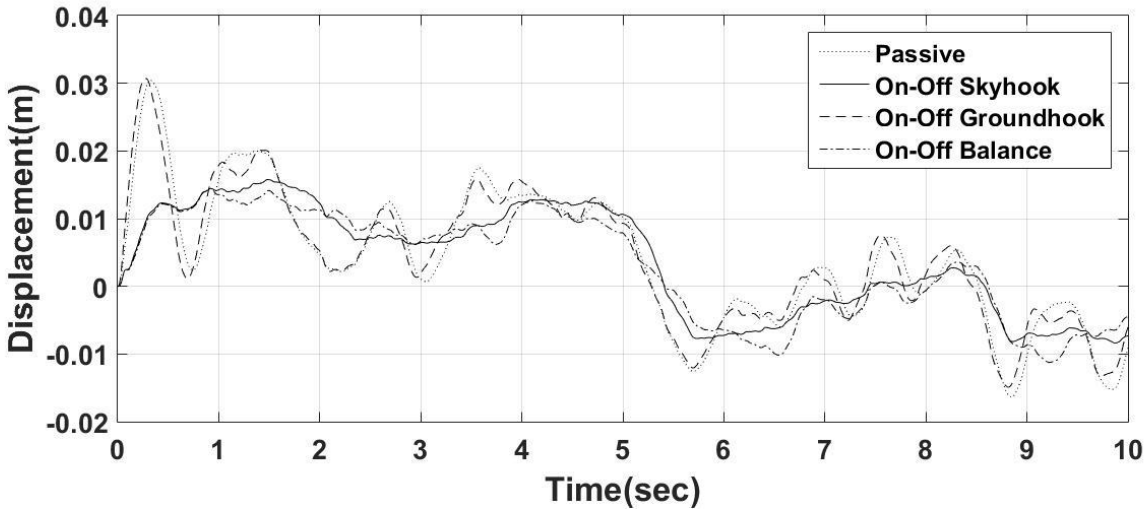

Fig. 6.34: Body displacement response of on-off logics for quarter car with random road input

6.4.2 Performance of continuous control strategies

Vehicle models with continuous control algorithms are simulated for the random type of road input. The results obtained are discussed in the following section.

6.4.2.1 Body acceleration

Fig. 6.35 shows the acceleration response of the continuous skyhook control for random road input. The initial magnitude has been reduced by the continuous logic to almost 2m/s^2, which

is almost half of that of a passive system. Moreover, there are no significant jerks available in this case like on-off skyhook logic. This will provide a comfortable ride in an irregular terrain.

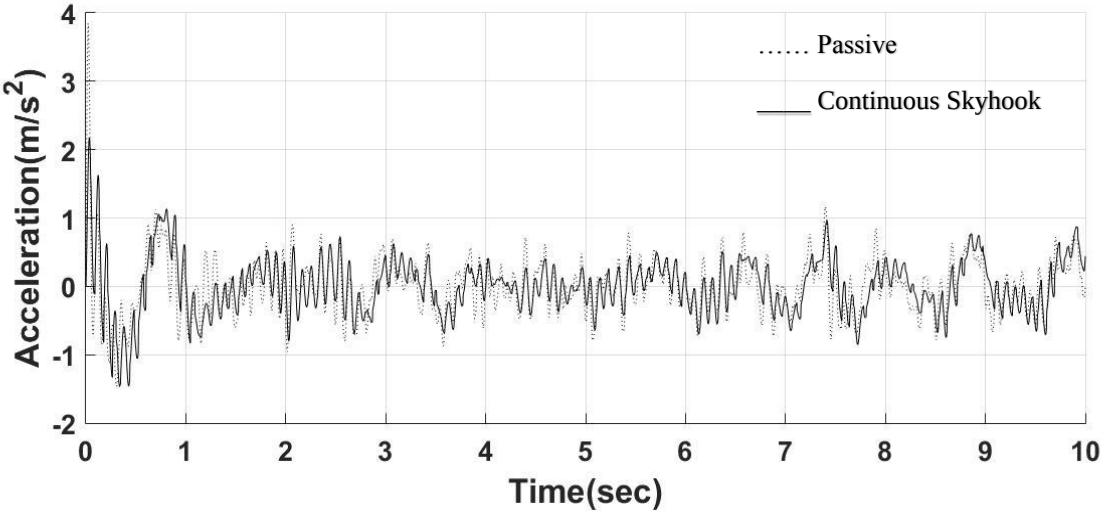

Fig. 6.35: Body acceleration response of quarter car continuous skyhook for random input

For continuous groundhook control however, the initial magnitude is slightly more than passive system. Moreover, the acceleration throughout the span has values greater than the passive system as can be seen from Fig. 6.36.

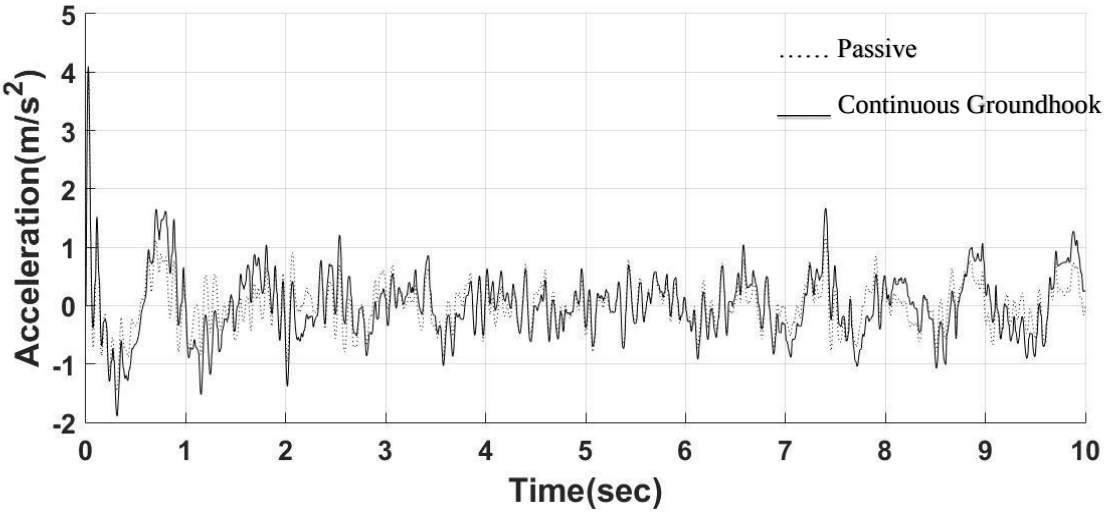

Fig. 6.36: Body acceleration response of quarter car continuous groundhook for random input

In Fig. 6.37, the response for continuous balance logic has been presented. Initial value has been reduced to almost $2m/s^2$. But the values over the time span of 10 seconds have been

found to be slightly more than continuous skyhook logic. The system provides comparable results to skyhook counterpart with slightly increased magnitude of acceleration.

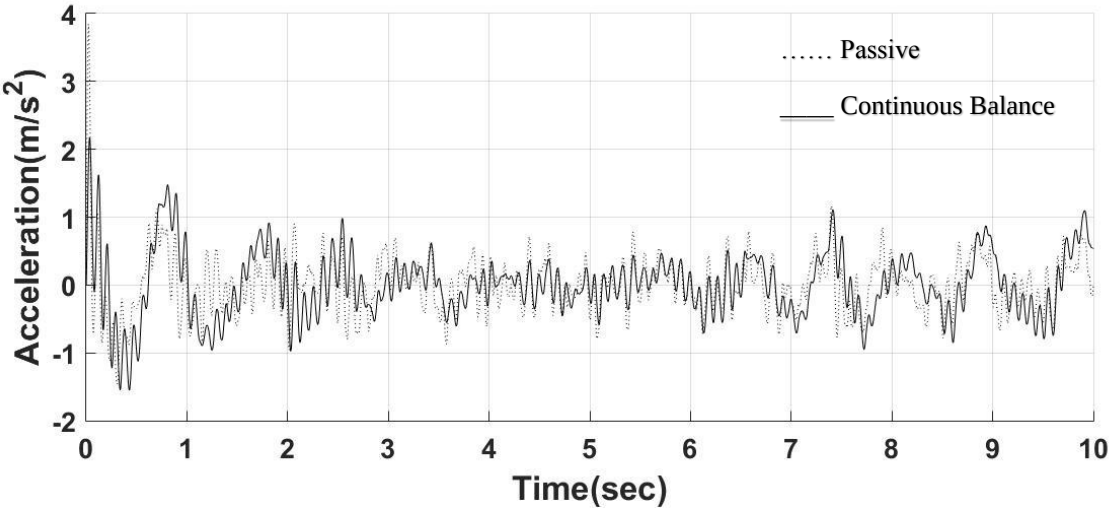

Fig. 6.37: Body acceleration response of quarter car continuous balance for random input

6.4.2.2 Body displacement

Body displacement vs time for all the continuous logics have been demonstrated in Fig. 6.38.

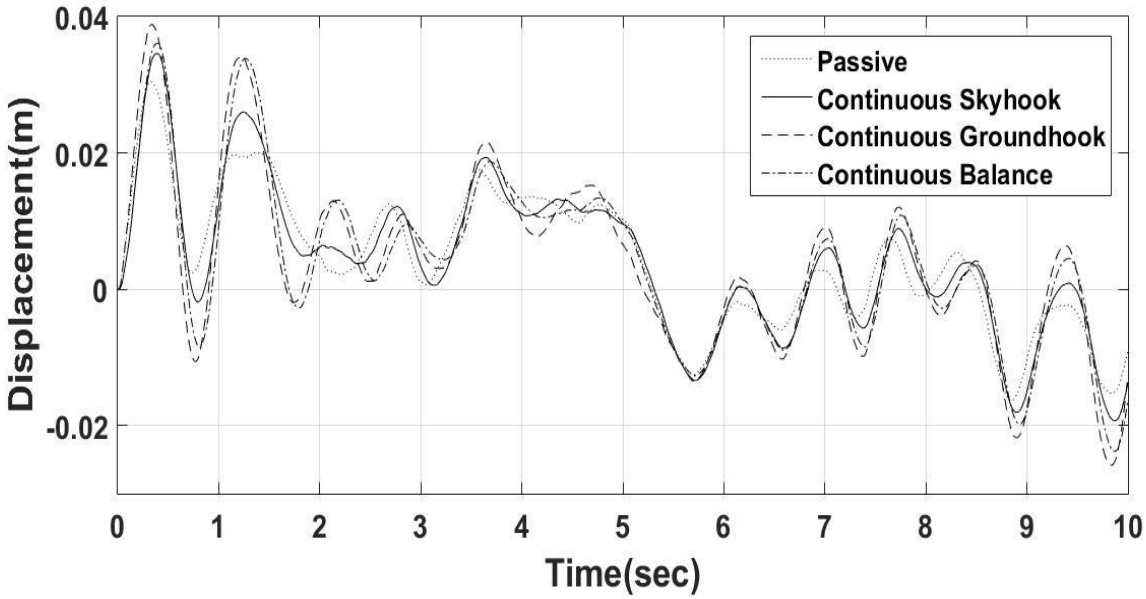

Fig. 6.38: Body displacement response of continuous logics for quarter car with random input

The magnitude of displacement is more than passive system throughout for all three continuous control logics. However, among the three continuous logics, continuous skyhook logic has better performance. For continuous skyhook logic, the body displacement is slightly more than that of a passive system. On the contrary, the maximum amplitudes achieved by continuous groundhook and balance logics are even more as shown in Fig. 6.38.

6.4.3 Performance of hybrid control strategies

Four hybrid control strategies have been considered for performance evaluation of semi-active suspension system for quarter car as discussed in the previous chapter. These are i) HY-SH-GH, ii) HY-SH-B, iii) HY-GH-B and iv) HY-SH-GH-B. The results are given in this section.

6.4.3.1 Body acceleration

Fig. 6.39 presents the acceleration response of the HY-SH-GH control strategy.

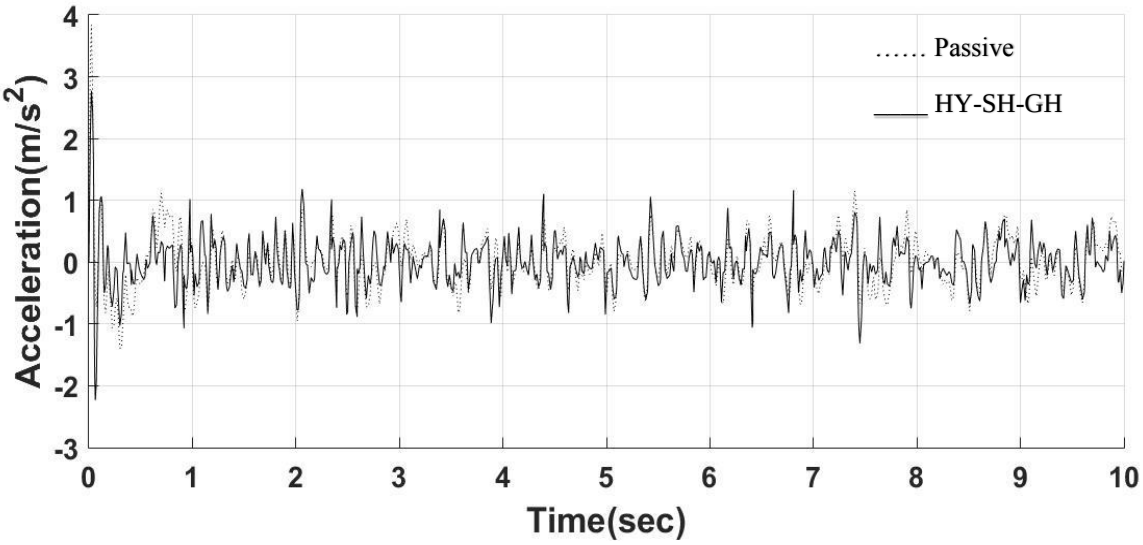

Fig. 6.39: Body acceleration response of quarter car HY-SH-GH control for random input

It can be observed that the initial magnitude has been reduced by almost $1m/s^2$ than passive system. Moreover, the sudden peaks in case of HY-SH-GH has been found to be less in number as well as less intense as compared to on-off skyhook logic.

For HY-SH-B control, the results are also found to be comparable with that of HY-SH-GH. The initial amplitude has been lowered to even less than $3m/s^2$ as shown in Fig. 6.40.

Severity and number of uncomfortable jerks have been significantly reduced in this case as well.

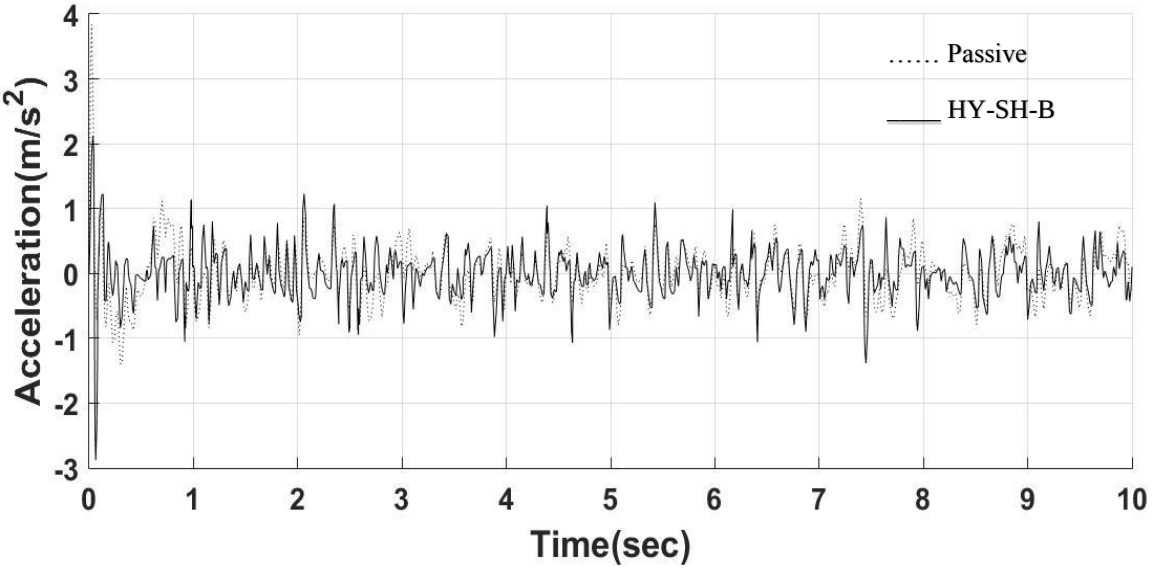

Fig. 6.40: Body acceleration response of quarter car HY-SH-B control for random input

Fig. 6.41 represents the acceleration response of HY-GH-B logic for random road input. In this case, the initial magnitude is slightly more than a passive system. The trend can be observed throughout the span of 10 seconds. The logic almost follows the passive response with somewhat less values at few places.

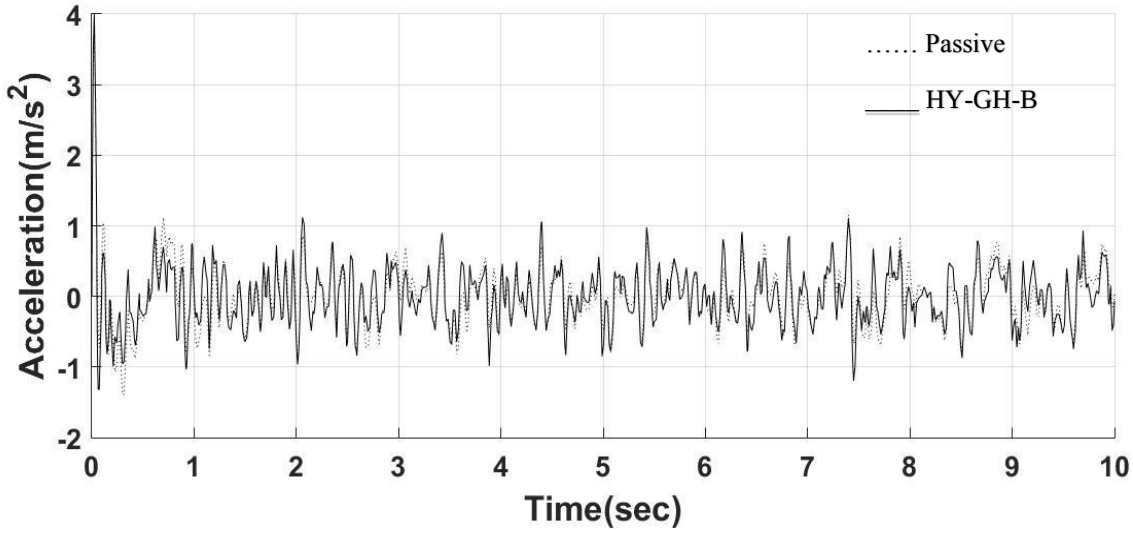

Fig. 6.41: Body acceleration response of quarter car HY-GH-B control for random input

For HY-SH-GH-B control, the initial value of acceleration is about 4.5 m/s^2 as shown in Fig. 6.42, which is even more than passive system. But, the system shows better performance in terms of severity of jerks. The amplitude in the opposite direction has immediately came down to -1 m/s^2 whereas, for other logics, it is more than -2 m/s^2 (except for HY-GH-B). The severity of the jerks has been found to be reduced in case of HY-SH-GH-B control than seen in HY-SH-GH control.

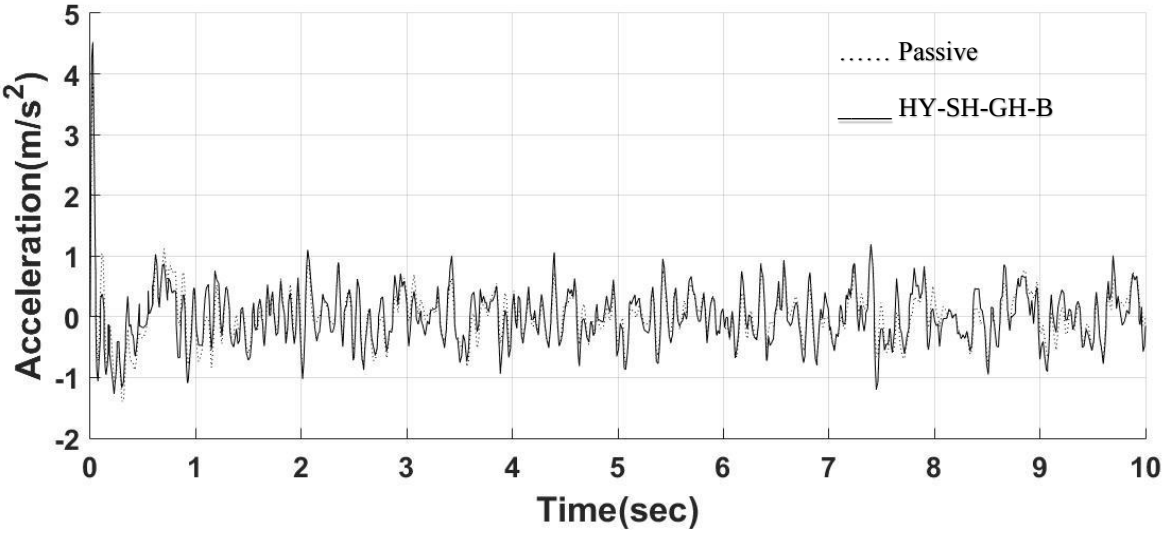

Fig. 6.42: Body acceleration response of quarter car HY-SH-GH-B control for random input

6.4.3.2 Body displacement

Body displacement vs time for all the continuous logics have been demonstrated in Fig. 6.43. In figure, it can be noticed that HY-SH-GH and HY-SH-B logics have better performance in terms of displacement neutralization. HY-GH-B and HY-SH-GH-B logics give comparable results. However, all the hybrid logics have better performance than passive system in terms of displacement neutralization. The peak value at the beginning is found to be 0.03m for passive, whereas, the same for HY-SH-GH-B is almost 0.025m. For HY-GH-B, its slightly less and around 0.023m. The values for HY-SH-GH and HY-SH-B has been found to be about 0.015m and 0.012 respectively.

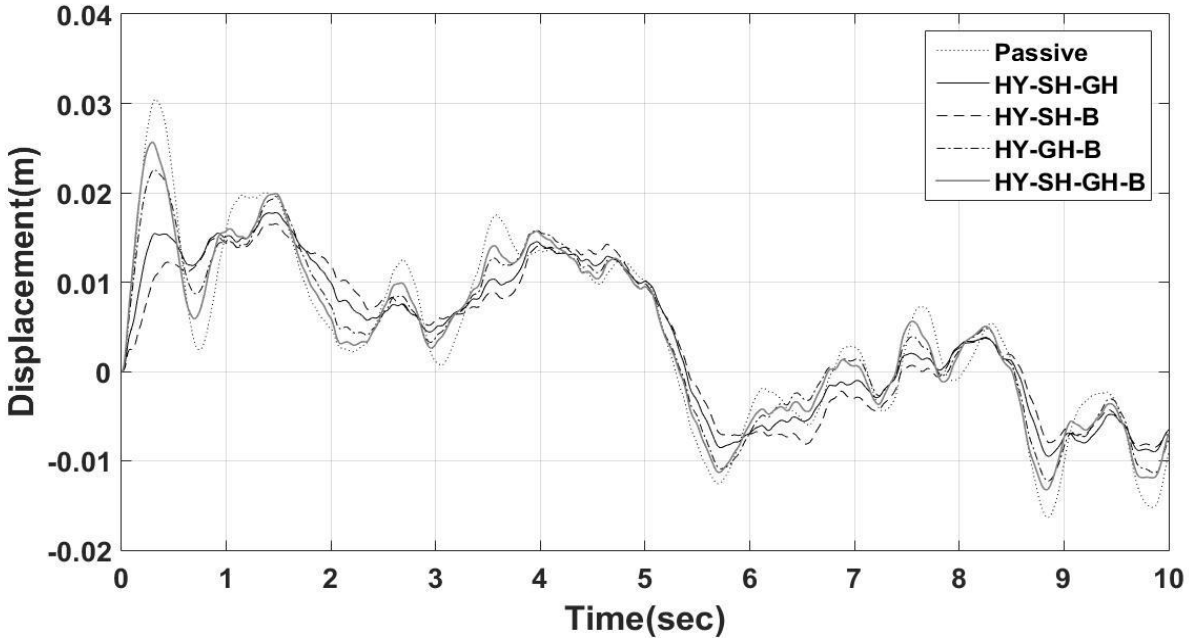

Fig. 6.43: Body displacement response of hybrid logics for quarter car with random input

6.5 Performance of Half Car Model for Random Road Input

A half car model has been subjected to a random road input as discussed in the previous chapter. Simulations have been carried out for the Simulink model of the quarter car model in the software environment of MATLab/Simulink®. The results have been presented in three sections- i) On-off strategies, ii) Continuous strategies and iii) Hybrid strategies.

6.5.1 Performance of on-off control strategies

The performance of the different on-off control algorithms as discussed in chapter 2 are presented in this section. The results were obtained in terms of body acceleration and body displacement.

6.5.1.1 Body acceleration

Fig. 6.44 shows the body acceleration vs time plot for the passive suspension system and semi-active system controlled with on-off skyhook strategy. It can be observed from figure that the response of on-off skyhook logic is mostly less than the passive system throughout the entire span of the simulation. However, whenever the condition function changes its direction, there will be sudden change in the damping force due to the switching of the damper in between on

and off states. So there will be sudden jerks shown by the sharp peaks in case of on-off skyhook logic. There are numerous such jerks can be seen from figure.

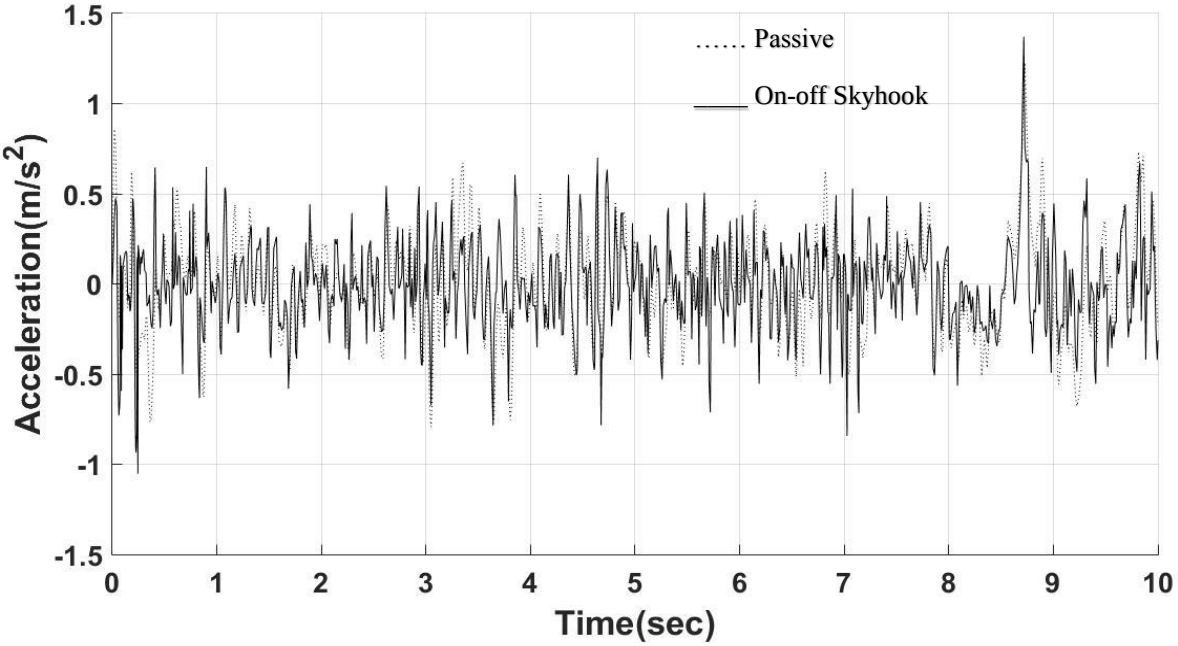

Fig. 6.44: Body acceleration response of half car on-off skyhook for random input

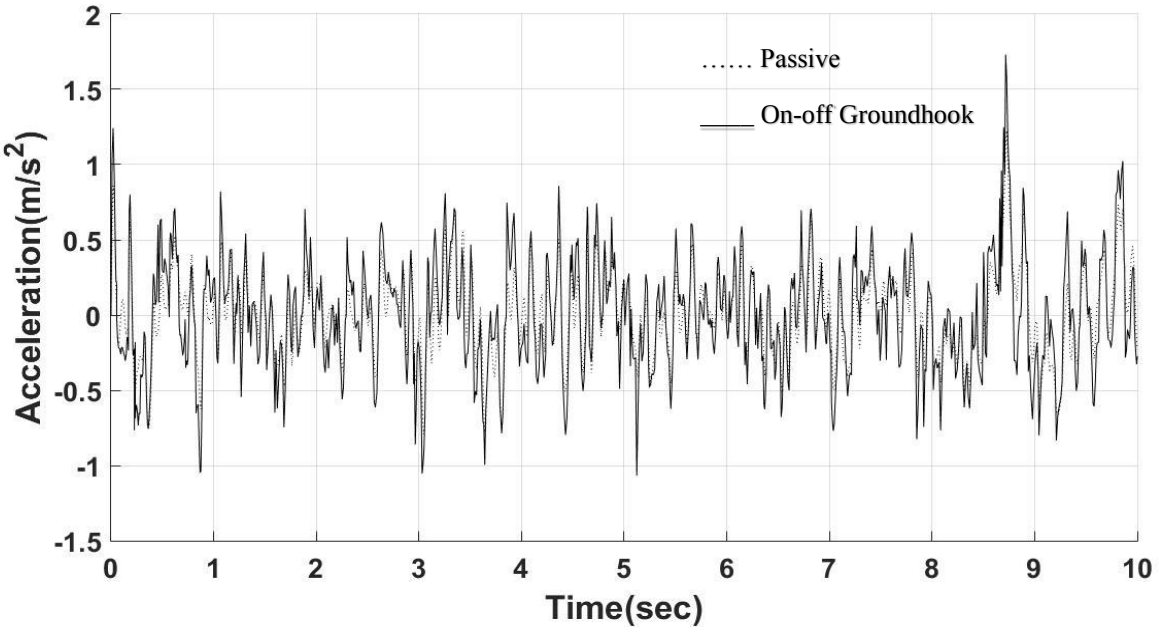

Fig. 6.45: Body acceleration response of half car on-off groundhook for random input

The response of on-off groundhook logic for random road input has been shown in Fig. 6.45. The magnitude throughout is found to be somewhat more than the passive system.

On the contrary, on-off balance control has better performance in terms of body acceleration. As shown in Fig. 6.46, the maximum magnitude achieved is less than $1 m/s^2$ and over the span of 10 seconds, the value of acceleration for on-off balance logic has found to be less. Moreover, the severity of jerks produced in this case is less than the skyhook logic to some extent.

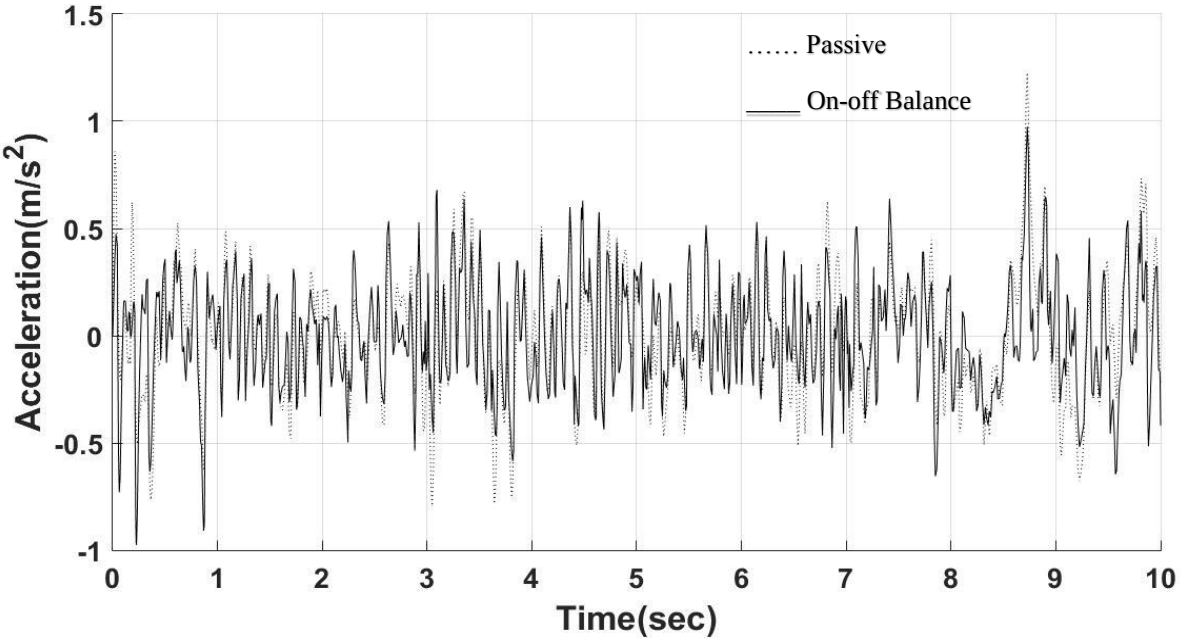

Fig. 6.46: Body acceleration response of half car on-off balance for random input

6.5.1.2 Body displacement

The displacement response of all on-off logics has been shown in Fig. 6.34. The trend shows that the on-off skyhook logic has the best performance as it has almost brought down the oscillating nature of response of the passive system to a neutral position throughout. On-off balance logic and on-off gorundhook logic has shown more displacement than on-off skyhook control. Although on-off groundhook logic almost follows the response of passive system, on-off balance logic tries to bring the magnitude down at times. But at other instances, the magnitude is found to be maximum for balance control.

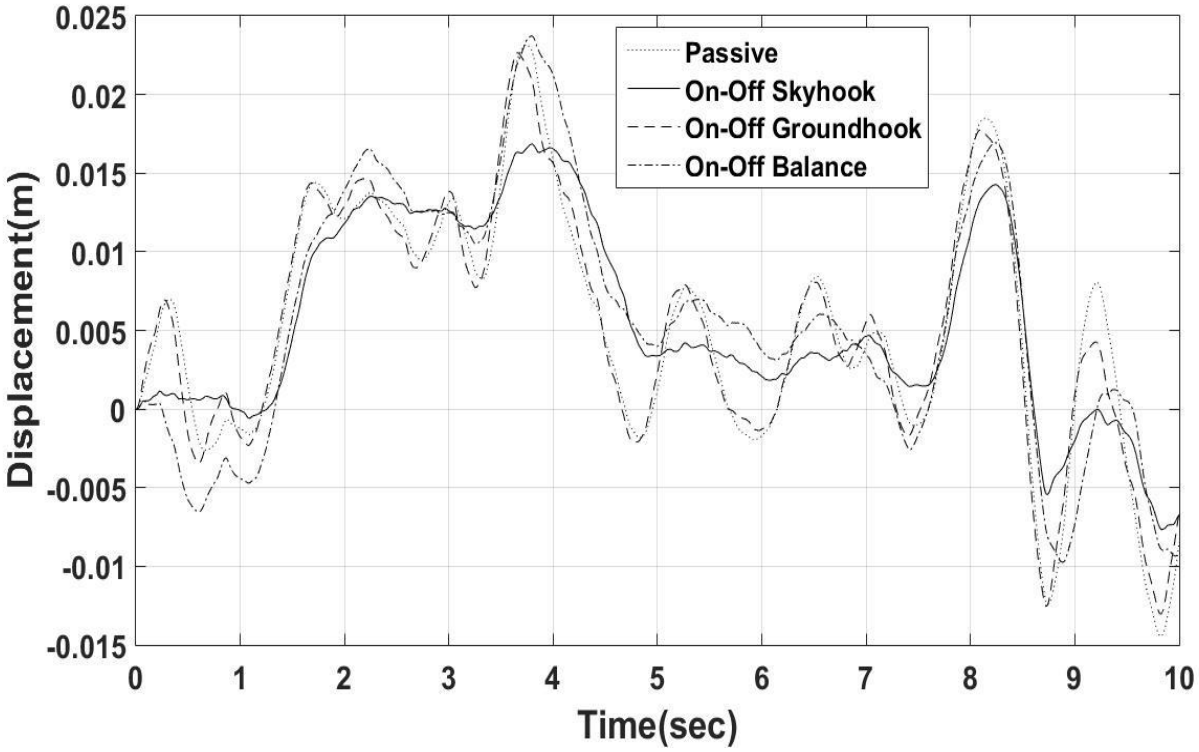

Fig. 6.47: Body displacement response of on-off logics for half car with random input

6.5.2 Performance of continuous control strategies

Vehicle models with continuous control algorithms are simulated for the random type of road input. The results obtained are discussed in the following section.

6.5.2.1 Body acceleration

Fig. 6.48 shows the acceleration response of the continuous skyhook control for random road input. The value of acceleration throughout has been found to be less than passive system. Moreover, the severity of jerks is less in this case unlike on-off skyhook logic. This will provide a comfortable ride in an irregular terrain.

For continuous groundhook control however, the magnitude of acceleration is slightly more than passive system throughout the span. The same is presented in Fig. 6.49. In Fig. 6.50, the response for continuous balance logic has been presented. The values over the time span of 10 seconds have been found to be slightly more than continuous skyhook logic. The system provides comparable results to skyhook counterpart with slightly increased magnitude of

acceleration. However, the intensity of the peaks is found to be less in this case as well. This ensures smooth ride as compared to the on-off counterparts, especially on-off skyhook logic.

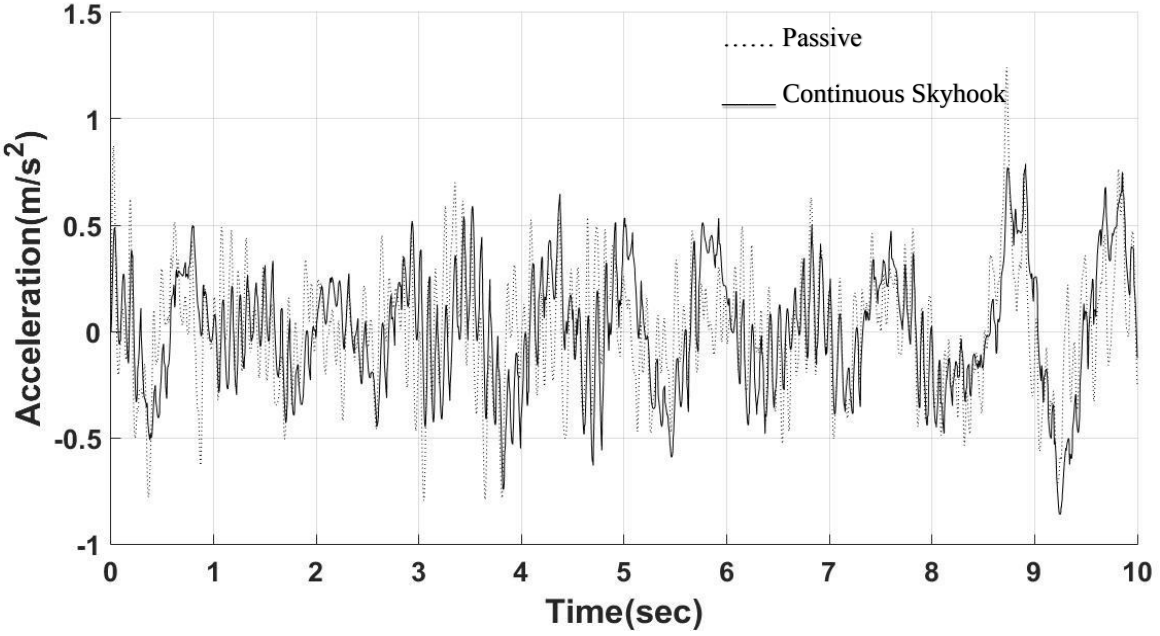

Fig. 6.48: Body acceleration response of half car continuous skyhook for random input

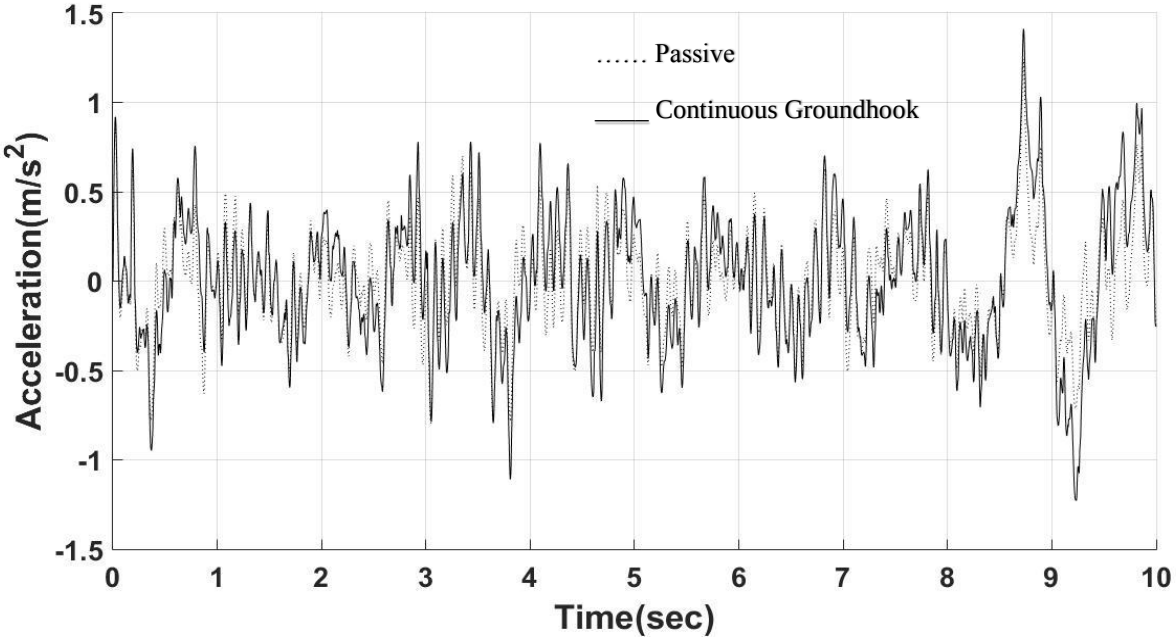

Fig. 6.49: Body acceleration response of half car continuous groundhook for random input

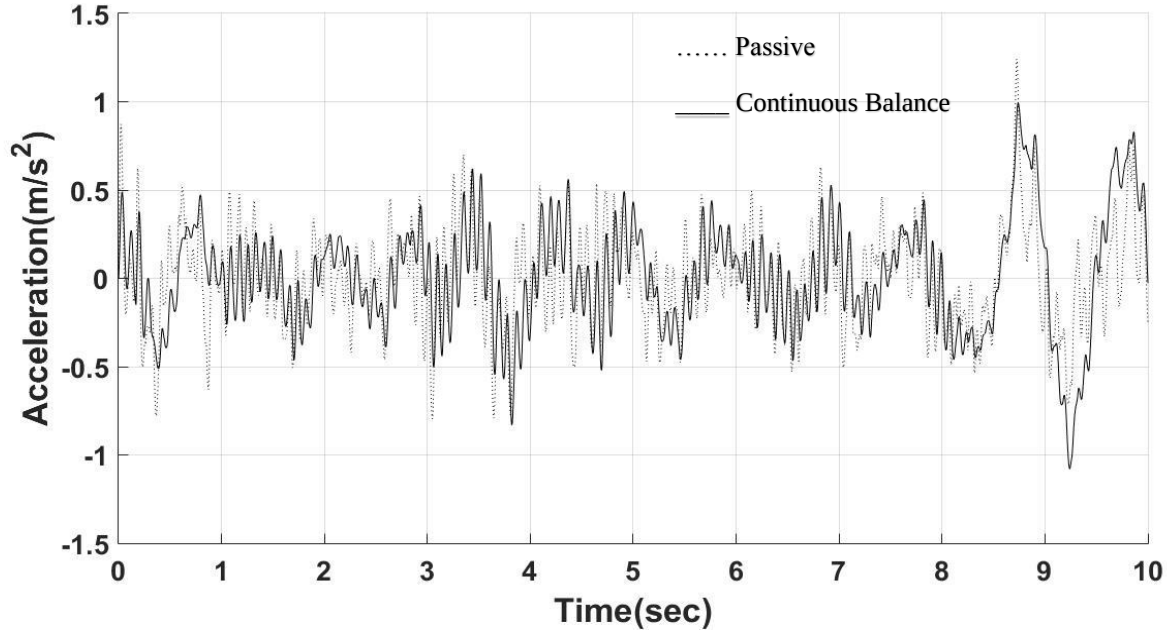

Fig. 6.50: Body acceleration response of half car continuous balance for random input

6.5.2.2 Body displacement

Body displacement vs time for all the continuous logics have been demonstrated in Fig. 6.51.

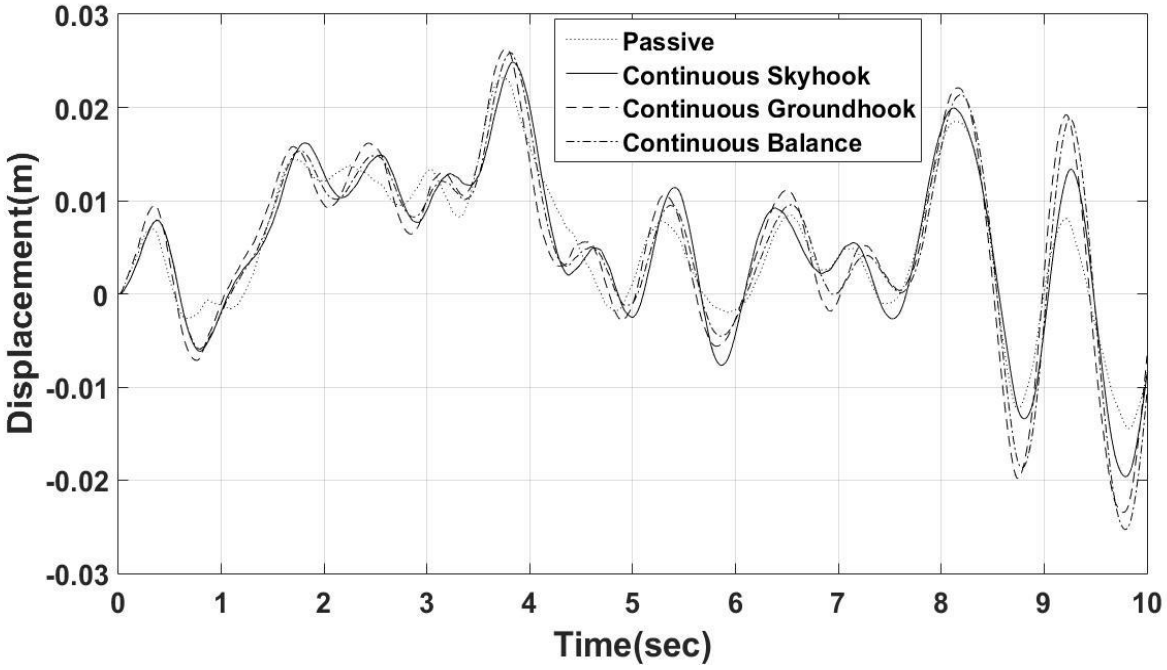

Fig. 6.51: Body displacement response of continuous logics for half car with random input

The displacement response of all the three continuous logics has been found to be more than passive system. The magnitude of displacement is more than passive system throughout. All three logics almost follow the response of the passive system. However, over time, skyhook logic shows a little better results than the other two.

6.5.3 Performance of hybrid control strategies

Four hybrid control strategies have been considered for performance evaluation of semi-active suspension system for half car as discussed in the previous chapter. The results are given in this section.

6.5.3.1 Body acceleration

Fig. 6.52 presents the acceleration response of the HY-SH-GH control strategy. It can be observed that the HY-SH-GH logic gives comparable results as on-off skyhook logic in case of random input for half car. The value of acceleration is less at some instances. However, the sharp jerks are present throughout the span.

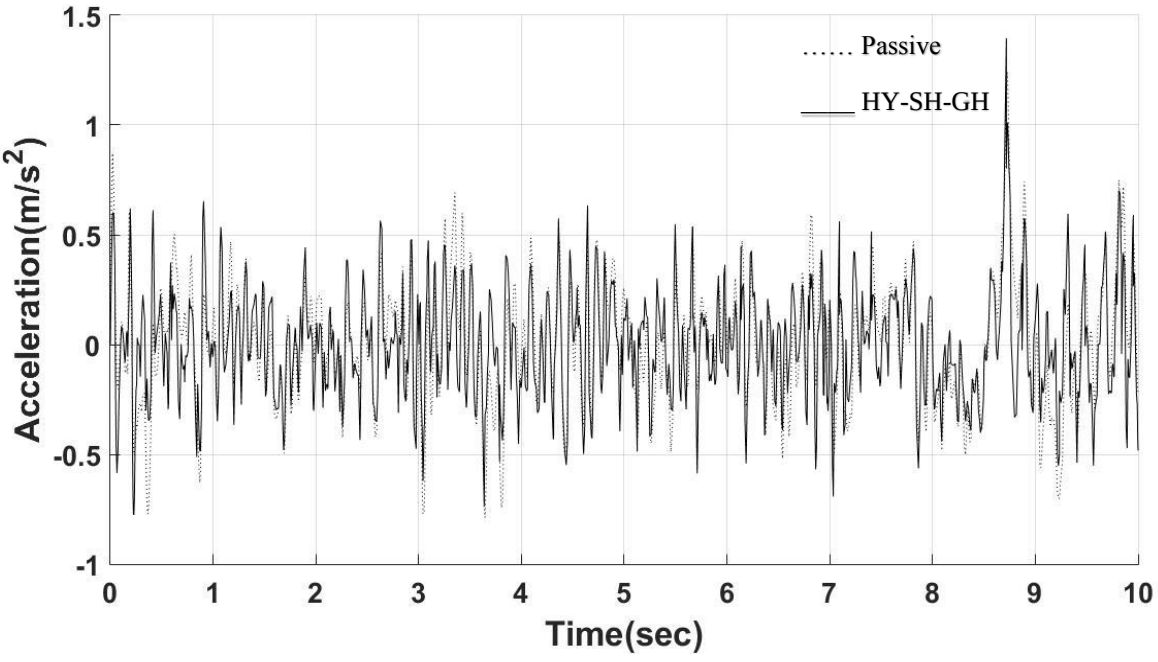

Fig. 6.52: Body acceleration response of half car HY-SH-GH control for random input

Response of HY-SH-B logic has been displayed in Fig. 6.53. It has been found that the magnitude of acceleration is less in case of HY-SH-B control than passive system for most of the time. The number of sharp peaks has also been found to be less in case of HY-SH-B logic.

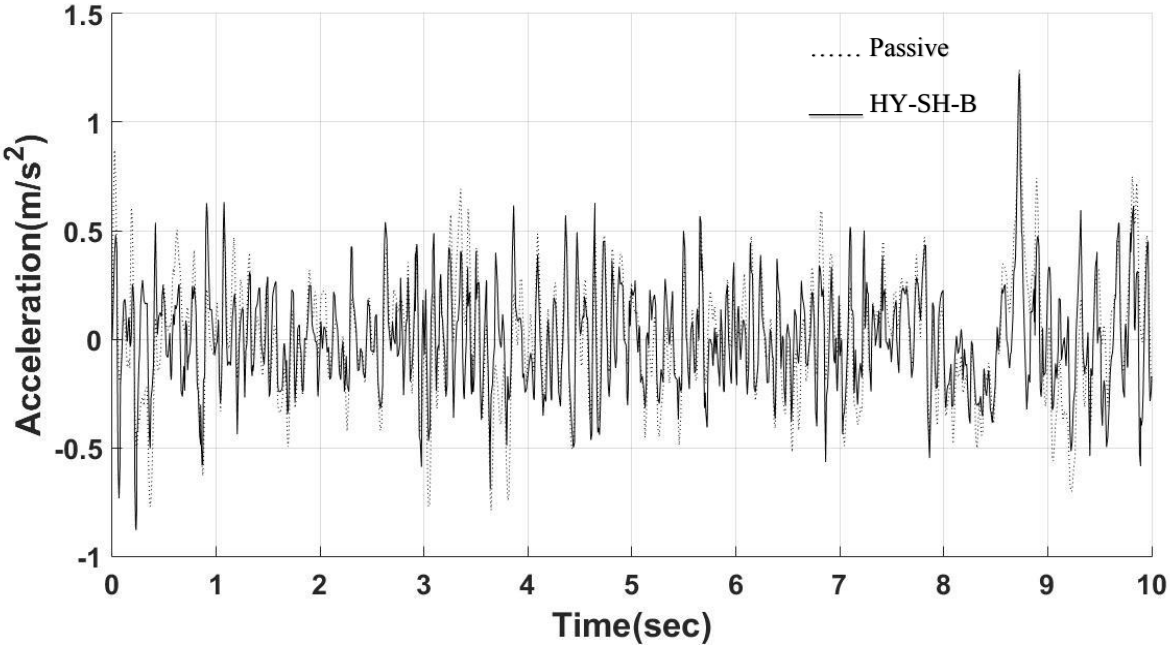

Fig. 6.53: Body acceleration response of half car HY-SH-B control for random input

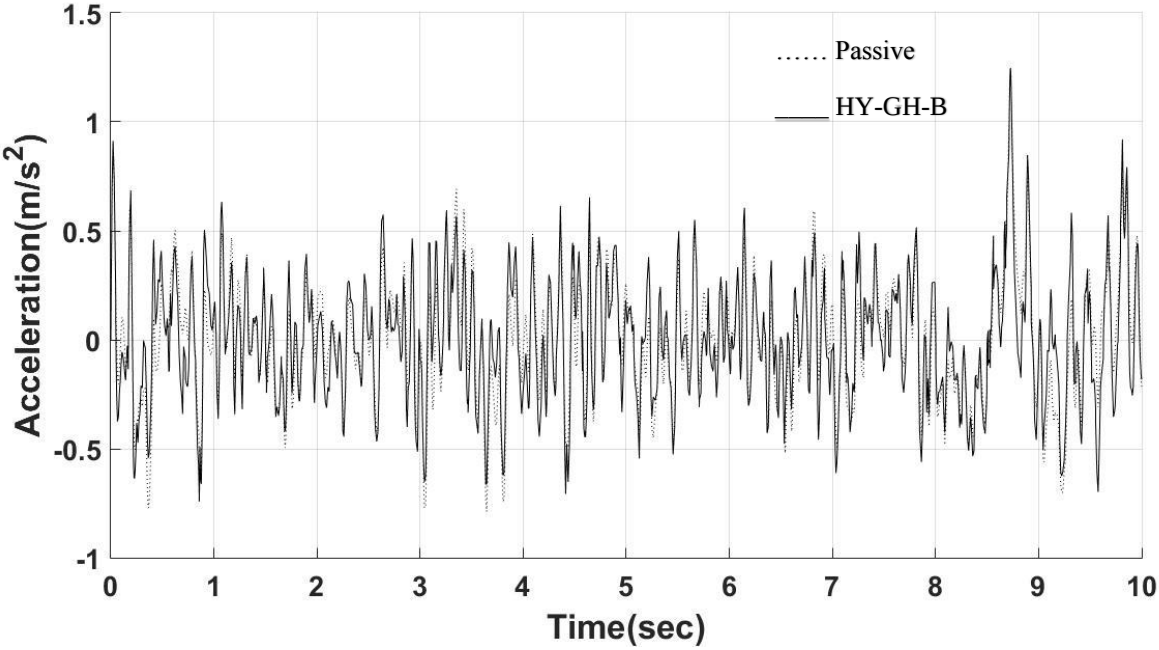

Fig. 6.54: Body acceleration response of half car HY-GH-B control for random input

Fig. 6.54 represents the acceleration response of HY-GH-B logic for random road input. In this case, the response of the system almost follows the passive system. However, there are numerous jerks present in this case as well. The magnitude of acceleration is found to be less at some instances and more at others.

For HY-SH-GH-B control as shown in Fig. 6.55, the magnitude of acceleration is found to be less than a passive system for most of the time. However, the intensity and density of jerks have been found to be almost same as HY-SH-GH control. Thus, HY-SH-GH and HY-SH-GH-B logics give comparable results for acceleration response of a half car in random road.

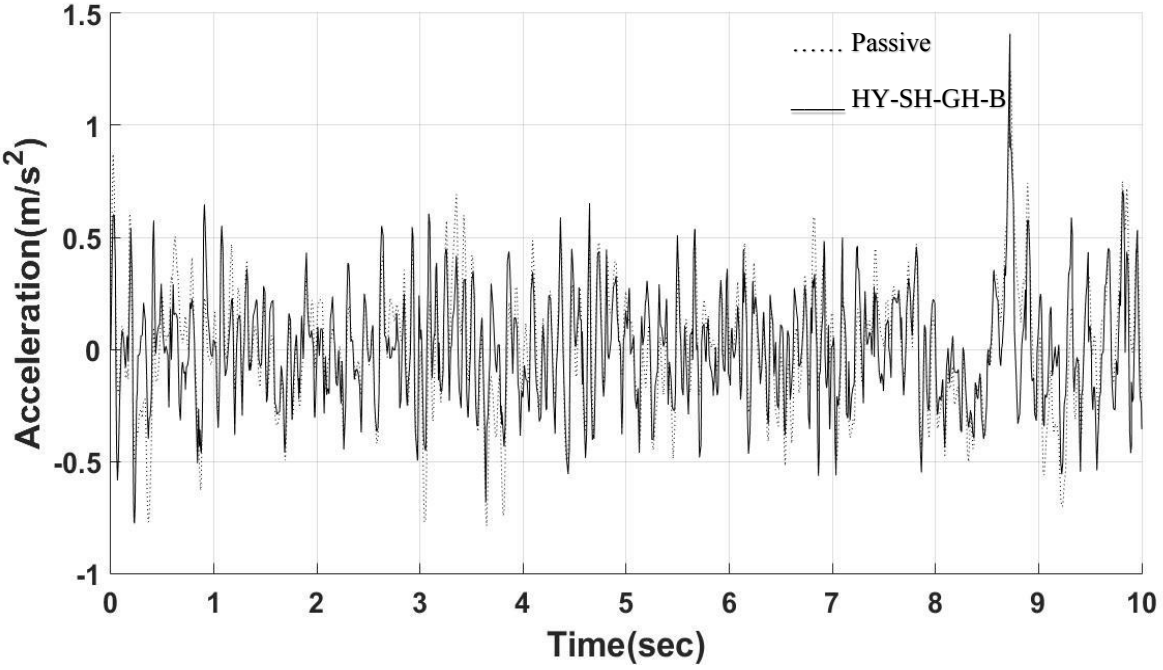

Fig. 6.55: Body acceleration response of half car HY-SH-GH-B control for random input

6.5.3.2 Body displacement

Body displacement vs time for all the continuous logics have been demonstrated in Fig. 6.56. In figure, it can be noticed that HY-SH-GH and HY-SH-GH-B logics have better performance in terms of displacement neutralization. The results for both these logics have been found to be overlapping. HY-SH-B logic gives comparable results with slightly higher value of

displacement than the former two logics. HY-GH-B has been found to be the poorest of all four hybrid strategies in terms of displacement response for half car in random road input. However, all the hybrid logics have better performance than passive system in terms of displacement neutralization.

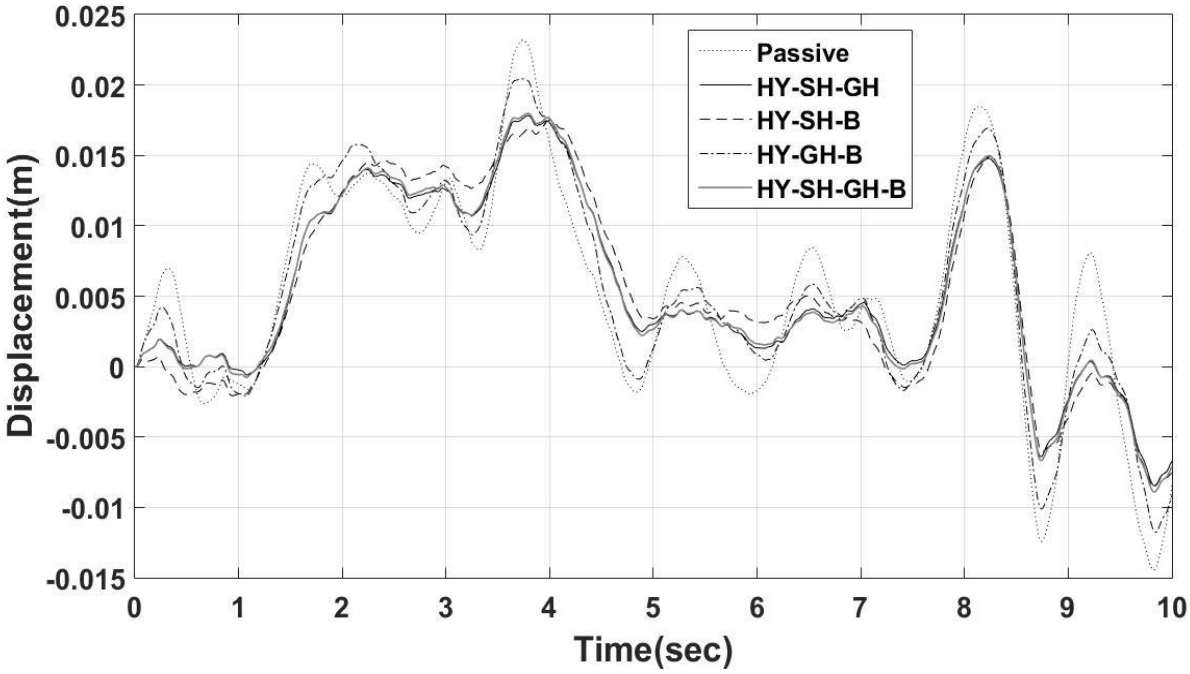

Fig. 6.56: Body displacement response of continuous logics for half car with random input

6.6 Summary of the chapter

This chapter has thoroughly discussed the performance of the different semi-active suspension control logics mentioned in previous chapters. The performance for both quarter car and half car have been evaluated for a half sine bump and random road input. Different performance parameters are considered for the evaluation of system performance. The major findings of the results will be presented in the next chapter.

CHAPTER 7

CONCLUSIONS AND FUTURE SCOPE

This dissertation work has been attempted to obtain the dynamic behaviour of semi-active suspension system for road vehicles through bond graph technique as well as MATLAB/Simulink® and to evaluate the different parameters through simulation. The model parameters are considered for a quarter car model and a half car model. The models were subjected to a bump type road profile input and a random road input. The results have been scrutinized to evaluate the performance of different control logics used for semi-active suspension control. The following conclusions were drawn in this work.

7.1 Conclusions

- The dynamic model of road vehicle had been constructed through bond graph technique and MATLAB/Simulink® environment.
- Vertical dynamics has been carried out for the road vehicle model. A 2-DOF quarter car model and a 4-DOF half car model is used for the analysis. Velocity input at the tire is given by considering half sine bump and random road irregularity.
- The results are obtained for vertical acceleration of sprung and unsprung masses, displacement of body and transmissibility of acceleration from wheel to vehicle body.
- Among on-off logics, on-off skyhook logic gives better performance in diminishing vertical acceleration of the body for bump type input. However, sudden jerks caused by this logic may lead to an uncomfortable ride. On-off groundhook logic on the other hand gives better performance regarding acceleration of unsprung mass. Hence, the vibration of the wheel will be terminated quickly providing better road holding force.
- The continuous logics have shown decline in the value of body acceleration. However, the settling time is found to be more.
- In case of the hybrid logics, HY-SH-GH and HY-SH-GH-B gives better results in terms of vertical acceleration of the vehicle body. The magnitude and the severity both were found to be less in these cases.

- For random road input however, the hybrid logics and on-off logics have shown comparable results.

7.2 Future Scope

- The performance of a full car model will be evaluated for the semi-active suspension system in future.
- In this work, the vertical and longitudinal (pitch) dynamics are investigated which can further be extended for the lateral dynamics of the vehicle model.
- Other different types of road inputs can be considered for the performance evaluation of the system.
- The work can be extended for active suspension system with different control strategies.

References

[1] *Road Accidents in India 2012*, Government of India, Ministry of Road Transport and Highways, Transport Research Wing, New Delhi, June 2013

[2] Dash, D. K., (2015). *Over 11,000 people killed by potholes, speed breakers last year*, The Times of India Report, (http://timesofindia.indiatimes.com/india/Over-11000-people-killed-by-potholes-speed-breakers-last-year/articleshow/48950267.cms)

[3] Granlund, J., (2012). *Vehicle and Human Vibration due to Road Condition*, ROADEX IV Project, EU Northern Periphery Programme.

[4] *Road Accidents in India 2013*, Government of India, Ministry of Road Transport and Highways, Transport Research Wing, New Delhi, August 2014

[5] Sun, L., (2002). *Optimum design of road-friendly vehicle suspension systems subjected to rough pavement surfaces*, Appl. Math. Modelling, Vol. 26, pp. 635–652.

[6] Chikhale, S. J., Deshmukh, S. P., (2013). *Comparative Analysis of Vehicle Suspension System in Matlab-SIMULINK and MSc- ADAMS with the help of Quarter Car Model*, International Journal of Innovative Research in Science, Engineering and Technology, Vol. 2, Issue 8.

[7] Xueying, L., Zhuoping, Y., Lu, X., (2012). *The Study on Accurate Modeling of Suspension Based on ADAMS*, International Journal of Machine Learning and Computing, Vol. 2, No. 2.

[8] Pathare, Y. S., Nimbalkar, S. R., (2014). *Design and Development of Quarter Car Suspension Test Rig Model and it's Simulation*, International Journal of Innovative Research & Development, Vol 3 Issue 2.

[9] Adibi-asl, H., Rideout, G., *Bond Graph Modeling and Simulation of a Full Car Model with Active Suspension*, Faculty of Engineering, Memorial University, St. John's, NL, Canada.

[10] Silva, L., Delarmelina, D., Junco, S., M'Sirdi, N. K., Noura, H., (2007). *Bond Graph Based Fault Diagnosis of 4W-Vehicles Suspension Systems I: Passive Suspensions*, 8th International Conference on Bond Graph Modeling and Simulation, Paper #2, pp. 15-17.

[11] Karnopp, D. C., Crosby, M. J., Harwood, R. A., (1974). *Vibration control using semi-active force generators*, American Society of mechanical Engineers, Journal of Engineering for Industry, 96 (2), 619-626.

[12] Karnopp, D. C., (1990). *Design principles for vibration control systems using semi-active dampers*, American Society of Mechanical Engineers, Journal of Dynamic Systems, Measurement, and Control 112, pp 448-455.

[13] Alanoly, J., Sankar, S., (1987). *A new concept in semi-active vibration isolation*, American Society of Mechanical Engineers, Journal of Mechanisms, Transmission, and Automation in Design 109 pp. 242-247.

[14] Alanoly, J., Sankar, S., (1988). *Semi-active force generators for shock isolation*, Journal of Sound and Vibration 126 (1) 145-156.

[15] Liu, Y., Waters, T. P., Brennan, M. J., (2005). *A comparison of semi-active damping control strategies for vibration isolation of harmonic disturbances*, Journal of Sound and Vibration 280 pp. 21-39.

[16] Shamsi, A., Choupani, N., (2008). *Continuous and Discontinuous Shock Absorber Control through Skyhook Strategy in Semi-Active Suspension System (4DOF Model)*, World Academy of Science, Engineering and Technology, International Journal of Mechanical, Aerospace, Industrial, Mechatronic and Manufacturing Engineering Vol:2, No:5, 697-701.

[17] Strecker, Z., Mazůrek, I., Roupec, J., Klapka, M., (2015). *Influence of MR damper response time on semiactive suspension control efficiency*, Meccanica 50:1949-1959.

[18] Bakar, S. A. A., Samin, P. M., Jamaluddin, H., Rahman, R. A., Sulaiman, S., (2015). *Semi Active Suspension System Performance under Random Road Profile Excitations*, in: International Conference on Computer, Communication, and ControlTechnology, April 21-23, Sarawak, Malaysia.

[19] Hailong, Z., Enrong, W., Fuhong, M., Rakheja, S., Chunyi, S., (2013). *Skyhook-based Semi-active Control of Full-vehicle Suspension with Magneto-rheological Dampers*, Chinese Journal of Mechanical Engineering, Vol. 26, No. 3, 498-505.

[20] Amin, M. H. I. M., Hudha, K., Kadir, Z. A., Amer, N. H., (2015). *Skyhook Control for 7 DOF Ride Model of Armored Vehicle due to Road Disturbance*, IEEE, 978-1-4799-7862-5/15

[21] Raj R., A., Shrivastava, S., Trikhande, M. W., (2015). *Modelling and Analysis of Skyhook and Fuzzy Logic Controls in Semi-Active Suspension System*, in: 2015 International Conference on Industrial Instrumentation and Control (ICIC), College of Engineering Pune, India. May 28-30, 2015.

[22] Strydom, A., Els, P.S., (2014). *The Applicability of Hybrid Control to a Small Off-Road Vehicle without a Differential*, in: Proceedings of the ASME 2014 International Design Engineering Technical Conferences & Computers and Information in Engineering Conference IDETC/CIE 2014, August 17-20, 2014, Buffalo, New York, USA DETC2014-34344.

[23] Kashem, S. B. A., Ektesabi, M., Nagarajah, R., (2015). *Comparison between different sets of suspension parameters and introduction of new modified skyhook control strategy incorporating varying road condition*, Vehicle System Dynamics, 50:7, 1173-1190.

[24] Bessinger, F. H., Cebon, D., Cole, D. J., (1995). *Force control of a semi-active damper*, J.Veh. Syst. Dyn. 24, pp. 695–723.

[25] Nguyen, Q. H., Choi, S. B., (2009). *Optimal design of MR shock absorber and application to vehicle suspension*, Smart Mater. Struct. 18, p. 035012.

[26] Espinoza, A. A. O., Ortega, A. M. C., Martinez, J. C. T., Alcantara, D. H., Menendez, R. M., (2014). *Analysis of On/Off Controllers of a Semi-Active Suspension in a CAN*, 19th IFAC World Congress, Cape Town, South Africa. August 24-29, 2014, 10902-10907.

[27] Goncalves, F. D., (2001). *Dynamic Analysis of Semi-Active Control Techniques for Vehicles Application*, M. S. Thesis, Dept. of Mechanical Engineering, Virginia Polytechnic Institute and State University, Virginia.

[28] Guglielmino, E., Sireteanu, T., Stammers, C. W., Ghita, G., Giuclea, M., (2008). *Semi-active Suspension Control- Improved Vehicle Ride and Road Friendliness*, Springer-Verlag London Limited, (ISBN 978-1-84800-230-2)

[29] Blanchard, E. D., (2003). *On the Control Aspects of Semiactive Suspensions for Automobile Applications*, M. S. Thesis, Dept. of Mechanical Engineering, Virginia Polytechnic Institute and State University, Virginia.

[30] Mukherjee, A., Karmakar, R., Samantaray, A. K., (2014). *Bond Graph in Modeling, Simulation and Fault Identification*, I. K. International Publishing House Pvt. Ltd., (Reprint).

[31] Agostinacchio, M., Ciampa, D., Olita, S., (2014). *The vibrations induced by surface irregularities in road pavements – a Matlab® approach*, Springer, European Transport Research Review, 6, 267-275

[32] Carter, A. K., (1998). *Transient Motion Control of Passive and Semi-Active Damping for Vehicle Suspensions*, M. S. Thesis, Dept. of Electrical Engineering, Virginia Polytechnic Institute and State University, Virginia.

[33] Krasnicki, E. J., (1980). *The experimental performance of an "on-off" active damper*, in: Proceedings of the 51st Shock and Vibration Symposium, San Diego, USA.

[34] Sireteanu, T., Stancioiu, D., Stammers, C. W., (2002). *Use of magnetorheological fluid dampers in semi-active driver seat vibration control*, in: ACTIVE 2002, ISVR, Southampton, UK.

[35] Rakheja, S., Sankar, S., (1985). *Vibration and shock isolation performance of a semi-active "on-off" damper*, American Society of Mechanical Engineers, Journal of Vibration, Acoustics, Stress, and Reliability in Design 107, pp. 398-403.

[36] Krasnicki, E. J., (1980). *Comparison of analytical and experimental results for semi-active vibration isolator*, Shock and Vibration Bulletin 50, pp. 69-76.

[37] Simon, D. E., (1998). *Experimental Evaluation of Semiactive Magnetorheological Primary Suspensions for Heavy Truck Application*, M. S. Thesis, Dept. of Mechanical Engineering, Virginia Polytechnic Institute and State University, Virginia.